

Patterns of Flavour Violation in Models with Vector-Like Quarks

Christoph Bobeth,^{1,2,4} Andrzej J. Buras,^{1,2} Alejandro Celis,³ Martin Jung^{1,4}

¹TUM Institute for Advanced Study, Lichtenbergstr. 2a, D-85748 Garching, Germany

²Physik Department, TU München, James-Frank-Straße, D-85748 Garching, Germany

³Ludwig-Maximilians-Universität München, Fakultät für Physik,
Arnold Sommerfeld Center for Theoretical Physics, 80333 München, Germany

⁴Excellence Cluster Universe, Technische Universität München, Boltzmannstr. 2, D-85748
Garching, Germany

Abstract

We study the patterns of flavour violation in renormalizable extensions of the Standard Model (SM) that contain vector-like quarks (VLQs) in a single complex representation of either the SM gauge group G_{SM} or $G'_{\text{SM}} \equiv G_{\text{SM}} \otimes U(1)_{L_\mu - L_\tau}$. We first decouple VLQs in the (1 – 10) TeV range and then at the electroweak scale also Z, Z' gauge bosons and additional scalars to study the resulting phenomenology that depends on the relative size of Z - and Z' -induced flavour-changing neutral currents, as well as the size of $|\Delta F| = 2$ contributions. In addition to rare decays like $M \rightarrow \ell\bar{\ell}$, $M \rightarrow M'\ell\bar{\ell}$, $M \rightarrow M'\nu\bar{\nu}$ with $M = K, B_s, B_d$ and $|\Delta F| = 2$ observables we analyze the ratio ε'/ε which appears in the SM to be significantly below the data. We study patterns and correlations between various flavour observables in VLQ models with left-handed (LH) and right-handed currents (RH), including experimental constraints. Among the highlights are large new physics (NP) effects in Kaon observables in G_{SM} models, mediated by tree-level Z exchanges with significant but generally smaller effects in $B_{s,d}$ -observables. ε'/ε can easily be made consistent with the data implying then uniquely the suppression of $K_L \rightarrow \pi^0\nu\bar{\nu}$. The enhancement of $K^+ \rightarrow \pi^+\nu\bar{\nu}$ branching ratio over its SM value is only possible in models with RH currents. While in G'_{SM} models NP effects are generally smaller, $K^+ \rightarrow \pi^+\nu\bar{\nu}$ can be enhanced for both LH and RH currents and ΔM_K is stronger affected than in G_{SM} models. We point out that the combination of NP effects to $|\Delta F| = 2$ and $|\Delta F| = 1$ observables in a given meson system allows to determine the masses of VLQs in a given representation independently of the size of VLQ couplings.

Contents

1	Introduction	2
2	The VLQ Models	4
2.1	VLQ Representations	4
2.2	Yukawa interactions of VLQs	5
2.3	Scalar sectors	7
3	Decoupling of VLQs	7
3.1	Tree-level decoupling and Z and Z' effects	9
3.2	Decoupling at one-loop level	12
3.3	Renormalisation group evolution	14
4	Implications for the down-quark sector	15
4.1	$ \Delta F = 2$	16
4.2	$ \Delta F = 1$: Semi-leptonic $d_j \rightarrow d_i + (\ell\bar{\ell}, \nu\bar{\nu})$	17
4.3	$ \Delta F = 1$: Hadronic $d_j \rightarrow d_i q\bar{q}$ and ε'/ε	18
5	Patterns of flavour violation	21
5.1	$ \Delta F = 2$	21
5.2	$ \Delta F = 1$	22
5.3	Determination of M	24
5.4	Kaon and B -meson systems	25
6	Numerics	26
6.1	G_{SM} models	28
6.2	$G'_{\text{SM}}(\Phi)$ model	37
7	Summary and Conclusions	39
A	Scalar sectors of G'_{SM}-models	43
A.1	$G'_{\text{SM}}(S)$ models	43
A.2	$G'_{\text{SM}}(\Phi)$ models	43
B	Master formulae for K and B decays	45
B.1	$ \Delta F = 2$	45
B.2	$d_j \rightarrow d_i \nu\bar{\nu}$	46
B.3	$d_j \rightarrow d_i \ell\bar{\ell}$	47
B.4	$d_j \rightarrow d_i q\bar{q}$ and ε'/ε	49
C	Statistical approach and numerical input	50
	References	50

1 Introduction

Among the simplest renormalizable extensions of the Standard Model (SM) that do not introduce any additional fine tunings of parameters are models in which the only new particles are vector-like fermions. Such fermions can be much heavier than the SM ones as they can acquire masses in the absence of electroweak symmetry breaking. If in the process of this breaking mixing with the SM fermions occurs, the generation of flavour-changing neutral currents (FCNC) mediated by the SM Z boson is a generic implication. If in addition the gauge group is extended by a second $U(1)$ factor, a new heavy gauge boson Z' is present and additional heavy scalars are necessary to provide mass for the Z' and to break the extended gauge-symmetry group down to the SM gauge group. There is a rich literature on FCNCs implied by the presence of vector-like quarks (VLQs), see in particular [1–12].

The goal of the present paper is an extensive study of patterns of flavour violation in models with VLQs that are based on the following gauge groups:

$$G_{\text{SM}} \equiv SU(3)_c \otimes SU(2)_L \otimes U(1)_Y, \quad (1)$$

$$G'_{\text{SM}} \equiv G_{\text{SM}} \otimes U(1)_{L_\mu - L_\tau}. \quad (2)$$

The choice of the particular symmetry group $U(1)_{L_\mu - L_\tau}$ [13, 14] is phenomenologically motivated by the fact that it allows in a simple manner to address successfully the LHCb anomalies [9, 15], while being anomaly-free and containing less parameters than general Z' models [16].

In our paper we will be guided by the analysis in Ref. [11] which identified all renormalizable models with additional fermions residing in a single vector-like complex representation of the SM gauge group with a mass M . It turns out that there are 11 models where new fermions have the proper quantum numbers so that they can couple in a renormalizable manner to the SM Higgs and SM fermions, thereby implying new sources of flavour violation. Our analysis will concentrate on FCNCs in the K , B_d and B_s systems, therefore only the five models with couplings to down quarks are relevant for us, as specified in Section 2. We call this class of models G_{SM} -models.

Consequently the models based on the gauge group G'_{SM} are called G'_{SM} -models. The VLQs in these models belong to the same representations under G_{SM} as in G_{SM} -models, but are additionally charged under $U(1)_{L_\mu - L_\tau}$. These models also contain new heavy scalars.

As we will discuss in detail in Section 2 and Section 5, the patterns of flavour violation in G_{SM} -models and G'_{SM} -models differ significantly from each other:

- In G_{SM} -models Yukawa interactions of the SM scalar doublet H involving ordinary quarks and VLQs imply flavour-violating Z couplings to ordinary quarks, which then dominate $|\Delta F| = 1$ FCNC transitions. However, for VLQ-masses above 5 TeV the corresponding NP contributions to $|\Delta F| = 2$ transitions are dominated by box diagrams with VLQs and scalars, while tree-level Z exchanges play a negligible role [11].
- In G'_{SM} -models the pattern of flavour violation depends on the scalar sector involved. We consider only models in which at least one of the additional scalars is charged

under $U(1)_{L_\mu-L_\tau}$ in such a way that Yukawa couplings between the given VLQ and ordinary quarks are allowed. If this is the case for a new scalar which is just a singlet S under the SM group, the latter imply flavour-violating Z' couplings to ordinary quarks without any FCNCs mediated by the Z . In the following we refer to these models as $G'_{\text{SM}}(S)$ -models. If, on the other hand, such a Yukawa coupling requires the scalar to be a doublet Φ , both tree-level Z' and Z contributions to flavour observables will be present. Their relative size depends on the model parameters, specifically the Z' mass. In these cases we introduce again an additional scalar singlet, but without Yukawa couplings, since otherwise the Z' mass would have to be of the order of the electroweak scale, which is phenomenologically very difficult to achieve. In the following we refer to these models as $G'_{\text{SM}}(\Phi)$ -models.

In this manner we will consider three classes of VLQ models with rather different patterns of flavour violation:

$$G_{\text{SM}}, \quad G'_{\text{SM}}(S), \quad G'_{\text{SM}}(\Phi), \quad (3)$$

in which $|\Delta F| = 1$ FCNCs are mediated by the Z , Z' and both, respectively. In G_{SM} and $G'_{\text{SM}}(\Phi)$ models $|\Delta F| = 2$ transitions are dominated for $M \geq 5$ TeV by box diagrams with VLQs and scalar exchanges, while in the $G'_{\text{SM}}(S)$ models also tree-level Z' exchanges can play an important, sometimes dominant, role.

In [11] an extensive analysis of the G_{SM} -models has been performed and a subset of G'_{SM} -models has been analyzed in [9, 15]. Therefore it is mandatory for us to state what is new in our article regarding these models:

- The authors of [11] concentrated on the derivation of bounds on the Yukawa couplings as functions of M but did not study the correlations between various flavour observables which is the prime target of our paper. Similar comments apply to [9].
- NP contributions to flavour observables depend in each model on the products of complex Yukawa couplings $\lambda_s^* \lambda_d$, $\lambda_b^* \lambda_d$ and $\lambda_b^* \lambda_s$ for $s \rightarrow d$, $b \rightarrow d$ and $b \rightarrow s$ transitions, respectively, as well as the VLQ mass M . This structure allows to set one of the λ_q -phases to zero, such that each model depends on only five Yukawa parameters and M , implying a number of correlations between flavour observables. The strongest correlations are, however, still found between observables corresponding to the same flavour-changing transition, and we concentrate our analysis on them. The correlations between observables with different transitions are weaker, but could turn out to be useful in the future when the data and theory improve, in particular in the context of models for Yukawa couplings.
- An important novelty of our paper, relative to [9, 11, 15], is the inclusion of the ratio ε'/ε in our study. Recent analyses indicate that the measurement of ε'/ε is significantly above its SM prediction [17–20]; it is hence of interest to see which of the models analyzed by us, if any, are capable of addressing this tension and what the consequences for other observables are.

Our paper is organized as follows. In Section 2 we present the particle content of the considered VLQ models, together with the gauge interactions, Yukawa interactions and

the scalar sector. In Section 3 we perform the decoupling of the VLQs and construct the effective field theory (EFT) for each model for scales $\mu_{\text{EW}} < \mu < M$. Section 4 is devoted to the matching of these EFTs to phenomenological ones describing $|\Delta F| = 1, 2$ processes below the scale μ_{EW} . This results in explicit flavour-violating couplings of the Z and Z' to the SM quarks. These enter the effective Lagrangians for the various flavour-changing processes, from which we derive the explicit formulae for the considered observables. In Section 5 we describe the patterns of flavour violation expected in different models, summarizing them with the help of two DNA tables. In Section 6, after formulating our strategy for the phenomenology, we present numerical results of our study. We conclude in Section 7. Several appendices collect additional information on the considered decays, some technical details and in particular the input and statistical procedure used in the numerical analysis.

2 The VLQ Models

Throughout the article we focus on models with vector-like fermions residing in complex representations, either of the the SM gauge group G_{SM} or its extension by an additional gauged $(L_\mu - L_\tau)$ symmetry, $U(1)_{L_\mu - L_\tau}$. For both models we adapt the usual SM fermion content of the three generations ($i = 1, 2, 3$) of quarks ($q_L^i = (u_L^i, d_L^i)^T$, u_R^i, d_R^i) and leptons ($L_L^i = (\nu_i, \ell_L^i)^T$, ℓ_R^i), which acquire masses via spontaneous symmetry breaking from the standard scalar $SU(2)_L$ doublet H .

The gauged $(L_\mu - L_\tau)$ symmetry is anomaly-free in the SM [13, 14]. The only non-vanishing $(L_\mu - L_\tau)$ charges of the SM fermions are introduced as

$$Q'(L_L^2) = Q'(\mu_R) = Q'_\ell, \quad Q'(L_L^3) = Q'(\tau_R) = -Q'_\ell. \quad (4)$$

Here $L_L^2 = (\nu_\mu, \mu_L)$ and $L_L^3 = (\nu_\tau, \tau_L)$ are left-handed $SU(2)_L$ doublets and μ_R and τ_R right-handed singlets. We normalize the $(L_\mu - L_\tau)$ charges of the leptons without loss of generality by setting $Q'_\ell = 1$. The SM quarks do not couple directly to the $U(1)_{L_\mu - L_\tau}$ gauge boson Z' . However, such couplings are generated in G'_{SM} models through Yukawa interactions of SM quarks with VLQs that couple directly to Z' .

2.1 VLQ Representations

As we are mainly interested in the phenomenology of down-quark physics, we will restrict our analysis to $SU(3)_c$ triplets and consider the following five models with $SU(2)_L$ singlets, doublets and triplets:

$$\begin{aligned} \text{singlets :} & \quad D(1, -1/3, -X), & \quad (\text{V}) \\ \text{doublets :} & \quad Q_V(2, +1/6, +X), \quad Q_d(2, -5/6, -X), & \quad (\text{IX, XI}) \\ \text{triplets :} & \quad T_d(3, -1/3, -X), \quad T_u(3, +2/3, +X), & \quad (\text{VII, VIII}) \end{aligned} \quad (5)$$

where the transformation properties are indicated as $(SU(2)_L, U(1)_Y, U(1)_{L_\mu - L_\tau})$, *i.e.* X denotes the charge under $U(1)_{L_\mu - L_\tau}$. It is implied that in G_{SM} -models the $U(1)_{L_\mu - L_\tau}$ charge should be omitted. The representations D , Q_V , Q_d , T_d , T_u correspond to the

models V, IX, XI, VII, VIII introduced in Ref. [11], where a complete list of renormalizable models with vector-like fermions under G_{SM} can be found. Concerning G'_{SM} , the combination of representations D , Q_V and additionally $U(1, +2/3, -X)$ has been studied first in [9].

The kinetic and gauge interactions of the new VLQs are given by

$$\mathcal{L}_{\text{kin}} = \bar{D}(i\mathcal{D} - M_D)D + \sum_{a=V,d} \bar{Q}_a(i\mathcal{D} - M_{Q_a})Q_a + \sum_{a=d,u} \text{Tr} [\bar{T}_a(i\mathcal{D} - M_{T_a})T_a], \quad (6)$$

with appropriate covariant derivatives \mathcal{D}_μ and we follow [11] for the triplet representations as given in (2.13) and (2.14) of that paper. The masses M of the VLQs introduce a new scale, which we will assume to be significantly larger than all other scales. The covariant derivative is, omitting the $SU(3)_c$ part,

$$\mathcal{D}_\mu = \partial_\mu - ig_1 \frac{\sigma^a}{2} W_\mu^a - ig_2 Y B_\mu - ig' Q' \hat{Z}'_\mu \quad (7)$$

with the gauge couplings $g_{2,1}$ and g' of $SU(2)_L$, $U(1)_Y$ and $U(1)_{L_\mu-L_\tau}$, respectively, and charges Y and Q' of $U(1)_Y$ and $U(1)_{L_\mu-L_\tau}$. The Pauli-matrices are denoted by σ^a . The “hat” on \hat{Z}'_μ indicates that we deal here with the gauge eigenstate and not mass eigenstate, see (76).

2.2 Yukawa interactions of VLQs

2.2.1 G_{SM}

The scalar sector consists of the SM scalar doublet H with its usual scalar potential. The VLQs interact with SM quarks (q_L , u_R , d_R) via Yukawa interactions

$$\begin{aligned} -\mathcal{L}_{\text{Yuk}}(H) = & \left(\lambda_i^D H^\dagger \bar{D}_R + \lambda_i^{T_d} H^\dagger \bar{T}_{dR} + \lambda_i^{T_u} \tilde{H}^\dagger \bar{T}_{uR} \right) q_L^i \\ & + \lambda_i^{V_u} \bar{u}_R^i \tilde{H}^\dagger Q_{VL} + \bar{d}_R^i \left(\lambda_i^{V_d} H^\dagger Q_{VL} + \lambda_i^{Q_d} \tilde{H}^\dagger Q_{dL} \right) + \text{h.c.} \end{aligned} \quad (8)$$

where $\tilde{H} \equiv i\sigma_2 H^*$. The complex-valued Yukawa couplings λ_i^{VLQ} give rise to mixing with the SM quarks and flavour-changing Z -couplings, which have been worked out in detail [11] and are discussed in Section 3.1.

2.2.2 $G'_{\text{SM}}(S)$

In models with an additional $U(1)_{L_\mu-L_\tau}$ the scalar sector has to be extended in order to generate the mass of the corresponding gauge boson Z' . A complex scalar $S(1, 0, X)$ ($SU(3)_c$ singlet) is added in the minimal version. As VLQs are charged under $U(1)_{L_\mu-L_\tau}$, their Yukawa couplings with the SM doublet H are forbidden. But the ones involving S are allowed for $Q'_S = \pm Q'_{\text{VLQ}}$ and given by [9]

$$-\mathcal{L}_{\text{Yuk}}(S) = \left(\lambda_i^D \bar{d}_R^i D_L + \lambda_i^V \bar{Q}_{VR} q_L^i \right) S + \text{h.c.} \quad (9)$$

In fact this scalar system is sufficient for models with VLQs having $U(1)_Y$ charges $Y = -1/3$ and $+1/6$ of the SM fermions d_R and q_L , respectively. In the following we refer to these models as $G'_{\text{SM}}(S)$ -models. The special feature of these models is that tree-level Z' exchanges dominate $\Delta F = 1$ transitions and in some part of the parameter space can also compete with contributions from box diagrams with VLQs and scalars in the case of $\Delta F = 2$ transitions.

2.2.3 $G'_{\text{SM}}(\Phi)$

For VLQs with G_{SM} quantum numbers different from one of the SM quark fields, the simple extension by a scalar singlet is not possible. In a next-to-minimal version we therefore add to the scalar sector an additional scalar $SU(2)_L$ doublet $\Phi(2, +1/2, X)$, besides the SM-like $H(2, +1/2, 0)$. We require $|X| \neq 1, 2$ in order to avoid lepton-flavour violating (LFV) Yukawa couplings — see for example [21] — and in consequence there are no LFV Z' couplings, which are subject to strong constraints at low energies. The vacuum expectation value (VEV) of Φ gives an unavoidable contribution to the Z' mass of the order of the electroweak scale, contributes to the mass of H and generates potentially large $Z - Z'$ mass mixing effects. The latter would be strongly constrained by electroweak precision tests [22], in particular there would be sizeable corrections to the Z couplings to muons. In order to avoid these difficulties, Φ is accompanied by an additional complex scalar singlet $S(1, 0, Y)$, which breaks the $U(1)_{L_\mu - L_\tau}$ symmetry at the TeV scale. The $L_\mu - L_\tau$ charge of S is chosen to be $Y = X/2$ in order to avoid the appearance of a Goldstone boson in the scalar sector and to forbid Yukawa couplings of S with SM fermions and VLQs.

The Yukawa interactions of the VLQs with Φ are

$$-\mathcal{L}_{\text{Yuk}}(\Phi) = \left(\lambda_i^D \Phi^\dagger \bar{D}_R + \lambda_i^{T_d} \Phi^\dagger \bar{T}_{dR} + \lambda_i^{T_u} \tilde{\Phi}^\dagger \bar{T}_{uR} \right) q_L^i + \lambda_i^{Q_d} \tilde{\Phi}^\dagger \bar{d}_R^i Q_{dL} + \text{h.c.}, \quad (10)$$

with $\tilde{\Phi} \equiv i\sigma_2 \Phi^*$ and we will refer to these models as $G'_{\text{SM}}(\Phi)$ -models. We note that the structure of couplings equals the one of G_{SM} models given in Eq. (8) upon $H \leftrightarrow \Phi$. For the VLQ $D(1, -1/3, X)$ we consider thus two versions, one in $G'_{\text{SM}}(S)$ and one in the $G'_{\text{SM}}(\Phi)$ -model. We refrain from the same procedure for $Q_V(2, +1/6, X)$. In $G'_{\text{SM}}(\Phi)$ models FCNCs are mediated by both Z and Z' but in the case of $\Delta F = 2$ transitions box diagrams with VLQs and scalars play the dominant role for sufficiently large M .

For ease of notation, we will sometimes refrain below from explicitly labeling the λ_i by the VLQ representation, as should be done if several of them are considered simultaneously.

2.2.4 Yukawa couplings of several representations

In our numerics we will consider one VLQ representation at a time as this simplifies the analysis significantly. In particular the number of parameters is quite limited. Still it is useful to make a few comments on the structure of flavour-violating interactions and at various places in our paper to state how our formulae would be modified through the presence of several VLQ representations in a given model. We plan to return to the phenomenology of such models in the future.

When admitting several VLQ representations F^m and F^n simultaneously, potentially additional locally gauge-invariant Yukawa couplings $\sim \tilde{\lambda}_{mn} \overline{F}_L^m \varphi_{mn} F_R^n$ with $\varphi_{mn} = H$ have to be included in the case of G_{SM} -models [3]. They give rise to flavour-changing neutral Higgs currents at tree level. In the G'_{SM} -models the $U(1)_{L_\mu-L_\tau}$ -charges of the additional $\varphi_{mn} = S, \Phi$ have been chosen following the criteria explained above, which fixes in turn the $U(1)_{L_\mu-L_\tau}$ -charges of the VLQs. In consequence such couplings to $\varphi_{mn} = S, \Phi$ are not permitted, however they are still allowed for $\varphi_{mn} = H$, which has zero $U(1)_{L_\mu-L_\tau}$ -charge. In $G'_{\text{SM}}(S)$ models, only the particular choice of the $U(1)_{L_\mu-L_\tau}$ charges $Q'_{Q_V} = -Q'_D$ [9] forbids these couplings to H , whereas the choice $Q'_{Q_V} = Q'_D$ would allow them, due to the possibility to replace $\overline{Q}_{VR} q_L^i \rightarrow \overline{q}_L^i Q_{VR}$ in Eq. (9), which maintains gauge invariance since S is a singlet. On the other hand, in $G'_{\text{SM}}(\Phi)$ models such couplings arise for Q_d with D and T_d .

2.3 Scalar sectors

In the G_{SM} -models, the scalar sector contains only the standard doublet $H(2, +1/2, 0)$, which provides masses to gauge bosons and standard fermions in the course of spontaneous symmetry breaking of $SU(2)_L \otimes U(1)_Y \rightarrow U(1)_{\text{em}}$ via the VEV $v \simeq 246$ GeV, where

$$\langle H \rangle = (0, v/\sqrt{2})^T. \quad (11)$$

In $G'_{\text{SM}}(S)$ -models the doublet $H(2, +1/2, 0)$ fulfils again the same role, whereas the singlet $S(1, 0, X)$ provides via its VEV $\langle S \rangle = v_S/\sqrt{2}$ a mass for the additional $U(1)_{L_\mu-L_\tau}$ Z' -gauge boson

$$M_{Z'}^2 = g'^2 v_S^2 X^2. \quad (12)$$

In $G'_{\text{SM}}(\Phi)$ -models the doublet $\Phi_2 \equiv H(2, +1/2, 0)$ gives masses to the chiral fermions, whereas $\Phi_1 \equiv \Phi(2, +1/2, X)$ contributes to the masses of the Z and Z' gauge bosons in combination with $S(1, 0, X/2)$.¹ The neutral components of the doublets acquire VEV's

$$\langle \Phi_a^0 \rangle = \frac{v_a}{\sqrt{2}}, \quad \tan \beta \equiv \frac{v_2}{v_1}, \quad v = \sqrt{v_1^2 + v_2^2} \simeq 246 \text{ GeV}, \quad (13)$$

with $0 \leq \beta \leq \pi/2$. In this case, neutral gauge boson mixing occurs with details given in Appendix A.2.

Further details on the scalar sectors of the $G'_{\text{SM}}(S)$ and $G'_{\text{SM}}(\Phi)$ models are collected in Appendix A.1 and A.2, respectively. In Table 1 we summarize all G'_{SM} -models and indicate which diagrams dominate NP contributions to $|\Delta F| = 1$ and $|\Delta F| = 2$ transitions in a given model.

3 Decoupling of VLQs

The VLQ models are characterised by the masses M of the VLQs, the various Yukawa couplings λ_i^{VLQ} ($i = 1, 2, 3$) of Section 2.2 and the VEVs of the respective scalar sectors,

¹This convention corresponds to that of the Type I 2HDM.

VLQ Representation	Scalar Singlet	Scalar Doublets	$ \Delta F = 1$	$ \Delta F = 2$
$D_a(3, 1, -1/3, -X)$	$S(1, 1, 0, X)$	$H(1, 2, 1/2, 0)$	Z'	Z', Box
$D_b(3, 1, -1/3, -X)$	$S(1, 1, 0, X/2)$	$\Phi_1(1, 2, 1/2, X), \Phi_2(1, 2, 1/2, 0)$	Z', Z	Box
$Q_V(3, 2, +1/6, +X)$	$S(1, 1, 0, X)$	$H(1, 2, 1/2, 0)$	Z'	Z', Box
$Q_d(3, 2, -5/6, -X)$	$S(1, 1, 0, X/2)$	$\Phi_1(1, 2, 1/2, X), \Phi_2(1, 2, 1/2, 0)$	Z', Z	Box
$T_d(3, 3, -1/3, -X)$	$S(1, 1, 0, X/2)$	$\Phi_1(1, 2, 1/2, X), \Phi_2(1, 2, 1/2, 0)$	Z', Z	Box
$T_u(3, 3, +2/3, +X)$	$S(1, 1, 0, X/2)$	$\Phi_1(1, 2, 1/2, X), \Phi_2(1, 2, 1/2, 0)$	Z', Z	Box

Table 1: Fermion and scalar representations under $SU(3)_c \otimes SU(2)_L \otimes U(1)_Y \otimes U(1)_{L\mu-L\tau}$ in G'_{SM} -models. In the last two columns we show which diagrams dominate NP contributions to $|\Delta F| = 1$ and $|\Delta F| = 2$ transitions for $M \geq 5$ TeV.

see Section 2.3. The present lower bound on M from the LHC is in the ballpark of 1 TeV, while the lower bounds on $M_{Z'}$ are typically close to 3 TeV if Z' has a direct coupling to light quarks. But as emphasized in [9, 15], Z' of $U(1)_{L\mu-L\tau}$ does not have such couplings, implying a much weaker lower bound on its mass, which could in fact be as low as the electroweak scale and even lower. While it could also be as heavy as the VLQ mass, we will assume the hierarchy

$$M_Z \lesssim M_{Z'} \ll M, \quad \text{or equivalently} \quad v \lesssim v_S \ll M, \quad (14)$$

in order to simplify the analysis. It is then natural to decouple first the VLQs and to consider EFTs for G_{SM} and G'_{SM} valid between the scales $\mu_M \sim M$ and $\mu_{\text{EW}} \sim v \simeq v_S$. These are subsequently matched in one step onto $SU(3)_c \otimes U(1)_{\text{em}}$ -invariant phenomenological EFTs of $|\Delta F| = 1, 2$ decays, which are valid between μ_{EW} and $\mu_b \sim m_b$, where m_b denotes the bottom mass. The coefficients determined in the process will indicate which operators are the most important. In principle one could consider an intermediate EFT which is constructed by integrating out Z' and the new scalars before integrating out top quark, W and Z , but from the point of view of renormalisation group effects, integrating out all these heavy fields simultaneously appears to be an adequate approximation.

In this section we present the results from the decoupling of the VLQs that are important for our phenomenological applications within the framework of the $G_{\text{SM}}^{(\prime)}$ -EFTs. The matching step of the $G_{\text{SM}}^{(\prime)}$ -EFTs to phenomenological EFT's of $|\Delta F| = 1, 2$ processes at the scale μ_{EW} is given in Section 4. The Lagrangian of the $G_{\text{SM}}^{(\prime)}$ -EFT consists of the dimension four interactions of the light fields and dimension six interactions generated by the decoupling of VLQs

$$\mathcal{L}_{G_{\text{SM}}^{(\prime)\text{-EFT}}} = \mathcal{L}_{\text{dim-4}} + \sum_a \mathcal{C}_a \mathcal{O}_a, \quad (15)$$

which are invariant under either G_{SM} or G'_{SM} , depending on the model. Thus in G_{SM} -models $\mathcal{L}_{\text{dim-4}}$ coincides with the SM Lagrangian and the corresponding non-redundant set of operators of dimension six has been classified in Ref. [23]. In G'_{SM} -models operators that are invariant under G'_{SM} must be added, which involve the Z' -boson and the addi-

tional scalar singlets and/or doublets. The Wilson coefficients \mathcal{C}_a ² are effective couplings, which are suppressed by v_i^2/M^2 with $v_i = (v, v_1, v_S)$, depending on the model. They are determined at the scale μ_M when decoupling VLQs. The decoupling proceeds either by explicit matching calculations starting at tree-level and including subsequently higher orders or by integrating them out in the path integral method [3]. The tree-level decoupling has been known for a long time for G_{SM} models [3] and is given for $G'_{\text{SM}}(S)$ models in Ref. [9].

Within the EFT, renormalisation group equations (RGE) allow to evolve the Wilson coefficients from μ_M down to μ_{EW} . At leading logarithmic (LL) order it has the approximate perturbative solution

$$\mathcal{C}_a(\mu_{\text{EW}}) = \left[\delta_{ab} - \frac{\gamma_{ab}}{(4\pi)^2} \ln \frac{\mu_M}{\mu_{\text{EW}}} \right] \mathcal{C}_b(\mu_M) \quad (16)$$

for not too large μ_M . The anomalous dimension matrices (ADM) γ_{ab} depend in general on couplings of the gauge, Yukawa and scalar sectors and are known for the G_{SM} -EFT [24–26]. Largest contributions might be expected for the case of $\gamma_{ab} \propto Y_u^\dagger Y_u \sim y_t^2$ mixing due to the top-quark Yukawa coupling $y_t \sim 1$ of the order of a few percent in the case of self-mixing ($a = b$) and from the mixing due to QCD under α_s . On the other hand, for $a \neq b$ non-zero Wilson coefficients can be generated at LL order.

The VLQs have a very limited set of couplings to light fields, which are either via gauge interactions (6) to the gauge bosons or via Yukawa interactions (8)–(10) to light — w.r.t. to VLQ mass M — SM quarks and scalars $\varphi = H, S$ or Φ , depending on the model. At tree-level, this particular structure of interactions can give rise only to flavour-changing Z and Z' couplings, whereas all other decoupling effects are loop-suppressed [27].

The decoupling of the VLQs proceeds in the unbroken phase of $SU(2)_L \otimes U(1)_Y$, hence quark fields are flavour-eigenstates and neutral components of scalar fields are without VEV at this stage. After the LL-evolution from μ_M to μ_{EW} , spontaneous symmetry breaking will take place within the $G_{\text{SM}}^{(l)}$ -EFTs and the transformation from flavour- to mass-eigenstates for fermions and gauge bosons can be performed, accounting for the dimension six part in Eq. (15).

3.1 Tree-level decoupling and Z and Z' effects

The couplings of the VLQs permit at tree level only a dimension six contribution from the generic 4-point diagram in Fig. 1a. Since its dimension-five contribution vanishes [3], it is equivalent to consider the 5-point diagram Fig. 1b, where either $SU(2)_L$ or $U(1)_Y$ gauge bosons in G_{SM} -models or in addition a \hat{Z}' in G'_{SM} -models is radiated off the VLQ [3, 9]. As a consequence, in G_{SM} - and G'_{SM} -models only operators of the type $\psi^2 \varphi^2 D \propto (\varphi^\dagger \overleftrightarrow{D}_\mu \varphi) [\bar{\psi}_i \gamma^\mu \psi_j]$ ($\varphi = H, S, \Phi$) receive non-vanishing contributions at tree-level, which are projected in part onto $\psi^2 \varphi^3$ -type operators via equation of motions (EOM) [23, 28].

After spontaneous symmetry breaking the $\psi^2 \varphi^3$ operators contribute to the quark

²The Wilson coefficients of $G_{\text{SM}}^{(l)}$ -EFTs are denoted with calligraphic \mathcal{C}_i , whereas the ones of phenomenological EFTs with C_i .

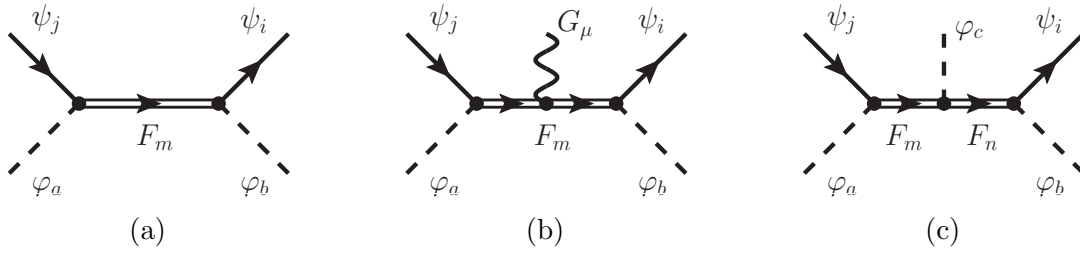


Figure 1: Tree-level graphs (a) and (b) of the decoupling of a VLQ F_m that give rise to $\psi^2\varphi^2D$ operators. They proceed via their Yukawa interactions with scalars $\varphi = (H, S, \Phi)$ and SM quarks $\psi = (q_L, u_R, d_R)$. The gauge boson G_μ depends on the representation. Tree-level graph (c) requires two representations $F_{m,n}$ with a Yukawa coupling via φ_c and give rise to $\psi^2\varphi^3$ operators.

masses m_ψ ($\psi = u, d$) at the scale μ_{EW} via

$$m_\psi^{ij} = \frac{v}{\sqrt{2}} \left(Y_\psi^{ij} - \frac{v^2}{2} \mathcal{C}_{\psi H}^{ij} - \frac{v_S^2}{2} \mathcal{C}_{\psi S}^{ij} - \cos^2\beta \frac{v^2}{2} \mathcal{C}_{\psi \Phi}^{ij} \right), \quad (17)$$

which allows to substitute Yukawa couplings Y_ψ in terms of measured m_ψ and new physics parameters $\mathcal{C}_{\psi^2\varphi^3} \propto Y_\psi \mathcal{C}_{\psi^2\varphi^2D}$. If several representations of VLQs are present in a given model and two of them $F_{m,n}$ couple to a scalar φ_c ³ via Yukawa couplings $\tilde{\lambda}_{mn}$, a third possibility is allowed at tree-level depicted in Fig. 1c, which contributes directly to $\psi^2\varphi^3$ operators and gives rise to flavour-changing neutral $H\bar{q}_i q_j$ interactions at tree-level [3]. The various possibilities for G_{SM} models, where $\varphi_c = H$, can be found in [3].

The relation of quark masses to the Yukawa interactions (17) includes now also $1/M^2$ contributions. Their diagonalisation proceeds as usual for the quark fields with the help of 3×3 unitary rotations in flavour space:

$$\psi_L \rightarrow V_L^\psi \psi_L, \quad \psi_R \rightarrow V_R^\psi \psi_R, \quad (18)$$

implying

$$V_L^{\psi\dagger} m_\psi V_R^\psi = m_\psi^{\text{diag}}, \quad V = (V_L^u)^\dagger V_L^d, \quad (19)$$

with diagonal up- and down-quark masses m_ψ^{diag} and the quark-mixing matrix V (CKM matrix). Throughout we will assume that down quarks are already mass eigenstates, which fixes also the basis for the VLQ Yukawa couplings λ_i^{VLQ} and implies $q_L = (V^\dagger u_L, d_L)^T$.

After spontaneous symmetry breaking the $\psi^2\varphi^2D$ operators give rise to flavour-changing Z and Z' interactions for fermions ($f = \ell, u, d$), which we parametrise as follows:

$$\mathcal{L}_{\text{VLQ}}^{(Z)} = \bar{f}^i [\Delta_L^{ij}(Z) \gamma^\mu P_L + \Delta_R^{ij}(Z) \gamma^\mu P_R] f^j Z_\mu, \quad (20)$$

$$\mathcal{L}^{(Z')} = \bar{f}^i [\Delta_L^{ij}(Z') \gamma^\mu P_L + \Delta_R^{ij}(Z') \gamma^\mu P_R] f^j Z'_\mu. \quad (21)$$

The flavour-diagonal ($i = j$) couplings of quarks and leptons to Z will be set to the ones of the SM as corrections from NP to them are in G_{SM} -models one-loop suppressed.

³As discussed above $\varphi_c = H$ in G_{SM} and G'_{SM} -models.

This is also the case of $G'_{\text{SM}}(S)$ models where Z does not play any role in FCNCs. In $G'_{\text{SM}}(\Phi)$ models modifications of the $Zf\bar{f}$ couplings come from $Z - Z'$ mixing. These shifts are relevant for leptons in partial widths of $Z \rightarrow \ell\bar{\ell}$ (see Appendix A.2) and could be of relevance in electroweak precision tests. In the semi-leptonic $|\Delta F| = 1$ FCNCs we will include them for consistency in $G'_{\text{SM}}(\Phi)$ models, although they are negligible in comparison to other effects.

3.1.1 G_{SM} -models

In the case of G_{SM} -models, the decoupling of VLQs gives the results for $\Delta_{L,R}(Z)$ couplings collected for down-quarks in Table 2, where

$$\Delta^{ij} \equiv \frac{\lambda_i^* \lambda_j}{g_Z} \frac{M_Z^2}{M^2}, \quad g_Z \equiv \sqrt{g_1^2 + g_2^2}. \quad (22)$$

Except for the sign in the case of T_u , our results agree with those in [11]. Furthermore, also non-zero couplings to up-type quarks arise [11] but they will not play any role in our paper.

Coupling	q	D	Q_V	Q_d	T_d	T_u
$\Delta_{L}^{q_i q_j}(Z)$	d	Δ^{ij}	0	0	$\Delta^{ij}/2$	$-\Delta^{ij}$
	u	0	0	0	$V_{im}\Delta^{mn}(V^\dagger)_{nj}$	$-V_{im}\Delta^{mn}(V^\dagger)_{nj}/2$
$\Delta_{R}^{q_i q_j}(Z)$	d	0	$-(\Delta^{ij})^*$	$(\Delta^{ij})^*$	0	0
	u	0	$(\Delta_u^{ij})^*$	0	0	0

Table 2: $\Delta_{L,R}^{q_i q_j}(Z)$ for down- and up-type-quark couplings ($i, j = 1, 2, 3$) to the Z boson in G_{SM} -models. Here V_{ij} is the CKM matrix and $\Delta_u = \Delta(\lambda_i^{V_d} \rightarrow \lambda_i^{V_u})$, see (8).

3.1.2 G'_{SM} -models

In the G'_{SM} -models, the $(L_\mu - L_\tau)$ symmetry fixes the Z' coupling to leptons to be

$$\Delta_{L}^{\ell\bar{\ell}}(Z') = \Delta_{R}^{\ell\bar{\ell}}(Z') = \Delta_{L}^{\nu_\ell \bar{\nu}_\ell}(Z') = g' Q'_\ell, \quad (23)$$

with $Q'_\ell = \{0, +1, -1\}$ for $\ell = \{e, \mu, \tau\}$. Here we have neglected $Z - Z'$ mixing effects existing in $G'_{\text{SM}}(\Phi)$ -models. However, for consistency we have to include these effects in the couplings of the Z to leptons

$$\Delta_{L}^{\ell\bar{\ell}}(Z) = -g_Z \left(\frac{1}{2} - s_W^2 \right) + g' Q'_\ell \xi_{ZZ'}, \quad \Delta_{R}^{\ell\bar{\ell}}(Z) = g_Z s_W^2 + g' Q'_\ell \xi_{ZZ'}, \quad (24)$$

to first order in the small mixing angle $\xi_{ZZ'}$ (see Appendix A.2 for details). On the other hand, the gauge couplings to quarks are model dependent.

In $G'_{\text{SM}}(S)$ -models the scalar sector of S and H generates only non-zero quark couplings to Z' , whereas in $G'_{\text{SM}}(\Phi)$ -models the scalar sector of S , H and Φ gives rise to non-zero couplings of SM quarks to both Z' and Z . We define

$$G^{ij} \equiv -\frac{\lambda_i^* \lambda_j}{2Xg'} \frac{M_{Z'}^2}{M^2}, \quad K^{ij} \equiv c_\beta^2 \frac{\lambda_i^* \lambda_j}{g_Z} \frac{M_Z^2}{M^2} = c_\beta^2 \Delta^{ij}, \quad (25)$$

with Δ^{ij} defined in Eq. (22) and the $Z - Z'$ mixing angle [see (78)]

$$\xi_{ZZ'} \simeq r' c_\beta^2 \frac{M_Z^2}{M_{Z'}^2}, \quad r' \equiv \frac{2Xg'}{g_Z}. \quad (26)$$

Here $c_\beta \equiv \cos \beta$ is a parameter associated with the scalar sector (see (13)) of $G'_{\text{SM}}(\Phi)$ -models, i.e. $v_1 = v \cos \beta$. The $\xi_{ZZ'}$ describes $Z - Z'$ mixing, which is phenomenologically constrained to be small, $\xi_{ZZ'} < 0.1$, due to constraints from the Z -boson mass, M_Z , and partial widths $Z \rightarrow \ell\bar{\ell}$ measured at LEP, as described in more detail in Appendix A.2. The down- and up-quark couplings to Z' and Z are collected for these models in Table 3. We confirm previous findings [9] for the $G'_{\text{SM}}(S)$ -models.

We note that the Z' couplings are suppressed/enhanced by the ratio r' w.r.t. the Z -couplings. Enhancement takes place for $2g'X > g_Z \approx 0.75$, such that for example $r' \approx 3$ can be reached with $g'X \approx 1.1$, still within the perturbative regime. The couplings of T_d and T_u differ just by a sign and factors 1/2. In distinction to Z -contributions in G_{SM} -models, both Z - and Z' -contributions in $G'_{\text{SM}}(\Phi)$ models decouple with large $\tan \beta$, see K^{ij} in Eq. (25).

Model	q	$\Delta_L^{q_i q_j}(Z')$	$\Delta_R^{q_i q_j}(Z')$	$\Delta_L^{q_i q_j}(Z)$	$\Delta_R^{q_i q_j}(Z)$
$G'_{\text{SM}}(S)$					
D	d	0	$(G^{ij})^*$	0	0
	Q_V	G^{ij}	0	0	0
	u	$V_{im} G^{mn} (V^\dagger)_{nj}$	0	0	0
$G'_{\text{SM}}(\Phi)$					
D	d	$-r' K^{ij}$	0	$[1 - r' \xi_{ZZ'}] K^{ij}$	0
Q_d	d	0	$-r' (K^{ij})^*$	0	$[1 - r' \xi_{ZZ'}] (K^{ij})^*$
T_d	d	$-r' K^{ij}/2$	0	$[1 - r' \xi_{ZZ'}] K^{ij}/2$	0
	u	$-r' V_{im} K^{mn} (V^\dagger)_{nj}$	0	$[1 - r' \xi_{ZZ'}] V_{im} K^{mn} (V^\dagger)_{nj}$	0
T_u	d	$r' K^{ij}$	0	$-[1 - r' \xi_{ZZ'}] K^{ij}$	0
	u	$r' V_{im} K^{mn} (V^\dagger)_{nj}/2$	0	$-[1 - r' \xi_{ZZ'}] V_{im} K^{mn} (V^\dagger)_{nj}/2$	0

Table 3: $\Delta_{L,R}^{q_i q_j}(Z')$ and $\Delta_{L,R}^{q_i q_j}(Z)$ for down- and up-type quark couplings ($i, j = 1, 2, 3$) in G'_{SM} -models. Here V_{ij} is the CKM matrix.

3.2 Decoupling at one-loop level

All other decoupling processes proceed via loops. Those that would lead to non-canonical kinetic terms in the $G_{\text{SM}}^{(\prime)}$ -EFTs can be absorbed by a suitable choice of wave-function

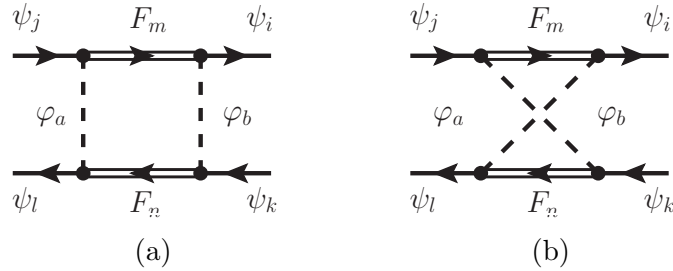


Figure 2: Box graphs for the decoupling of VLQs in representations $F_{m,n}$ due to their Yukawa interactions with scalars $\varphi = H, S, \Phi$ and SM quarks $\psi = (q_L, d_R, u_R)$. The crossed graph appears for certain representations $F_m \neq F_n$. The $|\Delta F| = 2$ graphs are found for $k = j$ and $l = i$.

renormalisation constants in the full theory above the scale μ_M , resulting in non-minimal renormalisation of interactions and giving rise to finite threshold effects of coupling constants. In G'_{SM} -models this is the case for kinetic mixing of B_μ and \hat{Z}'_μ , which enters our analysis only as a higher order effect.

All other effects enter as dimension six operators. The ones with four quarks are most important for quark-flavour phenomenology. They involve only VLQ-Yukawa interactions, as depicted in Fig. 2a and Fig. 2b, and give rise to ψ^4 -type operators, among which are also $|\Delta F| = 2$ operators. Here we match directly to the operators present in the phenomenological EFT of $|\Delta F| = 2$ decays, using the conventions in Appendix B.1, avoiding thereby the intermediate matching to the G_{SM} -invariant form.⁴ In principle this procedure hides the phenomenological interplay with other sectors in quark-flavour physics due to mixing effects taking place via the RGE, most prominently the ones enhanced by the top-Yukawa coupling, but here we are interested only in B -meson and Kaon phenomenology. The matching of ψ^4 operators in $G_{\text{SM}}^{(\prime)}$ -EFTs to the $|\Delta F| = 2$ phenomenological theory can be found in [29].

In G_{SM} -models VLQs contribute to $|\Delta F| = 2$ operators O_a^{ij} for $a = \text{VLL}, \text{VRR}, \text{LR1}$ via box diagrams (see Figs. 2a and 2b), which contain two heavy VLQ propagators with representations F_m and F_n and massless components of the standard doublet $H = (H^+, H^0)^T$. These box diagrams yield the general structure of the Wilson coefficients

$$\mathcal{C}_a^{ij} = \frac{\eta_{mn}}{(4\pi)^2} \frac{\Lambda_{ij}^m \Lambda_{ij}^n}{\mathcal{N}_{ij}} f_1(M_m, M_n) \quad (27)$$

at the scale μ_M . Here the prefactor \mathcal{N}_{ij} corresponds to the SM normalisation of the $|\Delta F| = 2$ EFT, see (82). The function

$$f_1(M_m, M_n) = \frac{\ln(M_m^2/M_n^2)}{M_m^2 - M_n^2}, \quad \text{with} \quad f_1(M_m, M_m) = \frac{1}{M_m^2}, \quad (28)$$

⁴Note that the set of ψ^4 -type operators is the same in all $G_{\text{SM}}^{(\prime)}$ models and a non-redundant set can be found in Ref. [23].

depends on the VLQ masses of representations $F_{m,n}$. The couplings Λ_{ij}^m are

$$\begin{aligned}\Lambda_{ij}^m &= (\lambda_i^m)^* \lambda_j^m & \text{for} & & F_m = D, T_d, T_u, \\ \Lambda_{ij}^m &= \lambda_i^m (\lambda_j^m)^* & \text{for} & & F_m = Q_d, Q_V.\end{aligned}\quad (29)$$

The index a of the operator and the numerical factors η_{mn} are collected in Table 4. Note that $a = \text{VLL}$ for $F_{m,n} = D, T_d, T_u$, and $a = \text{VRR}$ for $F_{m,n} = Q_d, Q_V$, whereas $a = \text{LR1}$ for $F_m = D, T_d, T_u$ and $F_n = Q_d, Q_V$. The factors η_{mn} are positive except for interference of $F_m = D, Q_d, T_d$ with $F_n = Q_V, T_u$, because in this case the scalar propagators are crossed, which gives rise to an additional sign w.r.t. the diagram with non-crossed scalar propagators. For $F_m = F_n$, these results agree with [11] for D, T_u, T_d , but for Q_d (model XI) we find an additional factor of 2. Concerning Q_V (model IX) we find a contribution to $\sim O_{\text{VRR}}$ instead of $\sim O_{\text{VLL}}$ and also opposite sign. For completeness we provide also the results for $F_m \neq F_n$.

(F_m, F_n)	D	Q_d	Q_V	T_d	T_u
D	VLL, +1/8	LR1, +1/4	LR1, -1/4	VLL, +1/16	VLL, -1/8
Q_d		VRR, +1/4	VRR, -1/4	LR1, +3/8	LR1, -3/8
Q_V			VRR, +1/4	LR1, -3/8	LR1, +3/8
T_d				VLL, +5/32	VLL, -1/8
T_u					VLL, +5/32

Table 4: The index $a = \text{VLL}, \text{VRR}, \text{LR1}$ appearing in Eq. (27) for representations (F_m, F_n) , followed by corresponding η_{mn} .

In $G'_{\text{SM}}(S)$ models we consider only VLQs D and Q_V and their interference

$$\begin{aligned}D : \quad \mathcal{C}_{\text{VRR}} &= \frac{1}{(4\pi)^2} \frac{(\lambda_i^D \lambda_j^{D*})^2}{\mathcal{N}_{ij}} \frac{1}{8M_D^2}, \\ Q_V : \quad \mathcal{C}_{\text{VLL}} &= \frac{1}{(4\pi)^2} \frac{(\lambda_i^V \lambda_j^{V*})^2}{\mathcal{N}_{ij}} \frac{1}{8M_V^2}, \\ D \times Q_V : \quad \mathcal{C}_{\text{LR1}} &= -\frac{1}{(4\pi)^2} \frac{(\lambda_i^D \lambda_j^{D*})(\lambda_i^V \lambda_j^{V*})}{\mathcal{N}_{ij}} \frac{f_1(M_D, M_V)}{4},\end{aligned}\quad (30)$$

which agrees with [9] except for a minus sign from crossed scalar propagators in the interference term $D \times Q_V$.

The results for $G'_{\text{SM}}(\Phi)$ models can be found straight-forwardly from the ones of the G_{SM} models, bearing in mind that (8) and (10) are equivalent up to the replacement $H \rightarrow \Phi$.

3.3 Renormalisation group evolution

The VLQ tree-level exchange generates only $\psi^2\varphi^2 D$ - and $\psi^2\varphi^3$ -type operators at the scale μ_M . The RG evolution from μ_M down to μ_{EW} affects firstly SM couplings, such as the

quartic Higgs coupling and quark-Yukawa couplings [24], and secondly via operator mixing also dimension-six Wilson coefficients at μ_{EW} . The quartic Higgs coupling is irrelevant for the processes discussed below and the quark masses are determined from low-energy experiments, i.e. much below μ_M . Potentially large enhancements appear if the ADM is proportional to the top-Yukawa coupling y_t or the strong coupling α_s . We neglect the y_t -contributions, because they appear only in self-mixing [25], where they are suppressed w.r.t the leading term in (16).

The LL RGE of $|\Delta F| = 2$ Wilson coefficients from QCD only [30] is given as

$$\begin{aligned} \mathcal{C}_{\text{VLL,VRR}}(\mu_{\text{EW}}) &= \eta_6^{2/7} \mathcal{C}_{\text{VLL,VRR}}(\mu_M), \\ \mathcal{C}_{\text{LR},1}(\mu_{\text{EW}}) &= \eta_6^{1/7} \mathcal{C}_{\text{LR},1}(\mu_M), \\ \mathcal{C}_{\text{LR},2}(\mu_{\text{EW}}) &= \frac{2}{3} \left(\eta_6^{1/7} - \eta_6^{-8/7} \right) \mathcal{C}_{\text{LR},1}(\mu_M) + \eta_6^{-8/7} \mathcal{C}_{\text{LR},2}(\mu_M), \end{aligned} \quad (31)$$

with $N_f = 6$ denoting the number of active quark flavours and $\eta_6 = \alpha_s^{(6)}(\mu_M)/\alpha_s^{(6)}(\mu_{\text{EW}})$. The initial conditions of $\mathcal{C}_a^{ij}(\mu_M)$ are collected in (27) and (30). Note that $\mathcal{C}_{\text{LR},2}(\mu_M) = 0$, and $\mathcal{C}_{\text{LR},1}(\mu_M) \neq 0$ only in the presence of several VLQ representations.

4 Implications for the down-quark sector

In the previous section the decoupling of the VLQs at tree-level and for $|\Delta F| = 2$ at one-loop level at the scale μ_M has been presented, including the most important effects from the RG evolution down to the electroweak scale μ_{EW} . In this section we discuss the decoupling of degrees of freedom of the order of μ_{EW} by matching onto phenomenological $|\Delta F| = 1, 2$ EFTs. In the G_{SM} -models these are the W and Z bosons, the top-quark and the standard Higgs h^0 that are all in the mass range $\mu_{\text{EW}} \in [80, 180]$ GeV. In G'_{SM} models additional Z' and scalars are present, which we allow to be heavier up to the ~ 1 TeV range. For the purpose of the decoupling, however, we ignore this hierarchy with the heavy standard sector ~ 100 GeV.

In our analysis we will frequently use general formulae for flavour observables in models with tree-level neutral gauge boson exchanges that are collected in [31]. These formulae were given in terms of the so-called master one-loop functions which have been already used before in many concrete extensions of the SM, see [32] for a review. Therefore our task is to calculate NP contributions to these functions in the VLQ models using the results obtained in the previous section. To this end it will be useful to adopt the notations of [31, 32].

We define the relevant CKM factors by⁵

$$\lambda_{ij}^{(U)} = V_{Ui}^* V_{Uj} \quad \text{with} \quad U \in \{u, c, t\} \quad \text{and} \quad i, j \in \{d, s, b\}. \quad (32)$$

We introduce further

$$g_{\text{SM}}^2 = 4 \frac{G_F^2 M_W^2}{2\pi^2} = 1.78137 \times 10^{-7} \text{ GeV}^{-2}. \quad (33)$$

⁵This notation differs sufficiently from the one for Yukawa couplings λ_i so that there should not be any problem in distinguishing them.

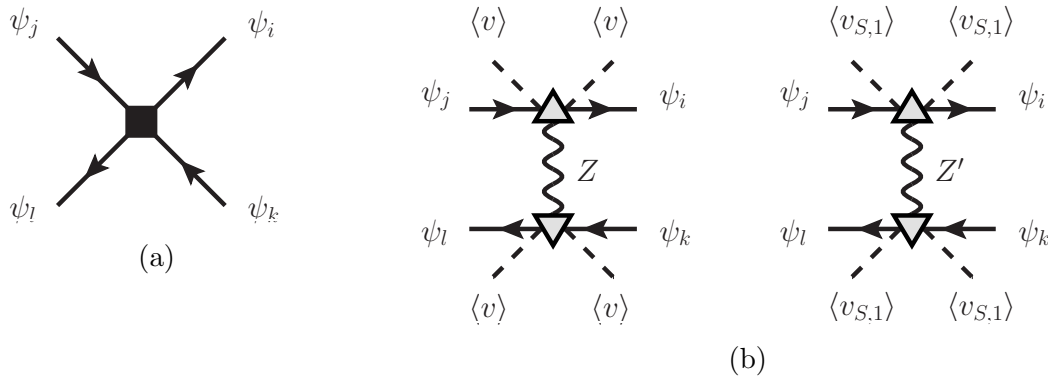


Figure 3: Fig. 3a shows flavour-changing four-quark transitions in the $G_{\text{SM}}^{(\prime)}$ -EFT that are mediated by local ψ^4 -operators, generated at the scale μ_M at one-loop level (indicated by the filled square). Fig. 3b shows contributions from double insertions of $\psi^2\varphi^2D$ -operators via intermediate Z or Z' exchange, which are formally of higher power, but are generated by tree-level VLQ exchange (indicated by the triangles).

The relevant master functions in the SM are

$$S_0(x_t), \quad X_0(x_t), \quad Y_0(x_t), \quad Z_0(x_t). \quad (34)$$

They are *flavour universal* and *real valued*. For completeness their explicit expressions can be found in the appendices. In the considered VLQ models new contributions not only break flavour universality, but also bring in new CP-violating phases, so that minimal flavour violation (MFV) is violated.

4.1 $|\Delta F| = 2$

The Wilson coefficients⁶ of $|\Delta F| = 2$ operators governing neutral kaon and B_q -meson mixing ($q = d, s$), defined in Appendix B.1, can receive at the scale μ_{EW} several contributions depicted in Fig. 3, depending on the model. Firstly, there are the local contributions, Fig. 3a, from the 1-loop decoupling presented in Section 3.2, which are formally of order v^2/M^2 , but one-loop suppressed. Secondly, there are double-insertions of flavour-changing $Z^{(\prime)}$ couplings, Fig. 3b, that count due to the double insertion formally as v^4/M^4 , but are generated already at tree-level. Thirdly, when considering several VLQ representations also double-insertions of $\psi^2\varphi^3$ -type operators [3], generating flavour-changing neutral Higgs exchange, can contribute in analogy to Fig. 3b when replacing the $Z^{(\prime)}$ by h^0 . As a consequence in this case also non-vanishing contributions can arise to the operators $O_{S\chi\chi,1}$ with $\chi = L, R$ and $O_{\text{LR},2}$ [29].

Unless we consider several VLQ representations simultaneously, new physics contributions involve only the operators O_{VLL}^{ij} and O_{VRR}^{ij} . They obey the same RG evolution (31) — with appropriate change of number of active quark flavours $N_f = 6 \rightarrow 5$ — and enter the M_{12} element of the mass-mixing matrix as the linear combination

$$[C_{\text{VLL}}^{ij} + C_{\text{VRR}}^{ij}] (\mu_{\text{EW}}) \equiv S_{ij} = S_0(x_t) + \Delta S_{ij} \quad (35)$$

⁶See footnote 2.

with ΔS_{ij} denoting VLQ contributions. The SM contribution is given at LO by $S_0(x_t)$, see (84). We have

$$\Delta S_{ij} = [\Delta S_{ij}]_{\text{VLL}} + [\Delta S_{ij}]_{\text{VRR}}, \quad (36)$$

although in a given model only one of these contributions is present. If two different models containing LH and RH couplings are combined then the most important in $|\Delta F| = 2$ transitions are not these two operators but $O_{\text{LR},1}^{ij}$ and $O_{\text{LR},2}^{ij}$.

The $[\Delta S_{ij}]_{\text{V}\chi\chi}$ with $\chi = L, R$ include quite generally box diagrams with VLQs and scalar exchanges as well as tree-level Z and Z' contributions. We can therefore write

$$[\Delta S_{ij}]_{\text{V}\chi\chi} = \mathcal{C}_{\text{V}\chi\chi}^{ij}(\mu_{\text{EW}}) + \frac{4r_Z}{g_{\text{SM}}^2 M_Z^2} \left[\frac{\Delta_\chi^{ij}(Z)}{\lambda_{ij}^{(t)}} \right]^2 + \frac{4r_{Z'}}{g_{\text{SM}}^2 M_{Z'}^2} \left[\frac{\Delta_\chi^{ij}(Z')}{\lambda_{ij}^{(t)}} \right]^2, \quad (37)$$

where $\mathcal{C}_{\text{V}\chi\chi}^{ij}(\mu_{\text{EW}})$ are given in (31). The r_V for $V = Z, Z'$ are NLO QCD corrections⁷ to Fig. 3b from decoupling of the V boson at the scale $\mu = \mu_{\text{EW}}$ [34], Note the model-dependence of the factors $\Delta_\chi^{ij}(Z)$ and $\Delta_\chi^{ij}(Z')$, given in Table 2 and Table 3, and the different dependence on the VLQ mass of these factors and $\mathcal{C}_{\text{V}\chi\chi}^{ij}(\mu_{\text{EW}})$.

When two or more representations are considered, also LR and SLL (SRR) operators contribute in principle. The Wilson coefficients of LR operators receive generally contributions from box diagrams and tree-level $Z^{(\prime)}$ exchanges, whereas SLL (SRR) and LR,2 from tree-level h^0 exchange. The results for all box contributions $\mathcal{C}_{\text{LR},1}^{ij}$ are given in formulae (27) and (30) and the RG evolution in (31). Adding the Z - and Z' -contributions, one arrives at

$$\mathcal{C}_{\text{LR},1}^{ij}(\mu_{\text{EW}}) = \mathcal{C}_{\text{LR},2}^{ij}(\mu_{\text{EW}}) + \frac{1}{\mathcal{N}_{ij}} \left[\frac{\Delta_L^{ij}(Z)\Delta_R^{ij}(Z)}{M_Z^2} + \frac{\Delta_L^{ij}(Z')\Delta_R^{ij}(Z')}{M_{Z'}^2} \right], \quad (38)$$

$$\mathcal{C}_{\text{LR},2}^{ij}(\mu_{\text{EW}}) = \mathcal{C}_{\text{LR},2}^{ij}(\mu_{\text{EW}}),$$

with the couplings $\Delta_\chi^{ij}(Z^{(\prime)})$ ($\chi = L, R$) collected in Table 2 and Table 3. \mathcal{N}_{ij} is defined in (82).

The RG evolution from μ_{EW} to m_b is done at NLL accuracy for the SM contribution and LL accuracy for the VLQ contribution.

4.2 $|\Delta F| = 1$: Semi-leptonic $d_j \rightarrow d_i + (\ell\bar{\ell}, \nu\bar{\nu})$

Semileptonic decays in the down-quark sector receive in VLQ models contributions via the Z and Z' tree-level exchanges depicted in Fig. 4a. They lead to modifications of the Wilson coefficients of the corresponding phenomenological EFTs of $d_j \rightarrow d_i \nu\bar{\nu}$ and $d_j \rightarrow d_i \ell\bar{\ell}$ decays given in Appendix B.2 and Appendix B.3, respectively. All Wilson coefficients in this section are formally at μ_{EW} , but since the corresponding operators are conserved currents under QCD, the RG evolution to the scale μ_b is trivial in all cases.⁸

⁷Since we decouple Z and Z' simultaneously at $\mu_{\text{EW}} \sim M_Z$, we do not resum logarithms between scales $M_{Z'}$ and μ_{EW} as for example in Ref. [33].

⁸The usual mixing of Q_9 operators with current-current operators $Q_{1,2}$ present in the SM and affecting C_9 coefficient is fully negligible here because NP contributions to $C_{1,2}$ are tiny in all models.

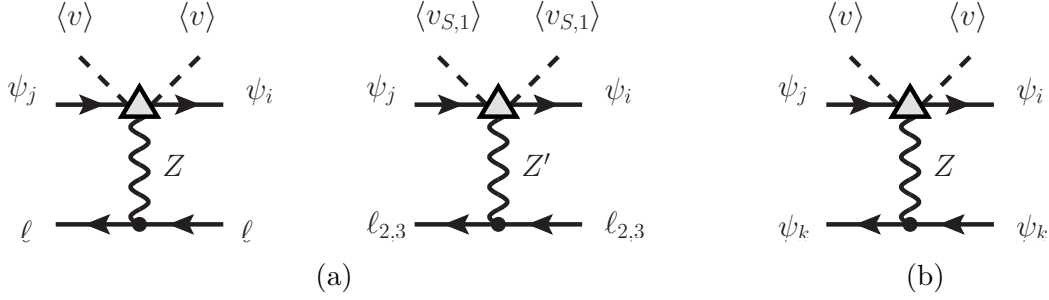


Figure 4: Flavour-changing $\Delta F = 1$ processes that are mediated in the $G_{\text{SM}}^{(\prime)}$ -EFTs by dimension six $\psi^2 \varphi^2 D$ -operators (indicated by the triangle), which are in turn generated at the scale μ_M at tree level. Semileptonic transitions $\psi_j \rightarrow \psi_i \ell \bar{\ell}$ in Fig. 4a can be mediated by both Z and Z' exchange, depending on the model. Not shown are analogous transitions $\psi_j \rightarrow \psi_i \nu \bar{\nu}$. Note that the Z' couples only to the second and third generations of leptons and neutrinos. Hadronic transitions $\psi_j \rightarrow \psi_i \psi_k \bar{\psi}_k$ in Fig. 4b are mediated only by Z exchange, with $\psi = (q_L, u_R, d_R)$, depending on the operator.

The $V = Z, Z'$ contributions modify the Wilson coefficients and one-loop functions

$$C_{L(R)}^{ij,\nu} = - \sum_V \frac{X_{L(R)}^{ij,\nu}(V)}{s_W^2}, \quad X_{L(R)}^{ij,\nu}(V) = \frac{\Delta_L^{\nu\bar{\nu}}(V)}{g_{\text{SM}}^2 M_V^2} \frac{\Delta_{L(R)}^{ij}(V)}{\lambda_{ij}^{(t)}}, \quad (39)$$

which enter the expressions for $d_j \rightarrow d_i \nu \bar{\nu}$ decays like $K^+ \rightarrow \pi^+ \nu \bar{\nu}$, $K_L \rightarrow \pi^0 \nu \bar{\nu}$ and also $B \rightarrow K^{(*)} \nu \bar{\nu}$ with more details in Appendix B.2.

The Wilson coefficients of the operators entering the $d_j \rightarrow d_i \ell \bar{\ell}$ transitions receive the following contributions

$$C_{9(9')}^{ij,\ell} = - \sum_V \frac{[\Delta_R^{\ell\bar{\ell}}(V) + \Delta_L^{\ell\bar{\ell}}(V)]}{s_W^2 g_{\text{SM}}^2 M_V^2} \frac{\Delta_{L(R)}^{ij}(V)}{\lambda_{ij}^{(t)}}, \quad (40)$$

$$C_{10(10')}^{ij,\ell} = - \sum_V \frac{[\Delta_R^{\ell\bar{\ell}}(V) - \Delta_L^{\ell\bar{\ell}}(V)]}{s_W^2 g_{\text{SM}}^2 M_V^2} \frac{\Delta_{L(R)}^{ij}(V)}{\lambda_{ij}^{(t)}}, \quad (41)$$

where the leptonic Z couplings are taken to be the ones of the SM except for $G'_{\text{SM}}(\Phi)$ models, where $Z - Z'$ mixing is included following (24). There are no Z' contributions to $C_{10(10')}$, as the lepton couplings are vectorial, see (23).

The purely leptonic decay $K_L \rightarrow \mu \bar{\mu}$ is described by ($\bar{s} \rightarrow \bar{d}$)

$$Y_A(K) = Y_L^{\text{SM}} + \frac{[\Delta_R^{\mu\bar{\mu}}(Z) - \Delta_L^{\mu\bar{\mu}}(Z)]}{g_{\text{SM}}^2 M_Z^2} \left[\frac{\Delta_L^{sd}(Z) - \Delta_R^{sd}(Z)}{\lambda_{sd}^{(t)}} \right], \quad (42)$$

with $Y_L^{\text{SM}} = 0.942$ [35].

4.3 $|\Delta F| = 1$: Hadronic $d_j \rightarrow d_i q \bar{q}$ and ε'/ε

Purely hadronic flavour-changing decays $d_j \rightarrow d_i q \bar{q}$ receive in the considered VLQ models predominantly contributions from Z exchange depicted in Fig. 4b. Other contributions

from scalar boxes, Fig. 3a, or double-insertions of Z or Z' exchange in Fig. 3b are either loop- or power-suppressed. The phenomenological EFT of these transitions is given in Appendix B.4. Since the flavour-diagonal Z couplings are given by the SM ones, no dependence on q arises to the order we are working in. The non-vanishing contributions to the $|\Delta F| = 1$ Wilson coefficients are conveniently rewritten as NP contributions to the Inami-Lim Z -penguin function C (see Appendices B.2 and B.3)

$$C_{L(R)}^{ij} = -\frac{g_Z}{2g_{\text{SM}}^2 M_Z^2} \frac{\Delta_{L(R)}^{ij}(Z)}{\lambda_{ij}^{(u)}}. \quad (43)$$

It contributes at the scale μ_{EW} to the Wilson coefficients of the QCD- and EW-penguin operators [36],

$$C_{3(5')}^{ij} = \frac{\alpha}{6\pi} \frac{C_{L(R)}^{ij}}{s_W^2}, \quad C_{7(9')}^{ij} = \frac{\alpha}{6\pi} 4C_{L(R)}^{ij}, \quad C_{9(7')}^{ij} = -\frac{\alpha}{6\pi} \frac{c_W^2}{s_W^2} 4C_{L(R)}^{ij}. \quad (44)$$

The RG evolution induces also non-vanishing contributions for the remaining QCD- and EW-penguin operators at lower scales relevant for Kaon and B -meson decays. Here we are mainly interested in CP violation in the Kaon sector, especially ε'/ε .

It is known from various analyses of ε'/ε , see [36] and references therein, that NP has to generate contributions to the Wilson coefficients of $O_8 \propto (V-A) \otimes (V+A)$ or $O'_8 \propto (V+A) \otimes (V-A)$ operators at the low energy scale in order to be able to modify significantly the SM predictions. This requires the presence of both LH flavour-violating couplings and RH flavour-diagonal couplings of Z or Z' in the case of O_8 , or RH flavour-violating couplings and LH flavour-diagonal couplings in the case of O'_8 . But in the models considered quark couplings of the Z' are either LH or RH, hence such contributions can only be generated as a higher-order effect. Given that $(V-A)$ and $(V+A)$ flavour-diagonal Z couplings to SM quarks are always present, tree-level Z exchanges fully dominate. NP contributions to $O_{9,10} \propto (V-A) \otimes (V-A)$ or $O'_{9,10} \propto (V+A) \otimes (V+A)$ operators are negligible due to their suppressed hadronic matrix elements relative to the ones of O_8 and O'_8 . This can be clearly seen in the semi-numeric expression (109) for ε'/ε , where the coefficients of $C_7^{(\prime)}$, which mixes into $C_8^{(\prime)}$, is largely enhanced w.r.t. all others. Whether O_8 or O'_8 is generated depends on whether a given model has $(V-A)$ or $(V+A)$ flavour-violating couplings:

- Within the G_{SM} - and $G'_{\text{SM}}(\Phi)$ -models, the pattern of NP contributions to ε'/ε is as follows

$$\begin{aligned} \text{singlets : } & D \quad \rightarrow \quad (O_8), \\ \text{doublets : } & Q_V, Q_d \rightarrow (O'_8), \\ \text{triplets : } & T_d, T_u \rightarrow (O_8). \end{aligned} \quad (45)$$

- In $G'_{\text{SM}}(S)$ -models ε'/ε remains SM-like, which could become problematic as we discuss briefly below.

Tree-level Z contributions to ε'/ε have been recently considered in detail in Ref. [36], where explicit expressions for the relevant hadronic matrix elements $\langle Q_8(m_c) \rangle_2$ and $\langle Q'_8(m_c) \rangle_2$

can be found. Whereas these matrix elements differ only by sign from each other, their Wilson coefficients differ also in magnitude, the one of Q'_8 being larger by a factor of $c_W^2/s_W^2 = 3.33$. This can also be seen in Eq. (44), remembering that the Wilson coefficients of Q_8 and Q'_8 at $\mu = m_c$ are directly related to the Wilson coefficients of Q_7 and Q'_7 at μ_{EW} , respectively.

The status of ε'/ε in the SM can be summarized as follows. The RBC-UKQCD lattice collaboration calculating hadronic matrix elements of all operators, but not including isospin-breaking effects, finds [17, 37]

$$(\varepsilon'/\varepsilon)_{\text{SM}} = (1.38 \pm 6.90) \times 10^{-4} \quad (\text{RBC} - \text{UKQCD}). \quad (46)$$

Using the hadronic matrix elements of QCD- and EW-penguin $(V-A) \otimes (V+A)$ operators from RBC-UKQCD lattice collaboration [17, 37] but extracting the matrix elements of $(V-A) \otimes (V-A)$ -penguin operators from the CP-conserving $K \rightarrow \pi\pi$ amplitudes and including isospin breaking effects, one finds [18]

$$(\varepsilon'/\varepsilon)_{\text{SM}} = (1.9 \pm 4.5) \times 10^{-4} \quad (\text{BGJJ}). \quad (47)$$

This result differs by 2.9σ from the experimental world average from the NA48 [38] and KTeV [39, 40] collaborations,

$$(\varepsilon'/\varepsilon)_{\text{exp}} = (16.6 \pm 2.3) \times 10^{-4}, \quad (48)$$

suggesting that models providing enhancement of ε'/ε are favoured. A new analysis in Ref. [20] confirms these findings

$$(\varepsilon'/\varepsilon)_{\text{SM}} = (0.96 \pm 4.96) \times 10^{-4} \quad (\text{KNT}). \quad (49)$$

These results are supported by upper bounds on the matrix elements of the dominant penguin operators from the large- N_c dual-QCD approach [19, 41], which allows to derive an upper bound on ε'/ε [18],

$$(\varepsilon'/\varepsilon)_{\text{SM}} \leq (8.6 \pm 3.2) \times 10^{-4}, \quad (50)$$

still 2σ below the experimental data. In particular it has been demonstrated in Ref. [41] that final state interactions are much less relevant for ε'/ε than previously claimed in Refs. [42–49]. These findings diminish significantly hopes that improved lattice QCD calculations will be able to bring the SM prediction for ε'/ε to agree with the experimental data in (48), motivating additionally to search for NP models capable of alleviating this tension.

In fact it has been demonstrated that in general models with flavour-changing Z and Z' exchanges [36, 50], in the Littlest Higgs model with T -parity [51], 331 models [52, 53] and supersymmetric models [54–56] agreement with the data for ε'/ε can be obtained, with interesting implications for other flavour observables.

We will see in Section 6 that also in VLQ models large NP contributions to ε'/ε are possible, such that agreement with the data in (48) can be obtained with a significant impact not only on rare K decays but also B decays.

5 Patterns of flavour violation

Our analysis involves three model variants G_{SM} , $G'_{\text{SM}}(S)$ and $G'_{\text{SM}}(\Phi)$, with up to five VLQ representations. In this section we describe the patterns of flavour violation in $|\Delta F| = 1, 2$ FCNC processes in the Kaon and $B_{d,s}$ -meson sectors that can be expected in these models, based on our results in Sections 3 and 4. The quantitative phenomenology depends in addition to the NP parameters on the CKM and hadronic ones and will be discussed in the next section. However, on the basis of the information collected so far, some general patterns of flavour violation emerge and it is possible to state whether in a given model relevant NP contributions to a given observable can be expected. We hope that the collection of observations below will be useful in monitoring the numerical analysis of the next section.

5.1 $|\Delta F| = 2$

In all models local VLQ contributions to $|\Delta F| = 2$ operators are generated at the VLQ-scale μ_M via one-loop box diagrams. The contributions from tree-level exchanges of Z and Z' at the scale μ_{EW} are power-suppressed due to the hierarchy (14) and should be therefore numerically subleading, at least for large VLQ masses. This property decouples $|\Delta F| = 1$ and $|\Delta F| = 2$ contributions to some extent, rendering it easier to accommodate potential tensions [57, 58] in $\Delta F = 2$ processes.

The $|\Delta F| = 2$ box contributions given in Eq. (27) and (30) depend only on the VLQ mass(es) M and their Yukawa couplings λ_i^{VLQ} , but neither on the gauge couplings nor on the scalar sector. Moreover for a given VLQ-representation, they are equal in G_{SM} and $G'_{\text{SM}}(\Phi)$ models owing to the equality of (8) and (10) upon $H \leftrightarrow \Phi$. Hence the measurements of $|\Delta F| = 2$ observables will result for a given M in the very same constraints on λ_i^{VLQ} in both G_{SM} and $G'_{\text{SM}}(\Phi)$ models.

Using (37), the relative size of box-to- Z exchange in G_{SM} and $G'_{\text{SM}}(\Phi)$ models is

$$\frac{(\Delta S)_{\text{Box}}}{(\Delta S)_Z} = a \eta_{LL} \frac{g_Z^2}{8\pi^2} \left[\frac{\eta_6^{2/7}}{r_Z} \right] \frac{M^2}{M_Z^2} \times \begin{cases} 1 & G_{\text{SM}} \\ c_\beta^{-4} & G'_{\text{SM}}(\Phi) \end{cases}, \quad (51)$$

with η_{LL} collected in Table 4, $r_Z \approx 1$, and $a = 4$ for T_d and unity otherwise. While the Z contribution is comparable to the box contribution for $M \approx 1 - 2$ TeV, it amounts only to a few percent for $M = 10$ TeV in G_{SM} models, whereas in $G'_{\text{SM}}(\Phi)$ models the Z -contributions are suppressed by c_β^4 . In $G'_{\text{SM}}(\Phi)$ models we have

$$\frac{(\Delta S)_{Z'}}{(\Delta S)_Z} = (r')^2 \left[\frac{r_{Z'}}{r_Z} \right] \frac{M_Z^2}{M_{Z'}^2}, \quad G'_{\text{SM}}(\Phi) \quad (52)$$

with $r_{Z'} \approx r_Z \approx 1$. Therefore Z exchange might be more important w.r.t. the Z' contribution for $M_Z < M_{Z'}$, depending on r' , see (26) but both are suppressed w.r.t. the box contribution.

In the $G'_{\text{SM}}(S)$ models the same picture holds qualitatively, however a Z -exchange is absent and the relative size of box-to- Z' exchange is different,

$$\frac{(\Delta S)_{\text{Box}}}{(\Delta S)_{Z'}} = \frac{(Xg')^2}{(4\pi)^2} \left[\frac{\eta_6^{2/7}}{r_{Z'}} \right] \frac{M^2}{M_{Z'}^2}, \quad G'_{\text{SM}}(S) \quad (53)$$

which for $X = 1$ reduces to the result in Ref. [9]. In contrast to G_{SM} and $G'_{\text{SM}}(\Phi)$ models, we note the particular structure of Z' couplings, not being suppressed by $M_Z^2/M_{Z'}^2$. A lower bound on $|X|v_S = M_{Z'}/g' \gtrsim 750$ GeV exists in $G'_{\text{SM}}(S)$ models, mainly from a combination of $Z \rightarrow 4\mu$ and the neutrino trident production [9]. This implies that only for $M \gtrsim 9$ TeV the ratio $(\Delta S)_{\text{Box}}/(\Delta S)_{Z'} \gtrsim 1$ and shows the numerical importance of the Z' contributions, unless one considers much larger VLQ masses.

The $|\Delta F| = 2$ observables are not sensitive to the chirality of the VLQ interactions as long as only one VLQ representation is present, because the contributions are additive as can be seen in Eq. (36).

5.2 $|\Delta F| = 1$

In semi-leptonic $|\Delta F| = 1$ processes governed by $d_j \rightarrow d_i + (\ell\bar{\ell}, \nu\bar{\nu})$, the VLQ contributions arise from tree-level Z exchange in G_{SM} models, Z' exchange in $G'_{\text{SM}}(S)$ models and both in $G'_{\text{SM}}(\Phi)$ models.

It is instructive to begin the discussion with $G'_{\text{SM}}(S)$ models considered already in Ref. [9], as they involve only Z' contributions to $\Delta F = 1$ processes and the leptonic Z' couplings have a special structure as given in Eq. (23). Moreover, as pointed out in that paper, the $|\Delta F| = 1$ contributions of VLQs in these models are independent of the scalar- and gauge-sector parameters, in contrast to $|\Delta F| = 2$ contributions that depend on v_S . We find the following pattern in NP contributions:

- Due to the equality of the LH and RH Z' couplings to leptons in (23), Z' exchange does neither contribute to $B_{s,d} \rightarrow \mu\bar{\mu}$ nor to $K_L \rightarrow \mu\bar{\mu}$. If future improved data will show the need for NP contributions to $B_{s,d} \rightarrow \mu\bar{\mu}$, this will be a problem for this scenario.
- The crucial virtue of $G'_{\text{SM}}(S)$ models, pointed out in [9], is the possibility of solving the LHCb anomalies; in particular, they can accommodate violation of lepton-flavour universality (LFU).
- In $B \rightarrow K(K^*)\nu\bar{\nu}$ only small contributions are possible due to cancellations among muon and tau contributions when averaging over neutrino flavours as a consequence of the $U(1)_{L_\mu-L_\tau}$ symmetry.
- These cancellations are less efficient in $K^+ \rightarrow \pi^+\nu\bar{\nu}$ due to interference with the charm component, see Appendix B.2.

Considering next G_{SM} and $G'_{\text{SM}}(\Phi)$ models in which tree-level Z contributions to $\Delta F = 1$ processes dominate, the most notable feature comes from the tree-level decoupling of the VLQs depicted in Fig. 1b, which implies a relationship between the flavour-changing Z and Z' couplings in these models, again owing to the equality of (8) and (10) upon $H \leftrightarrow \Phi$. Below the scale μ_M in both models a $\psi^2\varphi^2 D$ operator is generated, with the same Wilson coefficient, where $\varphi = H, \Phi$ in G_{SM} and $G'_{\text{SM}}(\Phi)$ models, respectively. The covariant derivative is the same in both models, up to the additional $U(1)_{L_\mu-L_\tau}$ part in $G'_{\text{SM}}(\Phi)$ models. Upon spontaneous symmetry breaking at the scale μ_{EW} , this operator becomes $\propto v^2$ in G_{SM} models and $\propto v_1^2 = c_\beta^2 v^2$ in $G'_{\text{SM}}(\Phi)$ models. Consequently, in

$G'_{\text{SM}}(\Phi)$ models all Z and Z' couplings $\propto c_\beta^2 \Delta^{ij}$ are suppressed by $c_\beta^2 = (1 + \tan^2 \beta)^{-1}$ w.r.t. Z couplings $\propto \Delta^{ij}$ in G_{SM} models, see (25), (22) and Table 3.

Note that the additional modifications from $Z - Z'$ mixing in $G'_{\text{SM}}(\Phi)$ models do not affect the dependence on the λ_i^{VLQ} . The suppression by c_β^2 can be only softened by going to very small $\tan \beta$. In order to guarantee perturbativity of the top-quark Yukawa coupling $0.3 \lesssim \tan \beta$ [59]. In Appendix A.2 we discuss further constraints on $\tan \beta$ in $G'_{\text{SM}}(\Phi)$ models from the measured Z mass and partial widths to leptons, which for $M_Z < M_{Z'}$ allow at most $2 \lesssim \tan \beta$, *i.e.* $c_\beta^2 \lesssim 0.2$. Depending on the choice of g' and v_S , this bound becomes even stronger. Therefore, VLQ effects in $|\Delta F| = 1$ FCNC processes are generically suppressed in $G'_{\text{SM}}(\Phi)$ models w.r.t. G_{SM} models. As an example one might consider the Wilson coefficient C_9^{ij} given in (40), governing $d_j \rightarrow d_i \ell \bar{\ell}$. The suppression factor in $G'_{\text{SM}}(\Phi)$ versus G_{SM} models is

$$\frac{(C_9^{ij})_{G'_{\text{SM}}(\Phi)}}{(C_9^{ij})_{G_{\text{SM}}}} = c_\beta^2 \left[1 - r' \xi_{ZZ'} - \frac{g'}{g_Z} \frac{4Q'_\ell}{(1 - 4s_W^2)} \xi_{ZZ'} - \frac{g'}{g_Z} \frac{4Q'_\ell}{(1 - 4s_W^2)} \frac{M_Z^2}{M_{Z'}^2} \right]. \quad (54)$$

The mixing angle $\xi_{ZZ'} \sim M_Z^2/M_{Z'}^2$ is small in most of the parameter space, such that $(1 - 4s_W^2)^{-1} \sim 10$ is overcompensated. The comparison of the first three terms with the last one in the brackets also shows the relative size of the Z' to Z contribution in $G'_{\text{SM}}(\Phi)$ models, which is also suppressed by $M_Z^2/M_{Z'}^2$. Consequently VLQ contributions to semileptonic $|\Delta F| = 1$ FCNC decays are in most cases suppressed in $G'_{\text{SM}}(\Phi)$ w.r.t. G_{SM} models.

However, there are exceptions related to the fact that with the parametric suppression of the Z and Z' couplings, the values of Yukawa couplings are weaker constrained by $\Delta F = 1$ transitions than in G_{SM} models and the constraints on Yukawas are governed this time by $\Delta F = 2$ processes. A detailed numerical analysis in the next section then shows that NP effects in ΔM_K turn out in fact significantly larger than in G_{SM} models.

For a given flavour-changing transition the correlations between different $|\Delta F| = 1$ observables depend on whether $Z^{(\prime)}$ have LH or RH flavour-violating quark couplings and the size of the corresponding leptonic $Z^{(\prime)}$ couplings. A summary is given in Table 5, where in addition to G_{SM} and $G'_{\text{SM}}(\Phi)$ models we include $G'_{\text{SM}}(S)$ models discussed already above. The generically small NP contributions in $C_9^{(\prime)ij,\ell}$ compared to $C_{10}^{(\prime)ij,\ell}$ and $C_{L(R)}^{ij,\nu}$ in G_{SM} models are due to the smallness of leptonic vector Z couplings relative to the axial-vector ones. The additional generic suppression of NP effects in $G'_{\text{SM}}(\Phi)$ w.r.t. G_{SM} is due to the aforementioned suppression by c_β^2 .

We observe that in G_{SM} models significant NP effects in $K^+ \rightarrow \pi^+ \nu \bar{\nu}$, $K_L \rightarrow \pi^0 \nu \bar{\nu}$, $B_{s,d} \rightarrow \mu \bar{\mu}$, $B \rightarrow K^{(*)} \mu \bar{\mu}$ and $B \rightarrow K^{(*)} \nu \bar{\nu}$ are possible, but the LHCb anomalies in angular observables in $B \rightarrow K^* \mu \bar{\mu}$ cannot be explained in these models because the vector coupling of Z to muons is suppressed by $(1 - 4s_W^2) \sim 0.1$ w.r.t. the axial-vector coupling of the Z . LFU of Z couplings precludes also the explanation of the violation of this universality in R_K , hinted at by LHCb data.

Due to the particular structure of Z' couplings, the general pattern of NP contributions to $K^+ \rightarrow \pi^+ \nu \bar{\nu}$, $K_L \rightarrow \pi^0 \nu \bar{\nu}$, $B_{s,d} \rightarrow \mu^+ \mu^-$, $B \rightarrow K^{(*)} \mu^+ \mu^-$ and $B \rightarrow K^{(*)} \nu \bar{\nu}$ in $G'_{\text{SM}}(\Phi)$ models is dominated by tree-level Z contributions as in G_{SM} models, but because of the aforementioned suppression by c_β^2 these contributions are smaller, with few exceptions mentioned above, than in the latter models. On the other hand, the presence of Z' with

	G_{SM}					$G'_{\text{SM}}(S)$		$G'_{\text{SM}}(\Phi)$			
	D	Q_V	Q_d	T_d	T_u	D	Q_V	D	Q_d	T_d	T_u
$C_9^{ij,\ell}$	■	—	—	■	■	—	★	■	—	■	■
$C_9^{\prime ij,\ell}$	—	■	■	—	—	★	—	—	■	—	—
$C_{10}^{ij,\ell}$	★	—	—	★	★	—	—	*	—	*	*
$C_{10}^{\prime ij,\ell}$	—	★	★	—	—	—	—	—	*	—	—
$C_L^{ij,\nu}$	★	—	—	★	★	—	★	*	—	*	*
$C_R^{ij,\nu}$	—	★	★	—	—	★	—	—	*	—	—

Table 5: “DNA” table for NP contributions to the $b \rightarrow s\mu^+\mu^-$ Wilson coefficients $C_{9,10}^{(\prime)}$ and to the $d_j \rightarrow d_i\nu\bar{\nu}$ ones $C_{L,R}^{\nu}$. ★ means that the NP contribution is potentially large, while ■ stands for a generically small contribution, due to the suppressed vector couplings of the Z to leptons compared to its axial-vector couplings. Smaller symbols in the $G'_{\text{SM}}(\Phi)$ models indicate the general suppression by c_β^2 w.r.t. G_{SM} models.

only vector lepton couplings allows in principle to address the LHCb anomalies more easily; however, given the generic suppression of the Z' couplings, this is harder than in $G'_{\text{SM}}(S)$ models.

Hadronic $|\Delta F| = 1$ processes governed by $d_j \rightarrow d_i q\bar{q}$ receive VLQ contributions only from tree-level Z exchange in G_{SM} and $G'_{\text{SM}}(\Phi)$ models. The suppression of VLQ effects by c_β^2 in $G'_{\text{SM}}(\Phi)$ models w.r.t. G_{SM} models is the same as discussed previously for semileptonic $|\Delta F| = 1$ processes. Such contributions are entirely absent in $G'_{\text{SM}}(S)$ models and ε'/ε is generated for example in the case of $d_j \rightarrow d_i d\bar{d}$ either by Z' double insertions or via box diagrams, which are both additionally suppressed by $|\lambda_d|^2$ compared to G_{SM} models.

5.3 Determination of M

There is a common claim that from flavour-violating processes it is only possible to measure the ratio $g_{\text{NP}}/M_{\text{NP}}$, where g_{NP} is the coupling present in a given theory, while M_{NP} is the NP scale. The scale tested by a given observable is typically quoted at the value of M_{NP} when setting $g_{\text{NP}} = 1$, and correspondingly changes when the latter is suppressed by some mechanism, as in the case of MFV.

Here we would like to point out that in concrete models with correlations between $|\Delta F| = 2$ and $|\Delta F| = 1$ processes, it is possible to determine M_{NP} without making any assumptions on the couplings involved. This is in particular important if M_{NP} should turn out to be beyond the reach of direct searches at the LHC.

In the context of 331 models the relevant correlations that allow the determination of $M_{Z'}$ can be found in Section 7.2 of [33], although this point has not been made there. In order to illustrate this in the case of VLQ models we consider the G_{SM} -models assuming for simplicity that M_{VLQ} is sufficiently large for the shift ΔS in ΔM_s to be dominated by box diagrams. On the other hand, ΔY entering the branching ratio for $B_s \rightarrow \mu\bar{\mu}$ is

	G_{SM}					$G'_{\text{SM}}(S)$		$G'_{\text{SM}}(\Phi)$			
	D	Q_V	Q_d	T_d	T_u	D	Q_V	D	Q_d	T_d	T_u
$ \Delta F = 2$	★	★	★	★	★	★	★	★	★	★	★
$B_{s,d} \rightarrow \mu\bar{\mu}$	★	★	★	★	★			*	*	*	*
$B \rightarrow K\mu\bar{\mu}$	★	★	★	★	★	★	★	*	*	*	*
$B \rightarrow K^*\mu\bar{\mu}$						★	★	*	*	*	*
$B \rightarrow K(K^*)\nu\bar{\nu}$	★	★	★	★	★			*	*	*	*
$K^+ \rightarrow \pi^+\nu\bar{\nu}$	★	★	★	★	★			*	*	*	*
$K_L \rightarrow \pi^0\nu\bar{\nu}$	★	★	★	★	★						
ε'/ε	★	★	★	★	★			*	*	*	*

Table 6: “DNA” of flavour effects in VLQ models. A star indicates that significant effects in a given model and given process are in principle possible, but could be reduced (see Section 6) through correlation among several observables. Empty space means that the given model does not predict sizable effects in that observable. The star ★ indicates left-handed currents and the star ★ right-handed ones, smaller stars indicate the suppression of $|\Delta F| = 1$ decays in $G'_{\text{SM}}(\Phi)$ models.

governed by tree-level Z exchange. Then we find independently of Yukawa couplings and CKM parameters a useful formula:

$$\frac{\sqrt{(\Delta S)^*}}{\Delta Y} = 1.90 b \sqrt{\eta_{mm}} \left[\frac{M}{10 \text{ TeV}} \right], \quad (\text{Boxes}), \quad (55)$$

where η_{mm} are given in Table 4 and $b = 1$ for D and Q_V , $b = -1$ for T_u and Q_d and $b = 1/2$ for T_d . Note that ΔS and ΔY are generally complex but their phases are related so that r.h.s of this equation is real valued. Extracting ΔS and ΔY from experiment, a range for M can be determined. This formula can easily be generalized to include Z contributions if necessary, but if VLQs are not found at the LHC, the value of M is sufficiently large for the above formula to be a good approximation. On the other hand, if VLQs are discovered at the LHC, we will know their masses and this determination will not be necessary — instead, the determination of the couplings would improve. Moreover for sufficiently low M the tree-level Z contributions to $|\Delta F| = 2$ dominate and then the dependence on M in the ratio in Eq. (55) drops out not allowing to determine M in this manner.

5.4 Kaon and B -meson systems

The correlations between flavour observables in different meson systems are governed by the Yukawa structure of the model in question, as will be elaborated quantitatively in Section 6. The important property of VLQ models is that the products defined in

Eq. (29),

$$\Lambda_{ij}^m = |\Lambda_{ij}^m| e^{i\varphi_{ij}^m}, \quad (56)$$

together with the VLQ mass M determine at the same time the flavour-violating $j \rightarrow i$ couplings of Z and Z' , as well as the flavour-diagonal Z' couplings to quarks. The relevant flavour-changing parameters are hence Λ_{ds}^m in Kaon decays, and $\Lambda_{db}^m, \Lambda_{sb}^m$ in $b \rightarrow d, s$ transitions of B mesons, respectively. Since only the *relative* phases of the λ_i^{VLQ} enter the Λ_{ij}^m , the phases φ_{ij}^m fulfill the relation

$$\varphi_{bs} = \varphi_{bd} - \varphi_{sd}, \quad (57)$$

dropping index m of the VLQ representation for convenience. This leaves us with five parameters for the three complex quantities Λ_{ij} . The phases φ_{ij} can vary in the full range $[-\pi, \pi]$, implying the occurrence of discrete ambiguities when determining them from experiment, as explicitly seen in the plots in Ref. [31] and in the plots in the next section. They can be resolved using observables where interference with the SM occurs. The absolute values λ_i^{VLQ} can be determined via

$$|\lambda_d| = \sqrt{\frac{\Lambda_{bd}\Lambda_{sd}^*}{\Lambda_{bs}}}, \quad |\lambda_s| = \sqrt{\frac{\Lambda_{bs}\Lambda_{sd}}{\Lambda_{bd}}}, \quad |\lambda_b| = \sqrt{\frac{\Lambda_{bd}\Lambda_{bs}^*}{\Lambda_{sd}}}. \quad (58)$$

One might expect the strongest constraints numerically to stem from $s \rightarrow d$ processes, because of the strong suppression of the SM contribution by $V_{td}V_{ts}^*$.

In a sense, as more explicitly seen in the next section, the flavour structure of VLQ models has some parallels to the one in 331 models [33, 52, 53, 60]. However, in 331 models the NP contributions are dominated by Z' tree-level exchanges and once the constraints from $B_{s,d}$ observables are taken into account, NP effects in the K system are found to be small, with the exception of ε'/ε . In the present analysis important Z boson contributions are present and this allows for more interesting NP effects than in 331 models in $K^+ \rightarrow \pi^+\nu\bar{\nu}$ and $K_L \rightarrow \pi^0\nu\bar{\nu}$ in G_{SM} , and to lesser extent in $G'_{\text{SM}}(\Phi)$ models. This was already signalled by the analysis in Ref. [36], but having concrete models allows us to be more specific with implications for the choice of favourite VLQ models. Furthermore, the partial decoupling of $|\Delta F| = 1$ and $|\Delta F| = 2$ processes in VLQ models discussed above modifies the corresponding correlations derived in Ref. [31], increasing the impact of $|\Delta F| = 2$ constraints on $|\Delta F| = 1$ processes relative to the one found in [31].

In Table 6 we summarize the patterns discussed above.

6 Numerics

In this section we perform the numerical analysis of the VLQ models presented above. For this purpose we start by constraining the VLQ couplings by the available flavour data and if applicable also by data from other sectors. We proceed by presenting the predictions for a number of key observables given these constraints, including their correlations where they are sizable. These fits are performed for different VLQ masses, in order to illustrate the explicit mass dependence of flavour observables discussed in Section 5.3.

Model-independent constraints on $\psi^2\varphi^2 D$ operators have been derived from Z - and W -boson observables [61], which are applicable to G_{SM} models. Although these constraints are not entirely independent from other operators, in VLQ-models the latter are loop-suppressed and can be neglected. The constraints on the modulus of the couplings are weak and of the order $|\lambda_i| \lesssim M/(1 \text{ TeV})$.⁹

More stringent constraints derive from $|\Delta F| = 2, 1$ flavour observables [11]. We constrain the five parameters $|\Lambda_{ij}|$ and φ_{ij} (56) with the $|\Delta F| = 2, 1$ processes listed in Table 7. Master formulae used in these constraints are collected in Appendix B. The SM predictions in Table 7 are based on the determination of CKM parameters from a tree-level fit given in Table 12. Some comments regarding the included observables are in order:

- The observable ΔM_K does not provide constraints in G_{SM} models and is omitted due to too large uncertainties from long-distance contributions in $G'_{\text{SM}}(\Phi)$ models. The prospects for controlling this long-distance part by lattice calculations are good [62] and in the future this constraint could play an important role.
- We find that huge NP effects in ε'/ε are not excluded by the constraints listed in Table 7 in G_{SM} - and $G'_{\text{SM}}(\Phi)$ -models, such that we impose bounds on the NP contribution $(\varepsilon'/\varepsilon)_{\text{NP}}$ itself

$$(\varepsilon'/\varepsilon)_{\text{NP}} \in [0, 20] \times 10^{-4}, \quad (59)$$

in order to avoid showing predictions for other observables that are easily excluded by ε'/ε , and to analyse its influence on the correlations of observables. This range roughly corresponds to NP required assuming present predictions from lattice QCD. We have checked that decreasing this range to $[5, 10] \times 10^{-4}$ as expected from the dual approach to QCD [19, 41] would have only minor impact on the global fit as what matters is the unique selection of the sign of the relevant phase required for the enhancement of ε'/ε .

- Due to the sizable experimental uncertainties, $Br(B_d \rightarrow \mu\bar{\mu})$ does not constrain the VLQ parameters further. It is thus omitted from the fit and we compare its prediction in our models to the present measurement.
- A full analysis of $B \rightarrow K^*\ell\bar{\ell}$ is beyond the scope of this work. We do therefore not include the LHCb anomalies [63–66] in our fits. The analysis of $b \rightarrow s\ell\bar{\ell}$ in $G'_{\text{SM}}(S)$ models has been already presented in [9, 15] and we have nothing to add here. In G_{SM} models the shift in C_9 is too small to be relevant while in $G'_{\text{SM}}(\Phi)$ models the effects are only moderately interesting and we will not address them here.

The three sectors $s \rightarrow d$, $b \rightarrow d$ and $b \rightarrow s$ are not independent, due to relation (57). In our analysis we show first the results separately for the three meson systems and demonstrate in a global fit that K -physics constraints have an impact on B physics but not vice versa.

⁹There is one tension from $[\hat{c}_{Hd}]_{33} = (-4.6 \pm 1.6) \times 10^{-2}$ [61] (A.9) for the VLQ representation Q_V .

$i \rightarrow j$	observable	measurement	ref.	SM (c.v. [95% CL])
$s \rightarrow d$	ε_K	$2.228(11) \times 10^{-3}$	[67]	$(2.21 [1.57, 2.98]) \times 10^{-3}$
	$Br(K^+ \rightarrow \pi^+ \nu \bar{\nu})$	$(17.3^{+11.5}_{-10.5}) \times 10^{-11}$	[68]	$(8.5 [7.3, 9.5]) \times 10^{-11}$
	$Br(K_L \rightarrow \mu \bar{\mu})_{\text{SD}}$	$< 2.5 \times 10^{-9}$	[69]	$\chi_{\text{SD}} : 1.81 [1.65, 1.94]$
	$(\varepsilon'/\varepsilon)_{\text{NP}}$	$[0, 20] \times 10^{-4}$	†	0×10^{-4}
$b \rightarrow d$	$\Delta M_d [\text{ps}^{-1}]$	0.5055(20)	[70]	0.62 [0.45, 0.78]
	$\sin(2\beta_d)$	0.691(17)*	[70]	0.734 [0.686, 0.796]
	$Br(B^+ \rightarrow \pi^+ \mu \bar{\mu})_{[15,22]}$	$3.29(84) \times 10^{-9}$	[71]	$(5.0 [3.8, 7.2]) \times 10^{-9}$
$b \rightarrow s$	$\Delta M_s [\text{ps}^{-1}]$	17.757(21)	[70]	19.0 [16.2, 21.9]
	$\sin(2\beta_s)$	-0.034(33)*	[70]	-0.040 [-0.044, -0.036]
	$Br(B_s \rightarrow \mu \bar{\mu})$	$(2.8^{+0.7}_{-0.6}) \times 10^{-9}$	[72]	$(3.41 [3.01, 3.81]) \times 10^{-9}$
	$Br(B^+ \rightarrow K^+ \mu \bar{\mu})_{[15,22]}$	$8.47(50) \times 10^{-8}$	[73]	$(11.0 [6.4, 15.6]) \times 10^{-8}$

Table 7: The list of $|\Delta F| = 2, 1$ flavour observables in $i \rightarrow j$ down-type transitions that are used to constrain the VLQ couplings. SM predictions are obtained with CKM parameters determined from the tree-fit. †We impose this conservative range on the NP contribution of ε'/ε to avoid values excluded by this observable in the predictions for other observables, see text for more details. * Note that we neglect potential “penguin pollution” in $b \rightarrow c\bar{c}s$ transitions, which have been shown in recent analyses to be at most of the size of the present experimental uncertainties [74–76].

6.1 G_{SM} models

In G_{SM} models the absence of additional scalars allows to vary the mass of the VLQ’s down to about 1 TeV without violating the hierarchy (14). The fits of the Λ_{ij} for the three types of transitions $j \rightarrow i = \{s \rightarrow d, b \rightarrow d, b \rightarrow s\}$ in G_{SM} models are shown in Fig. 5 for $M_{\text{VLQ}} = 10$ TeV and in Fig. 6 for $M_{\text{VLQ}} = 1$ TeV for the single-VLQ scenarios D and Q_V with LH and RH couplings, respectively. The plots for LH scenarios $T_{u,d}$ are qualitatively similar to D whereas the RH scenario Q_d is similar to Q_V . Quantitative differences arise due to changes of the sign in couplings and a factor 1/2 for T_d w.r.t. D and T_u , which are shown in Table 2. The statistical approach for these fits is detailed in Appendix C. We make the following observations:

- All included observables are compatible with the SM prediction at 95% CL. Correspondingly also the global fit allows for the SM solution at 95% CL in all planes in both scenarios, except for $\Lambda_{bd}^{Q_V}$ with $M_{\text{VLQ}} = 10$ TeV, where the SM is slightly outside that region. This is due to the slight tensions of ΔM_d and $Br(B^+ \rightarrow \pi^+ \ell \bar{\ell})$ with their SM predictions, which fortify each other in this case.
- For $M_{\text{VLQ}} = 10$ TeV, $|\Delta F| = 2$ constraints are competitive to the $|\Delta F| = 1$ ones,

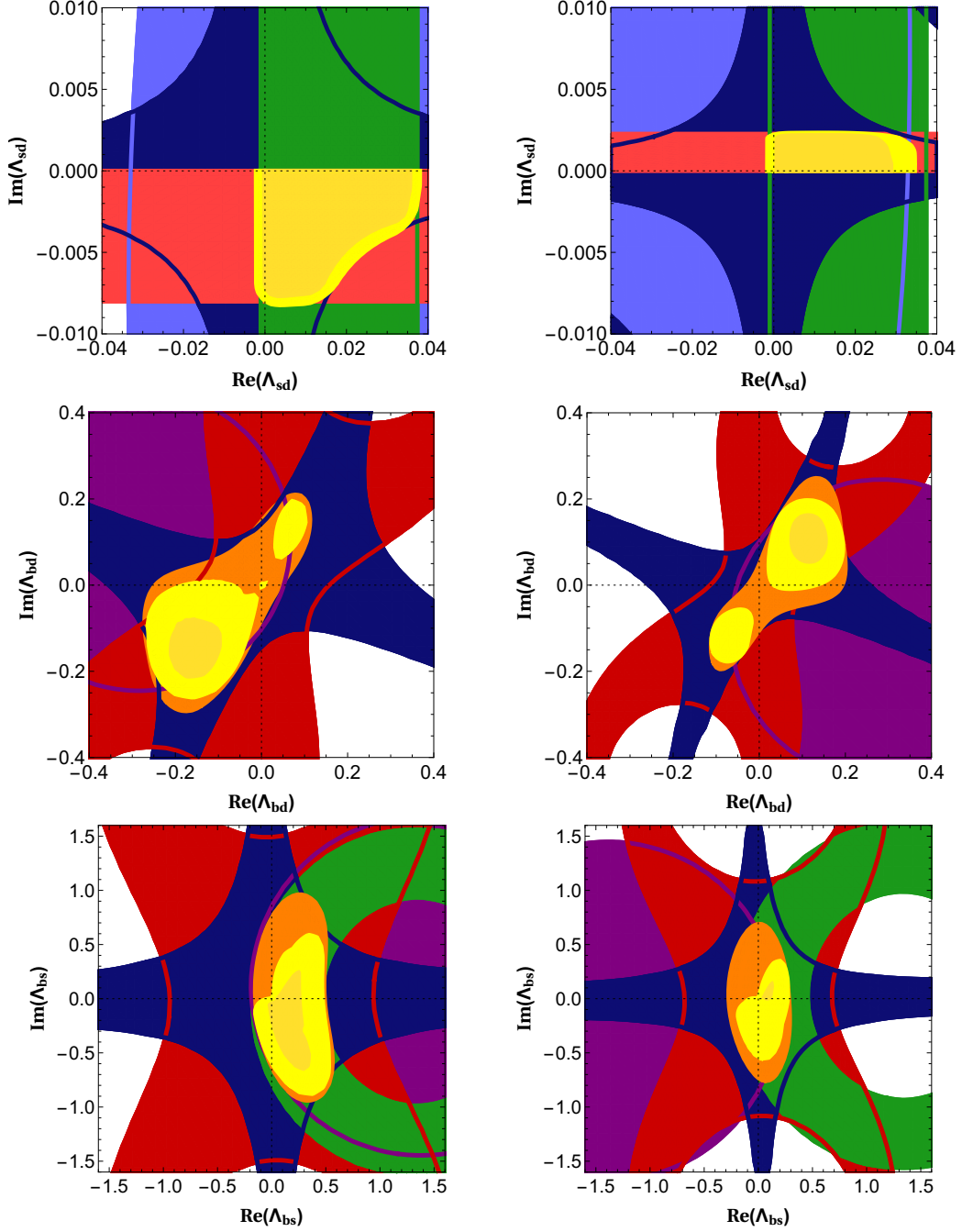


Figure 5: Fits of $\text{Im}(\Lambda_{ij})$ vs. $\text{Re}(\Lambda_{ij})$ for $ij = sd, bd, bs$ [upper, middle, lower] in G_{SM} -scenarios D [left] and Q_V [right] for $M_{\text{VLQ}} = 10$ TeV. Constraints from single observables and the combined fit for each separate sector [orange] are shown at 95% CL, the global fit [yellow] at 68% and 95%. For $ij = sd$: ε_K [dark blue], $Br(K^+ \rightarrow \pi^+ \nu \bar{\nu})$ [blue], $Br(K_L \rightarrow \mu \bar{\mu})_{\text{SD}}$ [green], and $(\varepsilon'/\varepsilon)_{\text{NP}}$ [red]. For $ij = bd$: ΔM_d [dark red], $\sin(2\beta_d)$ [dark blue] and $Br(B^+ \rightarrow \pi^+ \mu \bar{\mu})_{[15, 22]}$ [purple]. For $ij = bs$: ΔM_s [dark red], $\sin(2\beta_s)$ [dark blue], $Br(B_s \rightarrow \mu \bar{\mu})$ [green] and $Br(B^+ \rightarrow K^+ \mu \bar{\mu})_{[15, 22]}$ [purple].

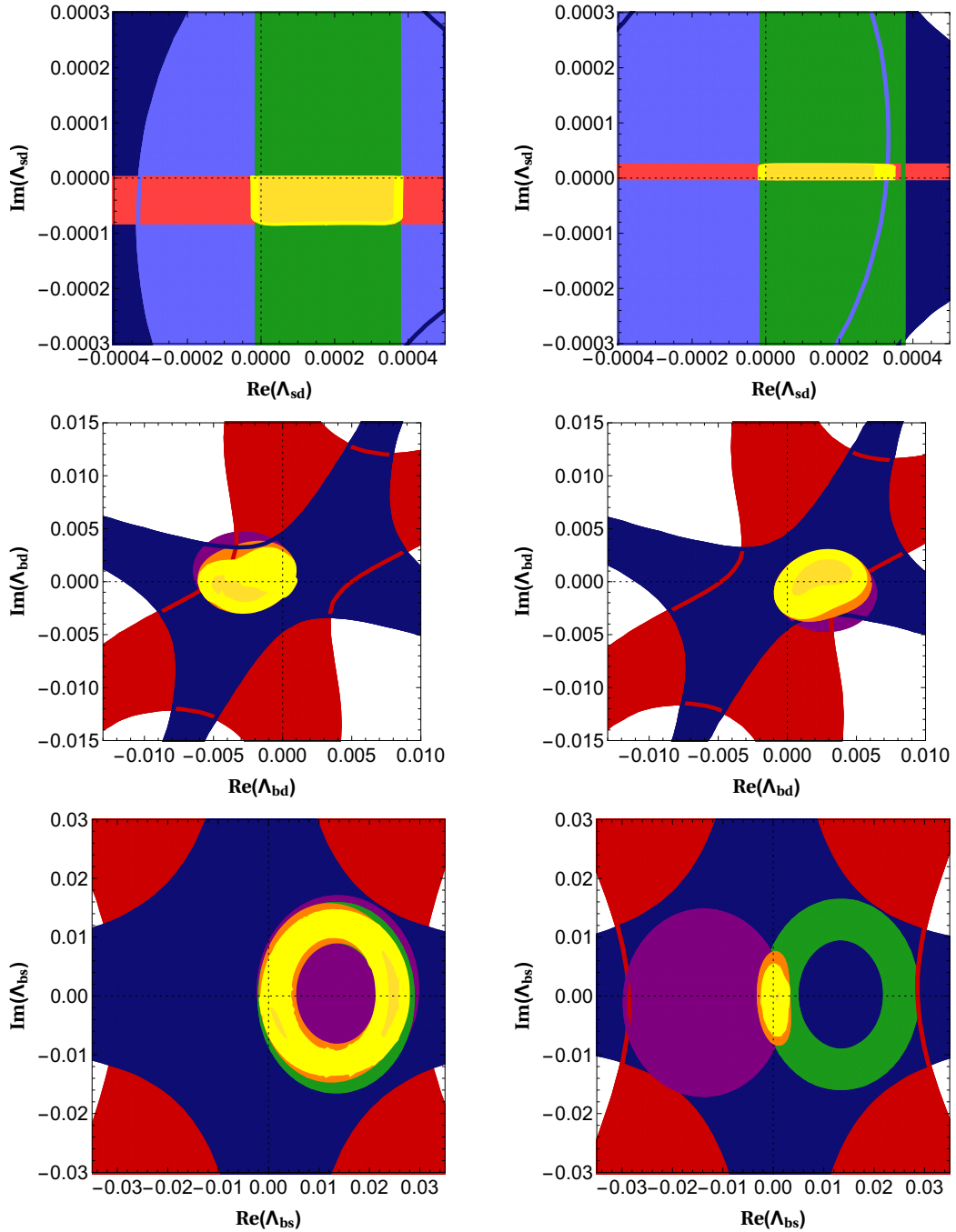


Figure 6: Fits of $\text{Im}(\Lambda_{ij})$ vs. $\text{Re}(\Lambda_{ij})$ for $ij = sd, bd, bs$ [upper, middle, lower] in G_{SM} -scenarios D [left] and Q_V [right] for $M_{\text{VLQ}} = 1$ TeV. The colour scheme is as in Fig. 5.

while for $M_{\text{VLQ}} = 1$ TeV the global fit is almost completely determined by $|\Delta F| = 1$ processes. This is in accordance with our previous discussion of the mass-dependence of these transitions. Specifically for ϵ_K , large effects are excluded by $|\Delta F| = 1$ observables.

- In $b \rightarrow s$, the $|\Delta F| = 1$ observables distinguish between scenarios with LH and RH currents due to their different dependences on the corresponding Wilson coefficients, most importantly C_{10} and C'_{10} ,

$$Br(B_s \rightarrow \mu\bar{\mu}) \propto |C_{10} - C'_{10}|^2, \quad Br(B^+ \rightarrow K^+ \mu\bar{\mu}) \propto |C_{10} + C'_{10}|^2. \quad (60)$$

The consequence is shown in Fig. 5 and Fig. 6 where allowed regions almost overlap for LH scenarios, but intersect only around the SM for RH scenarios, thereby diminishing the size of potential VLQ effects in other $b \rightarrow s$ observables. The same observation holds for $b \rightarrow d$ transitions, which will help once $B_d \rightarrow \mu\bar{\mu}$ is measured more precisely.

- In $s \rightarrow d$ transitions, the constraints from $(\epsilon'/\epsilon)_{\text{NP}}$ and $Br(K_L \rightarrow \mu\bar{\mu})_{\text{SD}}$ constrain the allowed values for φ_{sd} . This in combination with the slight tensions especially in $b \rightarrow d$ leads to stronger constraints in the global fit compared to the fits for the individual transitions in $b \rightarrow d, s$. As a consequence correlations between different transitions arise, but at the moment they are not very strong yet. This would change with significant measurements away from the SM for at least two of the transitions.
- The $|\Delta F| = 2$ CP-asymmetric observables ϵ_K and $\sin(2\beta_{d,s})$ impose star-shaped constraints in the complex Λ_{ij} -planes, which are not limited along the direction corresponding to the SM phase. Such a limit is provided by $\Delta M_{d,s}$, whereas in the case of $s \rightarrow d$ the one from ΔM_K is very weak and outside of the ranges shown.
- There is a complementarity in the constraints from $Br(K^+ \rightarrow \pi^+ \nu\bar{\nu})$ and $Br(K_L \rightarrow \mu\bar{\mu})_{\text{SD}}$ for every VLQ representations. Thus an improved measurement of $Br(K^+ \rightarrow \pi^+ \nu\bar{\nu})$ by NA62, which will operate until the LHC shut down in 2018 and aims at a 10% uncertainty [77, 78], will provide stronger cuts into the allowed parameter space. On the other hand, the constraints from $(\epsilon'/\epsilon)_{\text{NP}}$ and $Br(K_L \rightarrow \mu\bar{\mu})_{\text{SD}}$ are theoretically limited at the moment.

Using the above constraints, we obtain allowed ranges for observables that are yet to be measured (precisely), listed in Table 8. We furthermore analyze patterns for each transition, that will help to distinguish VLQ models from other NP scenarios, and different VLQs from each other. In this respect we point out that models Q_d and Q_V have the same experimental signatures in down-type quark FCNC transitions and are hence indistinguishable. Such a distinction might be possible after invoking additional constraints from up-type quark FCNC transitions, where both models differ from each other as indicated in Eq. (8). Still, in Q_V models strong correlations between the up- and down-type sectors can not be expected due to the in principle independent up- and down-type Yukawa couplings.

In the Kaon sector, we make the following observations, see also Fig. 7:

SM	measurement	D	Q_d, Q_V	T_u	T_d
$10^{11} \times Br(K_L \rightarrow \pi^0 \nu \bar{\nu}), \quad 10^{11} \times Br(K^+ \rightarrow \pi^+ \nu \bar{\nu})$					
3.2 [2.5, 4.3]	≤ 2600 [79]	[0, 4.3] [0, 4.3]	[1.3, 4.3] [1.3, 4.3]	[0, 4.3] [0, 4.3]	[0, 4.3] [0, 4.3]
8.5 [7.3, 9.5]	$17.3_{-10.5}^{+11.5}$ [79]	[0.8, 9.2] [0.8, 9.2]	[7.3, 40.3] [7.3, 40.3]	[0.7, 9.2] [0.8, 9.2]	[0.7, 9.2] [1.1, 9.2]
$10^{10} \times Br(B_d \rightarrow \mu \bar{\mu})$					
1.14 [0.94, 1.32]	≤ 6.3 [80]	[0.0, 1.7] [0.1, 1.8]	[0.8, 9.2] [1.1, 2.6]	[0.0, 1.7] [0.2, 1.9]	[0.0, 1.7] [0.5, 1.7]
$A_{\Delta\Gamma}(B_s \rightarrow \mu \bar{\mu}), \quad S(B_s \rightarrow \mu \bar{\mu})$					
1	—	[-1.00, 1.00] [0.12, 0.99]	[0.50, 1.00] [0.55, 1.00]	[-1.00, 1.00] [0.24, 1.00]	[-1.00, 1.00] [0.70, 1.00]
0	—	[-1.00, 1.00] [-0.99, 0.99]	[-0.79, 0.87] [-0.77, 0.83]	[-1.00, 1.00] [-0.96, 0.97]	[-1.00, 1.00] [-0.72, 0.72]
$10^2 \times A_{7,8,9}(B \rightarrow K^* \mu \bar{\mu})_{[1,6]}$					
< 0.1	4.5 ± 5.0 [81]	[-23.4, 23.3] [-14.5, 14.1]	[-10.4, 9.2] [- 9.8, 8.9]	[-23.9, 24.1] [-13.4, 13.1]	[-23.8, 24.2] [-8.3, 8.3]
< 0.1	-4.7 ± 5.8 [81]	[-0.9, 0.9] [-0.5, 0.5]	[-8.1, 7.2] [-7.7, 6.9]	[-0.9, 0.9] [-0.5, 0.5]	[-0.9, 0.9] [-0.3, 0.3]
< 0.1	3.3 ± 4.2 [81]	SM	[-5.6, 5.7] [-4.4, 5.0]	SM	SM
$10^2 \times A_{8,9}(B \rightarrow K^* \mu \bar{\mu})_{[15,19]}$					
< 0.1	2.5 ± 4.8 [81]	SM	[-6.1, 5.4] [-5.8, 5.2]	SM	SM
< 0.1	-6.1 ± 4.3 [81]	SM	[-9.7, 11.0] [-9.4, 10.4]	SM	SM
$\mathcal{R}_{B \rightarrow K \nu \bar{\nu}}, \quad \mathcal{R}_{B \rightarrow K^* \nu \bar{\nu}}, \quad \mathcal{R}_{FL}$					
1	≤ 4.3 [82]	[0.02, 1.10] [0.63, 1.10]	[0.79, 1.29] [0.79, 1.26]	[0.02, 1.10] [0.64, 1.10]	[0.02, 1.10] [0.69, 1.11]
1	≤ 4.4 [83]	[0.02, 1.10] [0.63, 1.10]	[0.86, 1.16] [0.86, 1.16]	[0.02, 1.10] [0.64, 1.10]	[0.02, 1.10] [0.69, 1.11]
1	—	SM	[0.91, 1.06] [0.91, 1.06]	SM	SM

Table 8: Ranges still allowed for observables when taking the constraints from Table 7 for the individual $s \rightarrow d$, $b \rightarrow d$ and $b \rightarrow s$ sectors into account, fitting at the time same CKM and hadronic parameters. Upper and lower intervals are for $M_{VLQ} = 1$ TeV and 10 TeV, respectively. Entries denoted as “SM” have tiny or no deviations from the SM. Experimental upper bounds are given at 90% CL.

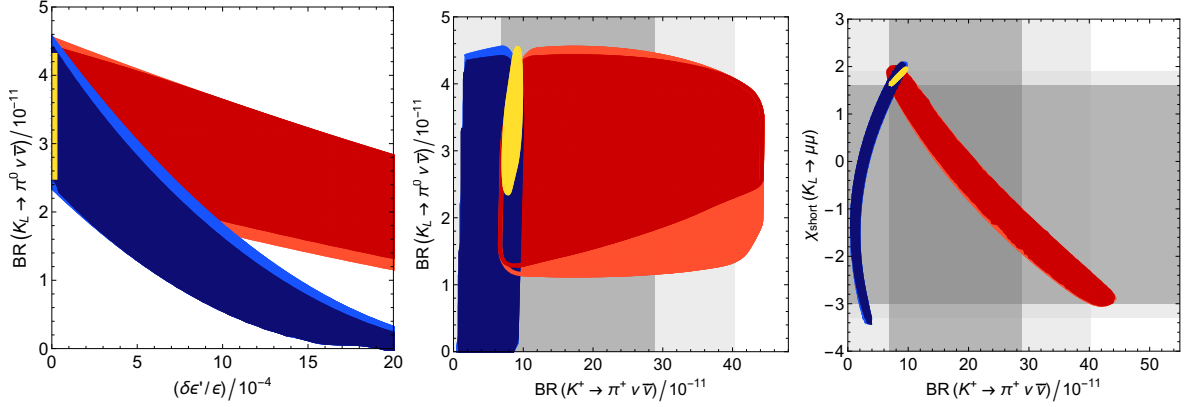


Figure 7: The correlations of observables in the Kaon sector in G_{SM} scenarios at 95% CL for the SM, as well as for $M_{\text{VLQ}} = 10$ TeV [darker colours] and $M_{\text{VLQ}} = 1$ TeV [lighter colours]. The colours correspond to the SM prediction [Yellow] and the VLQ-representations D [Blue] and Q_V [Red]; the results for $T_{u,d}$ and Q_d are very similar to the former and the latter, respectively. Dark and light grey bands show experimental measurements at 1- and 2σ .

- The VLQ models allow to enhance ε'/ε significantly, thereby addressing the apparent gap between the SM prediction and data, at the expense of suppressing $Br(K_L \rightarrow \pi^0 \nu \bar{\nu})$. This suppression is significantly weaker for Q_V and Q_d models (RH currents) than for D , T_d and T_u (LH currents), in accordance with the general study in [36]. Simultaneous agreement with the data for ε_K and ε'/ε can be obtained without fine-tuning of parameters.
- While the impact of ε'/ε on $K_L \rightarrow \pi^0 \nu \bar{\nu}$ is large as stated above, $K^+ \rightarrow \pi^+ \nu \bar{\nu}$ and ε'/ε are only weakly correlated and $Br(K^+ \rightarrow \pi^+ \nu \bar{\nu})$ can be enhanced by up to a factor of 4 compared to its SM value in models with RH currents. In models with LH currents, a strong suppression is possible, and the SM value corresponds to an upper bound in this case.
- The modes $K^+ \rightarrow \pi^+ \nu \bar{\nu}$ and $K_L \rightarrow \mu \bar{\mu}$ are strongly correlated in VLQ models, however, again differently so for LH and RH currents. While for RH currents one can easily infer the allowed range in one mode from a determination of the other, LH-current models are more strongly constrained from $K_L \rightarrow \mu \bar{\mu}$. Progress for the latter mode depends solely on the capability to separate the long-distance contributions to this mode from the short-distance ones, since the relevant data are already very precise, see Appendix B. Note that there is basically no correlation between ε'/ε and $K_L \rightarrow \mu \bar{\mu}$, as they are governed by imaginary and real parts of the corresponding couplings, respectively.
- The VLQ mass does not have a large impact on all these correlations, as can be seen by comparing the lighter and darker areas in Fig. 7. The reason is that $|\Delta F| = 1$ transitions are the dominant constraints at both masses, rendering the allowed ranges for other $|\Delta F| = 1$ processes mass-independent.

Correlation plots for observables in $b \rightarrow s$ processes are shown in Fig. 8. We observe the following patterns:

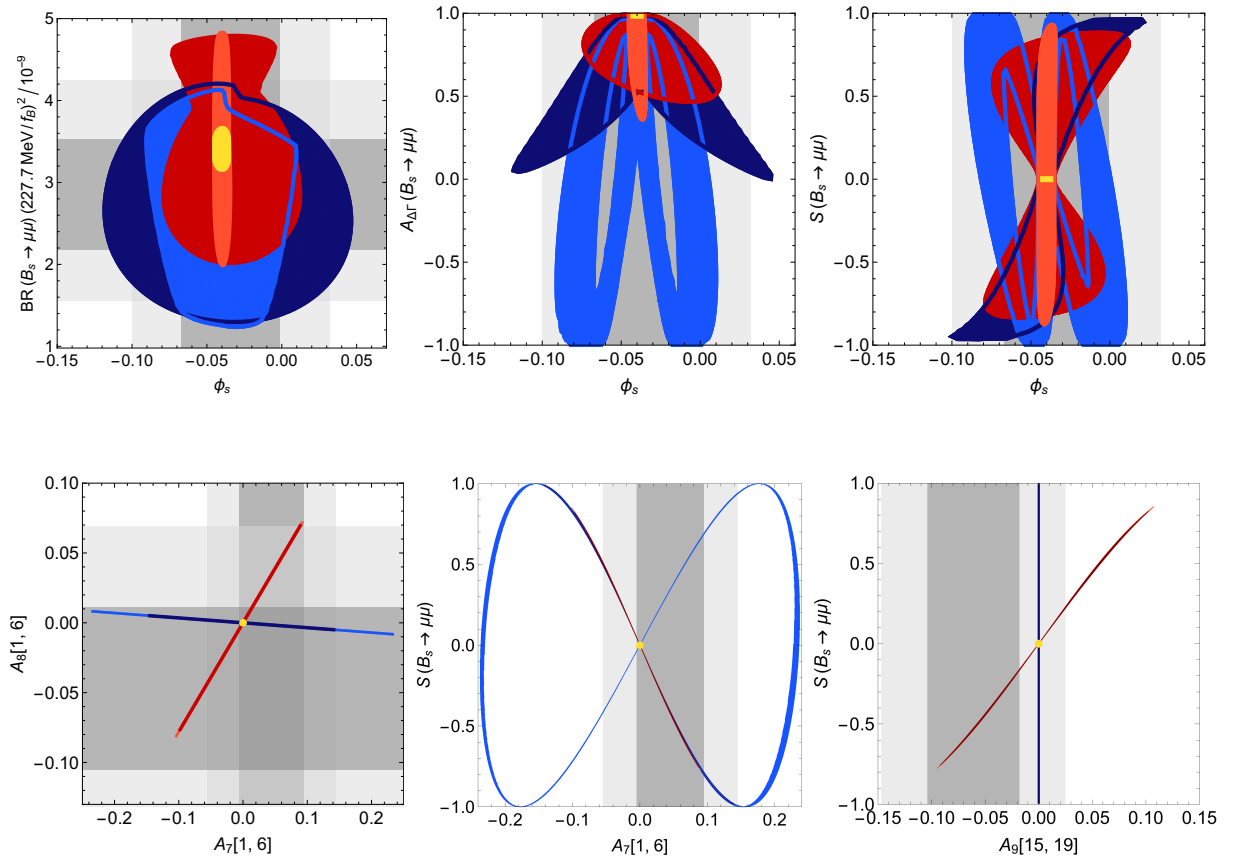


Figure 8: The correlations of observables in the $b \rightarrow s$ sector in G_{SM} -scenarios for $M_{\text{VLQ}} = 10$ TeV [darker colours] and 1 TeV [lighter colours] within the 95% CL regions. The colours are for VLQ-representations D [Blue] (similar to $T_{u,d}$), $Q_V = Q_d$ [Red]. Grey bands show experimental measurements at 1- and 2 σ and the yellow dots are the SM predictions.

- Since NP effects in all three quark transitions are governed by different parameters, the slight tensions in $|\Delta F| = 2$ observables hinted at by new lattice data [57] can easily be removed in VLQ models. This is in contrast to constrained-MFV models, where ε_K prohibits large effects in $\Delta M_{d,s}$ [58].
- $Br(B_s \rightarrow \mu\bar{\mu})$ can be strongly suppressed below its SM value, as slightly favoured by experiment, while still allowing for sizable NP effects in $\sin(2\beta_s)$, in particular in the case of models with LH currents. For $M_{\text{VLQ}} = 1$ TeV $|\Delta F| = 1$ observables constrain the NP effects in ϕ_s to be smaller than for larger VLQ masses. Specifically, for RH currents ϕ_s has to be very close to its SM value, in accordance with Fig. 6.
- Sizeable deviations from the SM prediction are still possible for the mass-eigenstate rate asymmetry $A_{\Delta\Gamma}(B_s \rightarrow \mu\bar{\mu})$ and the mixing-induced CP-asymmetry $S(B_s \rightarrow \mu\bar{\mu})$. Indeed, both can essentially vary in the full range $[-1, 1]$ for both LH and RH models for $M_{\text{VLQ}} = 1$ TeV. For $M_{\text{VLQ}} = 10$ TeV, the former is restricted to positive values in RH models. Of course, the experimental measurements are very challenging for $S(B_s \rightarrow \mu\bar{\mu})$. We note that to very good accuracy $A_{\Delta\Gamma}^2 + S^2 = 1$, since the direct CP-asymmetry $C(B_s \rightarrow \mu\bar{\mu})$ is negligible.
- CP-violating quantities are almost 100% correlated in $b \rightarrow s$ transitions as long as only one representation is considered. The reason is that the SM predictions are tiny and all NP contributions therefore directly proportional to the imaginary part of Λ_{bs} , which hence cancels in the ratio of two CP-violating quantities. For small NP contributions, the asymmetries are simply proportional to each other, for larger effects the relation depends on the normalisation of the asymmetry. These statements hold not only in VLQ models, but in all models that provide only a single new phase in $b \rightarrow s$ transitions, only the proportionality constant changes in other models.
- The imaginary parts of $b \rightarrow s\mu\bar{\mu}$ Wilson coefficients $C_{9,9',10,10'}$ can give rise to naive T-odd CP-asymmetries $A_{7,8,9}$ in $B \rightarrow K^*\mu\bar{\mu}$ that are tiny in the SM.¹⁰ The rough dependences on the Wilson coefficients are [84]

$$A_7 \propto \text{Im}[(C_{10} - C'_{10})C_7^*], \quad A_{8,9} \propto \text{Im}[C_9C_9'^* + C_{10}C_{10}'^* + \dots], \quad (61)$$

where the dots indicate other numerically suppressed interference terms of $C_{9,9'}$ with C_7 that are included in the numerical evaluation. The A_7 remains tiny at high dilepton invariant mass q^2 [85]. These CP-asymmetries have been measured in various q^2 -bins by LHCb [81] and we choose $q^2 \in [1, 6]$ and $[15, 19]$ GeV², which have smallest experimental and theoretical uncertainties. As can be seen in Table 8, the largest VLQ-effects in $A_{8,9}$ arise in RH G_{SM} -scenarios Q_d and Q_V , almost independent from the VLQ mass and with a strong anti-correlation shown in Fig. 8. The potential size of VLQ effects exceeds slightly the current experimental uncertainties, specifically for the CP asymmetry A_7 , such that improved measurements will provide additional bounds on VLQ couplings in the future, especially on their imaginary parts. The A_7 is correlated with A_8 and anti-correlated with A_9 in RH scenarios, whereas in LH scenarios $A_{8,9}$ remain SM-like.

¹⁰Note that we use different convention of angles w.r.t. LHCb: $A_{7,9} = -A_{7,9}^{\text{LHCb}}$ and $A_8 = A_8^{\text{LHCb}}$.

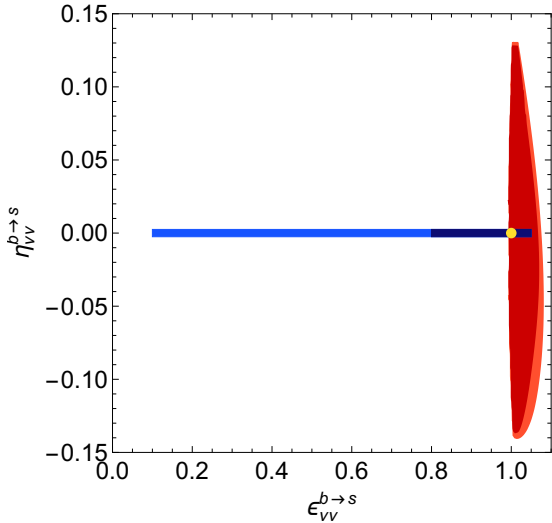


Figure 9: The correlations of the quantities η and ϵ , which determine the observables in the $b \rightarrow s\nu\bar{\nu}$ sector in G_{SM} -scenarios for $M_{\text{VLQ}} = 10$ TeV [darker] and 1 TeV [lighter] within the 95% CL regions. The colours are for VLQ-representations D [Blue] (similar to $T_{u,d}$), $Q_V = Q_d$ [Red].

- The decays $B \rightarrow K^{(*)}\nu\bar{\nu}$ are also sensitive probes of LH and RH NP effects due to Z -exchange and in order to exhibit these effect we consider the ratios [86]

$$\epsilon = \frac{\sqrt{|C_L|^2 + |C_R|^2}}{|C_L^{\text{SM}}|} \quad \text{and} \quad \eta = \frac{-\text{Re}(C_L C_R^*)}{|C_L|^2 + |C_R|^2}, \quad (62)$$

which are unity and zero in the SM, respectively, and which determine the observables

$$\mathcal{R}_{B \rightarrow K^{(*)}\nu\bar{\nu}} = \frac{Br(B \rightarrow K^{(*)}\nu\bar{\nu})}{Br(B \rightarrow K^{(*)}\nu\bar{\nu})_{\text{SM}}}, \quad \mathcal{R}_{F_L} = \frac{F_L(B \rightarrow K^{(*)}\nu\bar{\nu})}{F_L(B \rightarrow K^{(*)}\nu\bar{\nu})_{\text{SM}}} \quad (63)$$

via [87]

$$\mathcal{R}_{B \rightarrow K\nu\bar{\nu}} = (1 - 2\eta)\epsilon^2, \quad \mathcal{R}_{B \rightarrow K^*\nu\bar{\nu}} = (1 + \kappa_\eta\eta)\epsilon^2, \quad \mathcal{R}_{F_L} = \frac{1 + 2\eta}{1 + \kappa_\eta\eta}, \quad (64)$$

where κ_η is form-factor dependent and given in Ref. [87]. The Belle II experiment is expected to measure these branching ratios with 30% uncertainty [88] if they are of the size as predicted in the SM. In RH scenarios large VLQ effects are excluded due to the strong complementarity of the $|\Delta F| = 1$ constraints from $Br(B_s \rightarrow \mu\bar{\mu})$ and $Br(B^+ \rightarrow K^+\mu\bar{\mu})$ as mentioned above. ϵ has to be larger than one in these cases. The VLQ effects for $M_{\text{VLQ}} = 1$ TeV can lead to a rather large suppression in LH scenarios for ϵ while $\eta = 0$, leading to maximally correlated $\mathcal{R}_{B \rightarrow K^{(*)}\nu\bar{\nu}}$. The suppression is smaller for $M_{\text{VLQ}} = 10$ TeV, whereas $\mathcal{R}_{F_L} = 1$. The correlation plot is shown in Fig. 9. It will be challenging to distinguish the small deviations from SM predictions in RH scenarios; however, large (suppression) effects are possible and LH and RH scenarios are well distinguishable.

Similar correlation plots exist for $b \rightarrow d$ processes; however, given the CKM suppression of these modes compared to $b \rightarrow s$, precision measurements in $b \rightarrow d\ell\bar{\ell}$ and significant measurements of $b \rightarrow d\nu\bar{\nu}$ processes are not expected in the next couple of years. Nevertheless, we illustrate in Fig. 10 the impact of more precise measurements in this sector

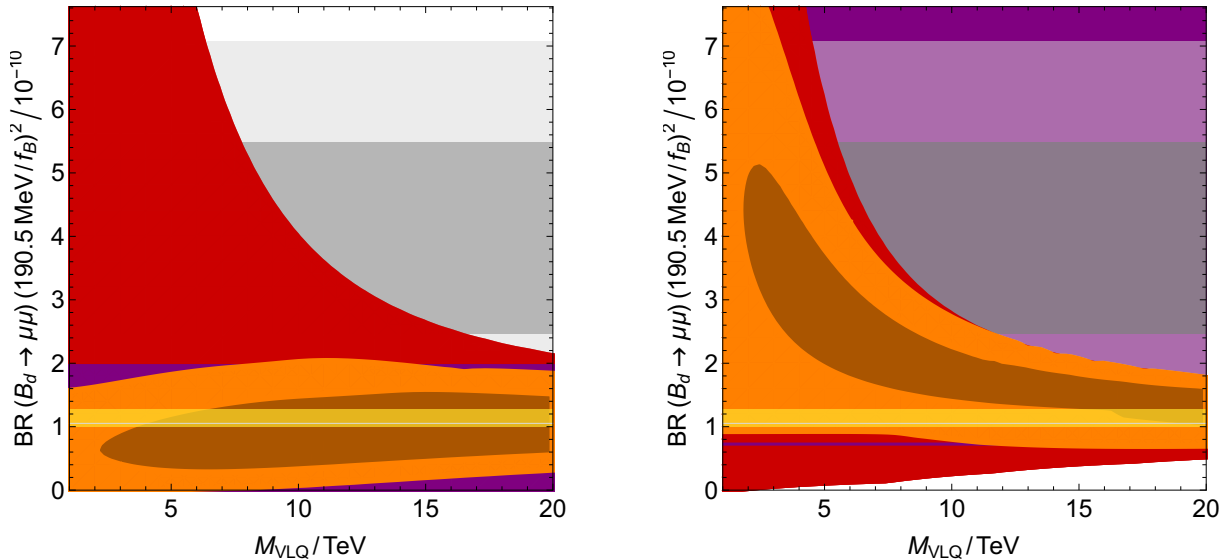


Figure 10: Predictions for $Br(B_d \rightarrow \mu\bar{\mu})$ for the LH G_{SM} scenario D [left] and RH G_{SM} scenario Q_V [right], in dependence on the VLQ mass. In dark red the constraint from $|\Delta F| = 2$ processes is shown, *i.e.* ΔM_d and $\sin 2\beta$, in purple the constraint from $B^+ \rightarrow \pi^+ \mu\bar{\mu}$, and in orange their combination. The yellow band corresponds to the SM prediction, the grey one to the measurement by the CMS and LHCb collaborations [72]. All constraints correspond to 95% CL, only inner darker bands to 68% CL.

exemplarily for $Br(B_d \rightarrow \mu\bar{\mu})$. All $|\Delta F| = 1$ processes depend only on the combination Δ_{ij} , see (22), of NP parameters; the allowed range predicted from one $|\Delta F| = 1$ process for another is therefore mass-independent, in contrast to the prediction from $|\Delta F| = 2$ processes. The present measurement from the CMS and LHCb collaborations is about 2σ larger than the SM prediction. As seen in Fig. 10 a confirmation of the present central value with higher precision would exclude LH G_{SM} scenarios and yield at least an upper limit on M_{VLQ} for the RH ones, in accordance with the discussion in Section 5.3.

6.2 $G'_{\text{SM}}(\Phi)$ model

In $G'_{\text{SM}}(\Phi)$ models $|\Delta F| = 1$ transitions are suppressed by $\tan \beta$ compared to G_{SM} models, such that $|\Delta F| = 2$ transitions dominate via the box contributions the constraints on VLQ couplings. In our numerical analysis of $G'_{\text{SM}}(\Phi)$ models we fix the parameters

$$g' = 1.5, \quad X = 1, \quad M_{\text{VLQ}} = 10 \text{ TeV}, \quad (65)$$

and choose two benchmark points BP1 and BP2:

$$\text{BP1:} \quad \tan \beta = 2, \quad v_S = 1.8 \text{ TeV}, \quad (66)$$

$$\text{BP2:} \quad \tan \beta = 3, \quad v_S = 1.3 \text{ TeV}, \quad (67)$$

in the lower range of possible values of $\tan \beta$ — see also Fig. 11 — from constraints described in Appendix A.2 to maximally enhance VLQ contributions in $|\Delta F| = 1$ transi-

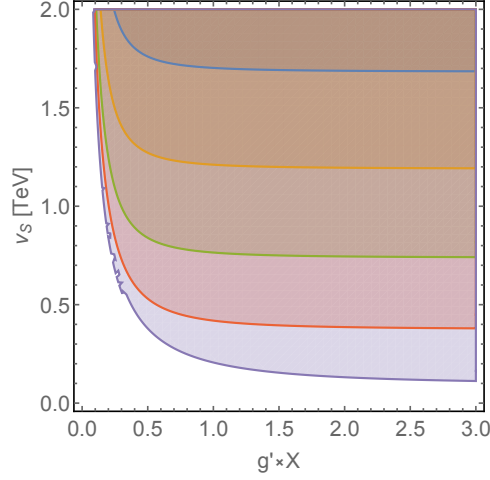


Figure 11: The allowed 95% CL regions in the v_S versus $g'X$ plane for fixed $\tan\beta = 2, 3, 5, 10, 40$ [Blue, Yellow, Green, Red, Purple] from the constraints M_Z and partial widths $\Gamma[Z \rightarrow \ell\bar{\ell}]$ ($\ell = e, \mu, \tau$), imposing $M_Z < M_{Z'}$.

tions. The corresponding Z and Z' masses and mixing angles are

$$\text{BP1:} \quad M_Z = 91.64 \text{ GeV}, \quad M_{Z'} = 1.35 \text{ TeV}, \quad \xi_{ZZ'} = 0.0011; \quad (68)$$

$$\text{BP2:} \quad M_Z = 91.63 \text{ GeV}, \quad M_{Z'} = 0.98 \text{ TeV}, \quad \xi_{ZZ'} = 0.0021. \quad (69)$$

The allowed regions of Λ_{ij} in $G'_{\text{SM}}(\Phi)$ models correspond to the regions allowed by $|\Delta F| = 2$ constraints in G_{SM} models given in Fig. 5. We find that $|\Delta F| = 1$ processes in Table 7 provide only tiny additional constraints in $b \rightarrow d, s$ and small ones in $s \rightarrow d$, allowing thus in $G'_{\text{SM}}(\Phi)$ models much larger values for Λ_{ij} compared to G_{SM} models.

The ranges still allowed for different observables with $|\Delta F| = 1, 2$ transitions are listed in Table 9, obtained by varying Λ_{ij} within the 95% CL regions, neglecting theory uncertainties. For this purpose $(\varepsilon'/\varepsilon)_{\text{NP}}$ has been restricted as given in Eq. (59). Notable features for the benchmark points are:

- ε'/ε can also be enhanced in $G'_{\text{SM}}(\Phi)$ models and thereby decrease the tension with the measurement. Especially in RH scenarios the constraint (59) is saturated, such that even larger effects are possible. The enhancement of ε'/ε falls off fast for larger values of $\tan\beta$ and v_S than in the benchmark points.
- Whereas VLQ effects in $Br(K_L \rightarrow \pi^0 \nu \bar{\nu})$ and $Br(K_L \rightarrow \mu \bar{\mu})_{\text{SD}}$ are small, $Br(K^+ \rightarrow \pi^+ \nu \bar{\nu})$ can still be enhanced by a factor of two to three over the SM prediction. Most notably, $(\Delta M_K)_{\text{SD}}$ can also be enhanced by a factor of more than two, in contradistinction to G_{SM} models, where VLQ effects are tiny. The reason for this enhancement is the absence of strong constraints from $|\Delta F| = 1$ on the real part of Λ_{sd} . Thus large $(\Delta M_K)_{\text{SD}}$ is independent of ε'/ε , since the latter is sensitive to the imaginary part of Λ_{sd} . This effect is enhanced with decreasing VLQ effects in $|\Delta S| = 1$ transitions as can be seen by comparing the results for BP1 and BP2.
- The VLQ effects on $B_{s,d} \rightarrow \mu \bar{\mu}$ are small except for $A_{\Delta\Gamma}(B_s \rightarrow \mu \bar{\mu})$ and $S(B_s \rightarrow \mu \bar{\mu})$. The CP asymmetries $A_{7,8,9}(B \rightarrow K^* \mu \bar{\mu})$ can still be significantly enhanced over the

SM to the percent level, but are a factor 2-3 smaller for BP1 than in G_{SM} models, see Table 8.

- VLQ effects in $B \rightarrow K^{(*)}\nu\bar{\nu}$ in $G'_{\text{SM}}(\Phi)$ models are smaller than in G_{SM} models, at the level of only (10 – 20)% deviation from the SM predictions.

We provide a summary of enhancements and/or suppressions w.r.t. the SM predictions of the observables discussed above due to VLQ effects in Table 10.

7 Summary and Conclusions

In this paper we have analysed flavour-violation patterns in the K and $B_{s,d}$ sectors in eleven models with vector-like quarks (VLQs). Five of them, called G_{SM} -models, contained only VLQs as new particles. Two of them, called $G'_{\text{SM}}(S)$ -models, have in addition a heavy Z' and a scalar S . The final four of them, called $G'_{\text{SM}}(\Phi)$ -models, contain a heavy Z' , a scalar S and a scalar doublet Φ . Our summary of patterns of flavour violation in these models in Section 5 accompanied by two DNA tables 5 and 6 and in particular our extensive numerical analysis in Section 6, see specifically tables 8 and 9, has shown that NP effects in several of these models can be still very large and that simultaneous consideration of several flavour observables should allow to distinguish between these models. This is also seen in Table 10, which shows that models with LH currents can be distinguished from models with RH currents through several observables.

As our results have been systematically summarized in the previous section, we list here only the main highlights. Most interesting NP effects are found in G_{SM} -models, even if they do not provide the explanation of the present LHCb anomalies. In particular

- Tree-level Z contributions to ε'/ε can be large, so that the apparent upward shift in ε'/ε can easily be obtained, bringing the theory to agree with data.
- Simultaneously the branching ratio for $K^+ \rightarrow \pi^+\nu\bar{\nu}$ can be significantly enhanced over its SM prediction, but only in models with flavour violating RH currents, because of the $K_L \rightarrow \mu\bar{\mu}$ constraint. On the other hand the positive shift in ε'/ε implies uniquely the suppression of the $K_L \rightarrow \pi^0\nu\bar{\nu}$ branching ratio.
- Potential tensions between $\Delta M_{s,d}$ and ε_K can be easily removed in these models, since no MFV relation is imposed on the couplings.
- Significant suppressions of the $Br(B_s \rightarrow \mu\bar{\mu})$ and of $A_{\Delta\Gamma}(B_s \rightarrow \mu\bar{\mu})$, in particular in models with LH currents, are possible. While such effects are also possible in 331 models, they cannot be as large as in VLQ models.
- CP-violating effects for a given quark transition are strongly correlated in all of these models, as long as only one representation is present, specifically for $b \rightarrow s$, where CP violation in the SM is tiny.

Having the LHCb anomalies in mind we have considered also VLQ models with a heavy Z' related to $U(1)_{L_\mu-L_\tau}$ symmetry. Our findings are as follows:

SM	measurement	D	Q_d	T_u	T_d
$10^4 \times (\varepsilon'/\varepsilon)_{\text{NP}}$					
(46, 47, 49)	(48)	[0.0, 20.0] [0.0, 20.0]	[0.0, 20.0] [0.0, 19.9]	[0.0, 20.0] [0.0, 20.0]	[0.0, 19.9] [0.0, 10.8]
$10^{11} \times Br(K_L \rightarrow \pi^0 \nu \bar{\nu}), \quad 10^{11} \times Br(K^+ \rightarrow \pi + \nu \bar{\nu})$					
3.2 [2.5, 4.3]	≤ 2600 [79]	[0.1, 3.2] [0.1, 3.2]	[1.8, 3.2] [1.8, 3.2]	[0.1, 3.2] [0.1, 3.2]	[0.1, 3.2] [0.9, 3.2]
8.5 [7.3, 9.5]	$17.3^{+11.5}_{-10.5}$ [68]	[1.5, 26.2] [1.6, 26.2]	[3.0, 49.7] [3.1, 48.5]	[1.5, 26.2] [1.8, 26.3]	[1.6, 26.2] [3.0, 23.7]
$10^9 \times Br(K_L \rightarrow \mu \bar{\mu})_{\text{SD}}$					
	≤ 2.5 [69]	[0.0, 5.5] [0.0, 5.5]	[0.0, 3.2] [0.0, 3.2]	[0.0, 5.5] [0.0, 5.6]	[0.0, 5.6] [0.0, 4.8]
$10^4 \times \Delta M_K$ [ps $^{-1}$]					
	52.93 ± 0.09 [67]	[47.2, 53.1] [45.5, 84.0]	[47.7, 83.9] [47.4, 191.8]	[47.0, 75.8] [45.0, 74.3]	[45.0, 75.7] [44.5, 131.1]
$10^{10} \times Br(B_d \rightarrow \mu \bar{\mu})$					
1.14 [0.94, 1.32]	≤ 6.3 [80]	[0.74, 1.32] [0.90, 1.21]	[0.90, 1.34] [0.97, 1.19]	[0.77, 1.30] [0.92, 1.19]	[0.92, 1.20] [1.00, 1.13]
$A_{\Delta\Gamma}(B_s \rightarrow \mu \bar{\mu}), \quad S(B_s \rightarrow \mu \bar{\mu})$					
1	—	[0.88, 1.00] [0.97, 1.00]	[0.95, 1.00] [0.98, 1.00]	[0.91, 1.00] [0.98, 1.00]	[0.97, 1.00] [0.99, 1.00]
0	—	[-0.47, 0.46] [-0.25, 0.25]	[-0.34, 0.34] [-0.18, 0.18]	[-0.43, 0.42] [-0.22, 0.22]	[-0.22, 0.22] [-0.11, 0.11]
$10^2 \times A_{7,8,9}(B \rightarrow K^* \mu \bar{\mu})_{[1,6]}$					
< 0.1	4.5 ± 5.0 [81]	[-5.0, 5.1] [-2.6, 2.7]	[-3.7, 3.7] [-1.9, 1.9]	[-4.5, 4.6] [-2.4, 2.4]	[-2.4, 2.4] [-1.2, 1.2]
< 0.1	-4.7 ± 5.8 [81]	[-0.6, 0.5] [-0.5, 0.4]	[-3.0, 2.9] [-1.6, 1.6]	[-0.5, 0.5] [-0.4, 0.4]	[-0.3, 0.2] [-0.2, 0.2]
< 0.1	3.3 ± 4.2 [81]	SM	[-1.7, 1.7] [-0.9, 0.9]	SM	SM
$10^2 \times A_{8,9}(B \rightarrow K^* \mu \bar{\mu})_{[15,19]}$					
< 0.1	2.5 ± 4.8 [81]	SM	[-2.4, 2.4] [-1.4, 1.4]	SM	SM
< 0.1	-6.1 ± 4.3 [81]	SM	[-4.4, 4.4] [-2.4, 2.5]	SM	SM
$\mathcal{R}_{B \rightarrow K \nu \bar{\nu}}, \quad \mathcal{R}_{B \rightarrow K^* \nu \bar{\nu}}, \quad \mathcal{R}_{F_L}$					
1	≤ 4.3 [82]	[0.78, 1.13] [0.88, 1.09]	[0.87, 1.15] [0.93, 1.08]	[0.80, 1.13] [0.89, 1.08]	[0.90, 1.08] [0.95, 1.05]
1	≤ 4.4 [83]	[0.78, 1.13] [0.88, 1.09]	[0.91, 1.10] [0.95, 1.05]	[0.80, 1.13] [0.90, 1.08]	[0.90, 1.08] [0.95, 1.05]
1	—	SM	[0.95, 1.04] [0.97, 1.02]	SM	SM

Table 9: Ranges still allowed for observables when varying Λ_{ij} of $G'_{\text{SM}}(\Phi)$ models in the 95% CL ranges for individual $s \rightarrow d$, $b \rightarrow d$ and $b \rightarrow s$ sectors for benchmark points BP1/BP2 [upper/lower]. Moreover $(\varepsilon'/\varepsilon)_{\text{NP}}$ is restricted as given in Eq. (59). Entries denoted as ‘‘SM’’ have tiny or no deviations from the SM. Experimental upper bounds are given at 90% CL.

	G_{SM}				$G'_{\text{SM}}(\Phi)$			
	D	$Q_{V,d}$	T_d	T_u	D	Q_d	T_d	T_u
ΔM_K					↑	↑	↑	↑
ε'/ε	↑	↑	↑	↑	↑	↑	↑	↑
$K^+ \rightarrow \pi^+ \nu \bar{\nu}$	↓	↑	↓	↓	↕	↕	↕	↕
$K_L \rightarrow \pi^0 \nu \bar{\nu}$	↓	↓	↓	↓	↓	↓	↓	↓
$Br(B_d \rightarrow \mu \bar{\mu})$	↕	↕	↕	↕				
$Br(B_s \rightarrow \mu \bar{\mu})$	↕	↕	↕	↕				
$A_{\Delta\Gamma}(B_s \rightarrow \mu \bar{\mu})$	↓	↓	↓	↓				
$S(B_s \rightarrow \mu \bar{\mu})$	↕	↕	↕	↕	↕	↕	↕	↕
$A_7(B \rightarrow K^* \mu \bar{\mu})_{[1,6]}$	↕	↕	↕	↕	↕	↕	↕	↕
$A_{8,9}(B \rightarrow K^* \mu \bar{\mu})_{[1,6]}$		↕				↕		
$A_{8,9}(B \rightarrow K^* \mu \bar{\mu})_{[15,19]}$		↕				↕		
$\mathcal{R}_{B \rightarrow K \nu \bar{\nu}}$	↓	↕	↓	↓				
$\mathcal{R}_{B \rightarrow K^* \nu \bar{\nu}}$	↓	↕	↓	↓				
\mathcal{R}_{FL}		↓						

Table 10: Summary of allowed VLQ effects in G_{SM} - and $G'_{\text{SM}}(\Phi)$ -models in flavour observables after the fit using experimental measurements of Table 7. Possible enhancement, suppression or both w.r.t. SM predictions are indicated by according ↑, ↓ or ↕. Empty space means that the given model does not predict sizable effects in that observable. Note that $(\varepsilon'/\varepsilon)_{\text{NP}}$ has been restricted (59), affecting other $s \rightarrow d$ observables.

- The $G'_{\text{SM}}(S)$ -models, considered already in Ref. [9], can explain LHCb anomalies by providing sufficient suppression of the coefficient C_9 , but NP effects in $B_s \rightarrow \mu\bar{\mu}$ and $K_L \rightarrow \mu\bar{\mu}$ are absent, those in $b \rightarrow s\nu\bar{\nu}$ transitions small and the ones in $K^+ \rightarrow \pi^+\nu\bar{\nu}$ and $K_L \rightarrow \pi^0\nu\bar{\nu}$ much smaller than in G_{SM} -models. Most importantly these models fail badly in explaining the ε'/ε anomaly.
- In the $G'_{\text{SM}}(\Phi)$ -models, the explanation of LHCb anomalies is more difficult than in $G'_{\text{SM}}(S)$ -models, but this time due to the presence of Z contributions interesting effects in other observables can be found.
- In particular, in contrast to G_{SM} -models, the parametric suppression of Z couplings by $\tan\beta$ allows for the increased values of Yukawa couplings that are this time mainly bounded by $|\Delta F| = 2$ transitions and not $|\Delta F| = 1$ transitions like in G_{SM} -models.
- We find that NP effects in ε'/ε , $K^+ \rightarrow \pi^+\nu\bar{\nu}$ can be large, even if smaller than in G_{SM} -models, but the corresponding effects in ΔM_K can be significantly larger than in G_{SM} -models. On the other hand NP effects in $K_L \rightarrow \pi^0\nu\bar{\nu}$, $K_L \rightarrow \mu\bar{\mu}$, $B \rightarrow K(K^*)\nu\bar{\nu}$ and $B_{d,s} \rightarrow \mu\bar{\mu}$ are beyond the reach of even presently planned future facilities. While effects in the CP asymmetries $A_{7,8,9}(B \rightarrow K^*\mu\bar{\mu})$ are also smaller than in G_{SM} models, they might be still within reach of LHCb.

Thus if NP will be found in $K^+ \rightarrow \pi^+\nu\bar{\nu}$ and $B_s \rightarrow \mu\bar{\mu}$, and the ε'/ε -anomaly will be confirmed by future lattice data, G_{SM} -models would offer the best explanation among VLQ models. If, on the other hand, the LHCb anomalies will be confirmed in the future and no visible NP will be found in rare K decays, $G'_{\text{SM}}(S)$ -models and $G'_{\text{SM}}(\Phi)$ -models would be favoured over G_{SM} -models. If all anomalies will survive and large NP effects in $K^+ \rightarrow \pi^+\nu\bar{\nu}$ will be found, we will have to extend the models analyzed by us by considering several VLQ representations simultaneously. We have also pointed out that in $G'_{\text{SM}}(\Phi)$ -models significant NP effects in ΔM_K can be found, larger than in G_{SM} and $G'_{\text{SM}}(S)$ -models.

While the discovery of VLQs at the LHC would give a strong impetus to the models considered by us, non-observation of them at the LHC would not preclude their importance for flavour physics. In fact, as we have shown, large NP effects in flavour observables can be present for $M_{\text{VLQ}} = 10$ TeV and in the flavour-precision era one is sensitive to even higher scales. In this context we have pointed out that the combination of $|\Delta F| = 2$ and $|\Delta F| = 1$ observables in a given meson system allows to determine the masses of VLQs in a given representation independently of the size of Yukawa couplings.

Acknowledgements

C.B. thanks Martin Gorbahn for numerical checks on ε'/ε . We thank Sebastien Descotes-Genon for providing us an update of a tree-level CKM fit from CKMfitter [89]. This research was done and financed in the context of the ERC Advanced Grant project “FLAVOUR” (267104) and was partially supported by the DFG cluster of excellence “Origin and Structure of the Universe”. The work of A.C. is supported by the Alexander von

Humboldt Foundation. This work is supported in part by the DFG SFB/TR 110 ‘‘Symmetries and the Emergence of Structure in QCD’’.

A Scalar sectors of G'_{SM} -models

A.1 $G'_{\text{SM}}(S)$ models

The scalar sector in $G'_{\text{SM}}(S)$ -models with one complex scalar $S(1, 0, X)$ and the SM doublet $H(2, +1/2, 0)$ is given by

$$\mathcal{L} = |\mathcal{D}_\mu H|^2 + |\mathcal{D}_\mu S|^2 - V \quad (70)$$

with the potential

$$V = m^2 H^\dagger H + \frac{\lambda}{2} (H^\dagger H)^2 + \frac{b_2}{2} |S|^2 + \frac{d_2}{4} |S|^4 + \frac{\delta}{2} H^\dagger H |S|^2. \quad (71)$$

We parametrize the SM Higgs doublet and the complex scalar as

$$H = \begin{pmatrix} H^+ \\ H^0 \end{pmatrix} = \begin{pmatrix} \varphi^+ \\ (v + \rho + i\eta)/\sqrt{2} \end{pmatrix}, \quad S = \frac{(v_S + R_0 + iI_0)}{\sqrt{2}}. \quad (72)$$

The neutral mass-eigenstates are given by $(h, H)^T \simeq (\rho, R_0)^T$ with approximate masses

$$m_h^2 \approx v^2 \left(\lambda - \frac{\delta^2}{2d_2} \right), \quad m_H^2 \approx v_S^2 \frac{d_2}{2}, \quad (73)$$

up to terms $\mathcal{O}(v^2/v_S^2)$. The general expressions can be found in [90].

Kinetic mixing of Z and Z' is caused by VLQ-exchange and depends on the VLQ masses M and the $U(1)_{L_\mu-L_\tau}$ -gauge coupling. It will be neglected in the following, see Ref. [9]. Mass mixing does not occur in $G'_{\text{SM}}(S)$ models.

A.2 $G'_{\text{SM}}(\Phi)$ models

The scalar sector in $G'_{\text{SM}}(\Phi)$ -models with one complex scalar $S(1, 0, X/2)$ and the two doublets $\Phi_1 \equiv \Phi(2, +1/2, X)$ and $\Phi_2 \equiv H(2, +1/2, 0)$ is given by

$$\mathcal{L} = |\mathcal{D}_\mu \Phi_1|^2 + |\mathcal{D}_\mu \Phi_2|^2 + |\mathcal{D}_\mu S|^2 - V, \quad (74)$$

with the potential

$$\begin{aligned} V = & m_a^2 \Phi_a^\dagger \Phi_a + \frac{\lambda_a}{2} (\Phi_a^\dagger \Phi_a)^2 + \lambda_3 (\Phi_1^\dagger \Phi_1) (\Phi_2^\dagger \Phi_2) + \lambda_4 (\Phi_1^\dagger \Phi_2) (\Phi_2^\dagger \Phi_1) \\ & + \frac{b_2}{2} |S|^2 + \frac{d_2}{4} |S|^4 + \frac{\delta_a}{2} \Phi_a^\dagger \Phi_a |S|^2 - \frac{\delta_3}{4} [\Phi_1^\dagger \Phi_2 S^2 + \Phi_2^\dagger \Phi_1 (S^*)^2]. \end{aligned} \quad (75)$$

We neglect kinetic mixing and parametrize the mass mixing via

$$\begin{pmatrix} \hat{Z}_\mu \\ \hat{Z}'_\mu \end{pmatrix} = \begin{pmatrix} \cos \xi_{ZZ'} & -\sin \xi_{ZZ'} \\ \sin \xi_{ZZ'} & \cos \xi_{ZZ'} \end{pmatrix} \begin{pmatrix} Z_\mu \\ Z'_\mu \end{pmatrix}. \quad (76)$$

After partial diagonalization of the neutral gauge boson system, the Z and Z' masses and their mass mixing are given by [91]

$$\hat{M}_Z^2 = g_Z^2 \frac{v^2}{4}, \quad \hat{M}_{Z'}^2 = (g'X)^2 \frac{v_S^2}{4} \left(1 + 4c_\beta^2 \frac{v^2}{v_S^2} \right), \quad \Delta^2 = -g_Z g'X c_\beta^2 \frac{v^2}{2}, \quad (77)$$

with $e = \sqrt{4\pi\alpha} = g_2 \hat{s}_W = g_1 \hat{c}_W = g_Z \hat{s}_W \hat{c}_W$. The $Z - Z'$ mixing angle

$$\tan 2\xi_{ZZ'} = \frac{2\Delta^2}{\hat{M}_Z^2 - \hat{M}_{Z'}^2} = c_\beta^2 \frac{4Xg'}{g_Z} \frac{\hat{M}_Z^2}{(\hat{M}_{Z'}^2 - \hat{M}_Z^2)} \quad (78)$$

is small unless X becomes large. The diagonalisation of the neutral gauge boson mass matrix gives mass eigenvalues

$$M_{Z,Z'}^2 = \frac{1}{2} \left[\hat{M}_{Z'}^2 + \hat{M}_Z^2 \mp \sqrt{(\hat{M}_{Z'}^2 - \hat{M}_Z^2)^2 + 4\Delta^4} \right], \quad (79)$$

which differ from the ones in Eq. (77) by terms $\mathcal{O}(v^2/v_S^2)$. Note that we present only the solution for which $M_Z < M_{Z'}$, i.e. throughout we will implicitly impose that the lighter mass eigenstate couples predominantly SM-like to quarks and leptons. As a consequence a lower bound on g' will be obtained. On the other hand, the decoupling limit $g' \rightarrow 0$ is not excluded, but it will lead to $M_{Z'} < M_Z$, i.e. that the heavier mass-eigenstate couples predominantly to SM-like fermions. The $\tan\beta$ dependence of $M_{Z'}$ becomes irrelevant once $v_S \gtrsim 0.5$ TeV. The mixing angle $\xi_{ZZ'}$ can be suppressed with large $\tan\beta$ and $M_{Z'}$, since we work in the part of the parameter space, where the other possibility of $g' \rightarrow 0$ is not an option.

In $\mathbf{G}'_{\text{SM}}(\Phi)$ -models we make use of the fact that photon- and W^\pm -interactions to leptons are SM-like in order to determine the values of the fundamental gauge couplings $g_{1,2}$ and the VEV v from $\alpha_e(M_Z)$, G_F and the W -boson pole mass M_W . As the remaining free parameters we choose $\tan\beta$, g' , X and v_S , whereas dependent parameters are $M_{Z,Z'}$ and $\xi_{ZZ'}$. Note that the latter depend only on the product $g'X$, such that there are effectively only three parameters. We will restrict this parameter space to

$$0.3 \leq \tan\beta \leq 40, \quad 0 \leq g'X \leq 3, \quad 0 \text{ TeV} \leq v_S \leq 2 \text{ TeV}. \quad (80)$$

The lower bound on $\tan\beta$ guarantees perturbativity of the top-quark Yukawa coupling [59], whereas v_S is bounded from above by the requirements (14) and yields $M_{Z'} \lesssim 1.5$ TeV within the above limits. Constraints on these parameters arise from the measured value of M_Z , which we impose with an error of $\delta M_Z = 5$ GeV to account for the use of tree-level relations only. Further constraints come from the partial widths of $Z \rightarrow \ell\bar{\ell}$ ($\ell = e, \mu, \tau$), constraining the new physics contributions of the Z -lepton couplings (24) that depend on the $\xi_{ZZ'}$ and g' due to gauge mixing. We find a small mixing angle $\xi_{ZZ'} \lesssim 0.1$ in the above specified parameter space of $\tan\beta$, $g'X$ and v_S if we impose the bound on new physics contributions to the partial widths of $Z \rightarrow \ell\bar{\ell}$ from LEP [22], allowing for 5σ deviations from the measured central values, together with the bound on M_Z . This justifies the expansion in the small mixing angle as done in Table 3.

B Master formulae for K and B decays

B.1 $|\Delta F| = 2$

The effective Lagrangian for neutral meson mixing in the down-type quark sector ($d_j \bar{d}_i \rightarrow \bar{d}_j d_i$ with $i \neq j$) can be written as [30]

$$\mathcal{H}_{\Delta F=2}^{ij} = \mathcal{N}_{ij} \sum_a C_a^{ij} O_a^{ij} + \text{h.c.}, \quad (81)$$

where the normalisation factor and the CKM combinations are

$$\mathcal{N}_{ij} = \frac{G_F^2}{4\pi^2} M_W^2 \left(\lambda_{ij}^{(t)} \right)^2, \quad (82)$$

with $ij = sd$ for kaon mixing and $ij = bd, bs$ for B_d and B_s mixing, respectively. The set of operators consists out of $(5 + 3) = 8$ operators [30],

$$\begin{aligned} O_{\text{VLL}}^{ij} &= [\bar{d}_i \gamma_\mu P_L d_j] [\bar{d}_i \gamma^\mu P_L d_j], \\ O_{\text{LR},1}^{ij} &= [\bar{d}_i \gamma_\mu P_L d_j] [\bar{d}_i \gamma^\mu P_R d_j], & O_{\text{LR},2}^{ij} &= [\bar{d}_i P_L d_j] [\bar{d}_i P_R d_j], \\ O_{\text{SLL},1}^{ij} &= [\bar{d}_i P_L d_j] [\bar{d}_i P_L d_j], & O_{\text{SLL},2}^{ij} &= -[\bar{d}_i \sigma_{\mu\nu} P_L d_j] [\bar{d}_i \sigma^{\mu\nu} P_L d_j], \end{aligned} \quad (83)$$

which are built out of colour-singlet currents $[\bar{d}_i^\alpha \dots d_j^\alpha] [\bar{d}_i^\beta \dots d_j^\beta]$, where α, β denote colour indices. The chirality-flipped sectors VRR and SRR are obtained from interchanging $P_L \leftrightarrow P_R$ in VLL and SLL. Note that the minus sign in $Q_{\text{SLL},2}$ arises from different definitions of $\tilde{\sigma}_{\mu\nu} \equiv [\gamma_\mu, \gamma_\nu]/2$ in Ref. [30] w.r.t. $\sigma_{\mu\nu} = i\tilde{\sigma}_{\mu\nu}$ used here. The ADM's of the 5 distinct sectors (VLL, SLL, LR, VRR, SRR) have been calculated in Refs. [30,92] at NLO in QCD, and numerical solutions are given in Ref. [93]. The NLO ADM's are also available for an alternative basis [94] with colour octet operators $Q_{\text{SLL},2} = [\bar{d}_i^\alpha P_L d_j^\beta] [\bar{d}_i^\beta P_L d_j^\alpha]$ and analogous $Q_{\text{SRR},2}$.

In the SM only

$$C_{\text{VLL}}^{ij}(\mu_{\text{EW}})|_{\text{SM}} = S_0(x_t), \quad S_0(x) = \frac{x(4 - 11x + x^2)}{4(x-1)^2} + \frac{3x^3 \ln x}{2(x-1)^3} \quad (84)$$

is non-zero at the scale μ_{EW} , depending on the ratio $x_t \equiv m_t^2/M_W^2$ of the top-quark and W -boson masses.

The $|\Delta F| = 2$ observables of interest $\Delta M_{K, B_d, B_s}$, ϵ_K and $\sin(2\beta_{d,s})$ derive all from the complex-valued off-diagonal elements M_{12}^{ij} of the mass-mixing matrices of the neutral mesons [95,96]. For the latter we use the full higher-order SM expressions in combination with the LO new physics contributions. In particular for M_{12}^{ds} , we make use of NLO and in part NNLO QCD corrections $\eta_{cc, tt, ct}$ collected in Table 12 and for the hadronic matrix element of $|\Delta S| = 2$ operators the value of \hat{B}_K . Concerning $|\Delta B| = 2$, we include the NLO QCD corrections η_B to the SM and use for the hadronic matrix elements the latest results for $F_{B_{d,s}} \sqrt{\hat{B}_{B_{d,s}}}$ [57].

B.2 $d_j \rightarrow d_i \nu \bar{\nu}$

The effective Lagrangian for $d_j \rightarrow d_i \nu \bar{\nu}$ ($i \neq j$) is adopted from Ref. [86],

$$\mathcal{L}_{d \rightarrow d \nu \bar{\nu}} = \frac{4G_F}{\sqrt{2}} \frac{\alpha_e}{4\pi} \lambda_{ij}^{(t)} \sum_a \sum_\nu C_a^{ij,\nu} O_a^{ij,\nu} + \text{h.c.}, \quad (85)$$

where the sums extend over $a = \{L, R\}$ and neutrino flavour $\nu = \{e, \mu, \tau\}$

$$O_{L(R)}^{ij,\nu} = [\bar{d}_i \gamma_\mu P_{L(R)} d_j] [\bar{\nu} \gamma^\mu (1 - \gamma_5) \nu]. \quad (86)$$

In the SM only

$$C_L^{ij,\nu}|_{\text{SM}} = \frac{4B - C}{s_W^2} \equiv -\frac{X_0}{s_W^2} \quad (87)$$

has non-vanishing contribution at the scale μ_{EW} , whereas $C_R^\nu = 0$. The functions B and C depend on the ratio $x_t \equiv m_t^2/M_W^2$ of the top-quark and W -boson masses and enter as the gauge-independent linear combination $X_0(x_t) \equiv C(x_t) - 4B(x_t)$ [97, 98],

$$X_0(x) = \frac{x}{8} \left(\frac{x+2}{x-1} + \frac{3x-6}{(x-1)^2} \ln x \right). \quad (88)$$

It is given by

$$X_0 \rightarrow X_L^{\text{SM}} = 1.481 \pm 0.009, \quad (89)$$

when including higher order QCD and electroweak corrections [99–102] as extracted in Ref. [103] from original papers.

The theoretical predictions for $b \rightarrow s \nu \bar{\nu}$ observables defined in Eq. (63) are based on formulae given in Ref. [87]. These expressions account for the lepton-non-universal contribution of VLQ's w.r.t. the neutrino flavour in G'_{SM} models. However, the particular structure of the gauged $U(1)_{L_\mu - L_\tau}$ (4) leads to a cancellation of the numerically leading interference contributions of the SM and new physics [9].

The $Br(K^+ \rightarrow \pi^+ \nu \bar{\nu})$ receives in the SM the numerically leading contribution from the “top”-sector, when decoupling heavy degrees of freedom at μ_{EW} , which yields directly the local $\mathcal{O}_L^{sd,\nu}$ operator ($\nu = e, \mu, \tau$). Further, a non-negligible “charm”-sector arises from double-insertions of hadronic and semi-leptonic $|\Delta S| = 1$ operators when decoupling the charm quark at $\mu_c \sim m_c$, which is enhanced due to the strong CKM hierarchy ($\lambda_{sd}^{(t)} \propto \lambda^5$) \ll ($\lambda_{sd}^{(c)} \propto \lambda^2$), where $\lambda = |V_{us}|$ is the Cabibbo angle. This is usually expressed in the effective Hamiltonian of the SM as [104]

$$\mathcal{H}_{\text{eff}} = \mathcal{N} \sum_\nu \left[\lambda_{sd}^{(c)} X_c^\nu + \lambda_{sd}^{(t)} X_L^{\text{SM}} \right] \mathcal{O}_L^{sd,\nu}, \quad (90)$$

with $\mathcal{N} = G_F \alpha_e / (2\sqrt{2}\pi s_W^2)$, where $X_c^e = X_c^\mu \neq X_c^\tau$.

The NP contributions in VLQ-models cannot compete with the SM contribution to the tree-level processes entering the “charm”-sector, since they are suppressed by an additional factor $(M_W/M_{\text{VLQ}})^2$. In consequence, NP contributes to the “top”-sector only

$$X_L^{\text{SM}} \rightarrow X_t^\nu = X_L^{\text{SM}} + X_L^{sd,\nu} + X_R^{sd,\nu} \equiv X_L^{\text{SM}} + X_{\text{NP}}^\nu, \quad (91)$$

with $X_{L,R}^{sd,\nu}$ given in Eq. (39), such that the top-sector becomes neutrino-flavour dependent.

The experimental measurement averages over the three neutrino flavours,

$$Br(K^+ \rightarrow \pi^+ \nu \bar{\nu}) = \frac{\kappa_+(1 + \Delta_{EM})}{\lambda^{10}} \frac{1}{3} \sum_{\nu} \left[\text{Im}^2 \left(\lambda_{sd}^{(t)} X_t^{\nu} \right) + \text{Re}^2 \left(\lambda_{sd}^{(c)} X_c^{\nu} + \lambda_{sd}^{(t)} X_t^{\nu} \right) \right], \quad (92)$$

with the assumption that $\lambda_{sd}^{(c)} X_c^{\nu}$ is real. The NNLO QCD results of the functions X_c^{ν} [104] are combined into

$$P_c = \frac{1}{\lambda^4} \left(\frac{2}{3} X_c^e + \frac{1}{3} X_c^{\tau} \right) = \left(\frac{0.2252}{\lambda} \right)^4 (0.404 \pm 0.024), \quad (93)$$

where $\lambda = 0.2252$ has been used in Ref. [103]. The factor

$$\kappa_+ = r_{K^+} \frac{3\alpha^2(M_Z)\lambda^8}{2\pi^2 s_W^4} Br(K \rightarrow \pi e \bar{\nu}_e) = 0.5173(25) \times 10^{-10} \left[\frac{\lambda}{0.225} \right]^8 \quad (94)$$

contains the experimental value $Br(K \rightarrow \pi e \bar{\nu}_e)$ and the isospin correction r_{K^+} and has been evaluated in Ref. [105] (table 2) including various corrections. Further $\Delta_{EM} = -0.003$ for $E_{\max}^{\gamma} \approx 20$ MeV [105]. If one takes into account the different value of $s_W^2 = 0.231$ taken in Ref. [105] compared to our value in Table 12, then $\kappa_+ = 0.5150 \times 10^{-10} (\lambda/0.225)^8$.

The sum (92) contains the SM contribution and further the interference of SM \times NP and NP \times NP. Besides P_c at NNLO in the SM contribution, the NLO numerical values

$$X_c^e = 10.05 \times 10^{-4}, \quad X_c^{\tau} = 6.64 \times 10^{-4}, \quad (95)$$

for $\mu_c = 1.3$ GeV are used for the interference of SM \times NP.

The branching fraction of $K_L \rightarrow \pi^0 \nu \bar{\nu}$ is obtained again by averaging over the three neutrino flavours

$$Br(K_L \rightarrow \pi^0 \nu \bar{\nu}) = \frac{\kappa_L}{\lambda^{10}} \frac{1}{3} \sum_{\nu} \text{Im}^2 \left(\lambda_{sd}^{(t)} X_t^{\nu} \right), \quad (96)$$

with

$$\kappa_L = \kappa_+ \frac{r_{K_L} \tau_{K_L}}{r_{K^+} \tau_{K^+}} = 2.231(13) \times 10^{-10} \left[\frac{\lambda}{0.225} \right]^8. \quad (97)$$

The numerical value is from Ref. [105] (table 2) and it decreases to $\kappa_L = 2.221 \times 10^{-10} (\lambda/0.225)^8$ when rescaling with our value of s_W^2 .

B.3 $d_j \rightarrow d_i \ell \bar{\ell}$

The effective Lagrangian for $d_j \rightarrow d_i \ell \bar{\ell}$ ($i \neq j$) is adopted from Ref. [106],

$$\mathcal{L}_{d \rightarrow d \ell \bar{\ell}} = \frac{4G_F \alpha_e}{\sqrt{2} 4\pi} \lambda_{ij}^{(t)} \sum_a \sum_{\ell} C_a^{ij,\ell} O_a^{ij,\ell} + \text{h.c.}, \quad (98)$$

were the sum over a extends over the $|\Delta F| = 1$ operators

$$O_{9(9')}^{ij,\ell} = [\bar{d}_i \gamma_\mu P_{L(R)} d_j][\bar{\ell} \gamma^\mu \ell], \quad O_{10(10')}^{ij,\ell} = [\bar{d}_i \gamma_\mu P_{L(R)} d_j][\bar{\ell} \gamma^\mu \gamma_5 \ell], \quad (99)$$

whereas scalar $O_{S,P(S',P')}^\ell$ and tensorial operators $O_{T(T5)}^\ell$ are not generated in the context of VLQ models. In the SM the only non-zero Wilson coefficients,

$$C_9^{ij,\ell}|_{\text{SM}} = \frac{1}{s_W^2} [(1 - 4s_W^2)C - B - s_W^2 D] \equiv \frac{Y_0}{s_W^2} - 4Z_0, \quad (100)$$

$$C_{10}^{ij,\ell}|_{\text{SM}} = \frac{1}{s_W^2} (B - C) \equiv -\frac{Y_0}{s_W^2}, \quad (101)$$

are lepton-flavour universal and also universal w.r.t down-type quark transitions, as the CKM elements have been factored out. All other Wilson coefficients vanish at the scale μ_{EW} . The functions B, C, D depend again on the ratio $x_t \equiv m_t^2/M_W^2$ of the top-quark and W -boson masses and give two gauge-independent combinations $Y_0(x_t) \equiv C(x_t) - B(x_t)$ and $Z_0(x_t) \equiv C(x_t) + D(x_t)/4$, that are given in the SM as

$$Y_0(x) = \frac{x}{8} \left(\frac{x-4}{x-1} + \frac{3x \ln x}{(x-1)^2} \right), \quad (102)$$

$$Z_0(x) = \frac{18x^4 - 163x^3 + 259x^2 - 108x}{144(x-1)^3} + \frac{32x^4 - 38x^3 - 15x^2 + 18x}{72(x-1)^4} \ln x - \frac{1}{9} \ln x. \quad (103)$$

In the predictions of $Br(B_{d,s} \rightarrow \mu\bar{\mu})$ and the mass-eigenstate rate asymmetry $A_{\Delta\Gamma}(B_{d,s} \rightarrow \mu\bar{\mu})$ we include for the SM contribution the NNLO QCD [107] and NLO EW [35] corrections, whereas NP contributions are included at LO. The values of the decay constants $F_{B_{d,s}}$ are collected in Table 12.

The branching fractions $Br(B^+ \rightarrow (\pi^+, K^+)\mu\bar{\mu})$ at high dilepton invariant mass q^2 are predicted within the framework outlined in Refs. [108–110]. We neglect contributions from QCD penguin operators, which have small Wilson coefficients and the NLO QCD corrections to matrix elements of the charged-current operators [111, 112], but include the contributions $\sim V_{ub}V_{ud(s)}^*$. The form factors and their uncertainties are adapted from lattice calculations [113, 114] for $B \rightarrow \pi$ and [115] for $B \rightarrow K$ with a summary given in [116]. We add additional relative uncertainties of 15% for missing NLO QCD corrections and 10% for possible duality violation [109] in quadrature.

The predictions for observables of $B \rightarrow K^*\mu\bar{\mu}$ are based on Refs. [84] and [117] for low- and high- q^2 regions, respectively. The corresponding results for $B \rightarrow K^*$ form factors in the two regions are from the LCSR calculation [118] and the lattice calculations [119, 120].

The measurement of $Br(K_L \rightarrow \mu\bar{\mu})$ provides important constraints on its short-distance (SD) contributions, despite the dominating long-distance (LD) contributions inducing uncertainties that are not entirely under theoretical control. We utilise the approach [69] that derived bounds on the SD part χ_{SD} of the decay amplitude of $K_L \rightarrow \mu\bar{\mu}$. A conservative bound allows for both signs of the interference of SD- and LD-parts $|\chi_{\text{SD}}| \leq 3.1$, whereas we will use the more stringent bound $-3.1 \leq \chi_{\text{SD}} \leq 1.7$ in our fits, which has been derived by relying on predictions of this sign based on the quite general assumptions stated in [69, 121].

B.4 $d_j \rightarrow d_i q \bar{q}$ and ε'/ε

The effective Lagrangian for $d_j \rightarrow d_i q \bar{q}$ ($i \neq j$) is adopted from Ref. [122], where the definition of the operators can be found and here we restrict ourselves to $\bar{s} \rightarrow \bar{d}$, i.e. $ij = sd$. At the scale μ_{EW} ($N_f = 5$) it reads

$$\begin{aligned} \mathcal{L}_{d \rightarrow dq\bar{q}} = & -\frac{G_F}{\sqrt{2}} \lambda_{sd}^{(u)} \left\{ (1 - \tau) [z_1(O_1 - O_1^c) + z_2(O_2 - O_2^c)] \right. \\ & \left. + \sum_{a=3}^{10} (\tau v_a + v_a^{\text{NP}}) O_a + \sum_{a=3}^{10} v'_a O'_a \right\} + \text{h.c.}, \end{aligned} \quad (104)$$

where $O_{1,2}^{(c)}$ denote current-current operators. The sum over a extends over the QCD- and EW-penguin operators and we included their chirality-flipped counterparts $O'_a = O_a[\gamma_5 \rightarrow -\gamma_5]$. Thereby we assume that VLQ contributions to other operators are strongly suppressed. The Wilson coefficients are denoted as z_a , $v_a^{(\text{NP})}$ and v'_a , taken at the scale μ_{EW} . For the SM-part, CKM unitarity was used,

$$\tau \equiv \lambda_{sd}^{(u)} / \lambda_{sd}^{(t)}, \quad (105)$$

and we introduced a new physics contribution v_a^{NP} as shown above, which is related to the VLQ-contribution (44) as

$$v_a^{\text{NP}} = C_a^{sd}, \quad v'_a = C_{a'}^{sd}. \quad (106)$$

The RG evolution at NLO in QCD and QED leads to the effective Hamiltonian at a scale $\mu \lesssim \mu_c \sim m_c$ ($N_f = 3$)

$$\mathcal{H}_{d \rightarrow dq\bar{q}} = \frac{G_F}{\sqrt{2}} \lambda_{sd}^{(u)} \left\{ z_1 O_1 + z_2 O_2 + \sum_{a=3}^{10} [z_a + \tau y_a + v_a^{\text{NP}}] O_a + \sum_{a=3}^{10} v'_a O'_a \right\} + \text{h.c.}, \quad (107)$$

after decoupling of b - and c -quarks at scales $\mu_{b,c}$ [122], where $y_a \equiv v_a - z_a$ and all Wilson coefficients are at the scale μ .

The contributions of new physics can then be accounted for in ε'/ε by the replacement

$$y_a(\mu) \rightarrow y_a(\mu) + \frac{v_a^{\text{NP}}(\mu) - v'_a(\mu)}{\tau}, \quad (108)$$

where the minus sign is due to $\langle (\pi\pi)_I | O_a | K \rangle = -\langle (\pi\pi)_I | O'_a | K \rangle$ for the pseudo-scalar pions in the final state [123]. For the readers convenience we provide a semi-numerical formula for ε'/ε with initial conditions of Wilson coefficients from new physics in QCD- and EW-penguins $a = 3^{(\prime)}, 5^{(\prime)}, 7^{(\prime)}, 9^{(\prime)}$ at the electroweak scale μ_{EW} :

$$\frac{\varepsilon'}{\varepsilon} = \left[-2.58 + 24.01 B_6^{(1/2)} - 12.70 B_8^{(3/2)} \right] \times 10^{-4} + \sum_a P_a \text{Im}(v_a^{\text{NP}} - v'_a) [\mu_{\text{EW}}]. \quad (109)$$

The coefficients are

$$P_a = p_a^{(0)} + p_a^{(6)} B_6^{(1/2)} + p_a^{(8)} B_8^{(3/2)} \quad (110)$$

with $p_a^{(n)}$ given in Table 11, where the last column gives P_a for $B_6^{(1/2)}(\mu) = 0.57$ and $B_8^{(3/2)}(\mu) = 0.76$. For this purpose $\mu_{\text{EW}} = M_W$, $\mu_b = m_b(m_b)$, $\mu_c = 1.3$ GeV and $\mu = 1.53$ GeV have been used. The central value of the SM prediction is $(\varepsilon'/\varepsilon)_{\text{SM}} = 1.5 \times 10^{-4}$ compared to 1.9×10^{-4} in [18] due to different numerical inputs.

a	$p_a^{(0)}$	$p_a^{(6)}$	$p_a^{(8)}$	P_a
3	7.45	-3.40	-3.50	2.85
5	1.70	30.62	-18.74	4.91
7	-102.02	-1.32	2040.38	1447.91
9	36.72	4.42	-21.28	23.06

Table 11: Values of the coefficients entering the semi-numerical formular of ε'/ε in Eq. (109). The last column gives P_a for $B_6^{(1/2)} = 0.57$ and $B_8^{(3/2)} = 0.76$.

C Statistical approach and numerical input

The input quantities included in our analysis are collected in Table 12. The CKM parameters have to be determined independently of contributions from the VLQs. The “tree-level” fit carried out by the CKMfitter collaboration achieves such a determination, taking only measurements into account that are unaffected in our NP scenarios, *i.e.* (semi-)leptonic tree-level decays, tree-level determinations of γ and $B \rightarrow \pi\pi, \pi\rho, \rho\rho$, used as a constraint on γ . The results of this fit are again quoted in Table 12.

As a statistical procedure, we choose a frequentist approach. The fits include as parameters of interest the VLQ couplings and in addition nuisance parameters, which constitute theoretical uncertainties. The nuisance parameters are listed in Table 12 and consist of

- CKM parameters from a “tree-level” fit¹¹;
- hadronic parameters: decay constants, form factors, $|\Delta F| = 2$ hadronic matrix elements.

The 1- and 2-dimensional confidence regions (CL) of parameters are obtained by profiling over the remaining parameters, *i.e.* maximisation of the likelihood function over the subspace of remaining parameters for a fixed value of the (pair of) parameter(s) of interest. Similarly, correlation plots for pairs of observables are obtained by profiling over all parameters and imposing in addition the specific values for the pair observables. The 2-dimensional 68% and 95% confidence regions are determined then for two degrees of freedom. The SM predictions of observables are found in the same way by setting VLQ contributions to zero and profiling only over the CKM and hadronic nuisance parameters.

References

- [1] Y. Nir and D. J. Silverman, *Z Mediated Flavor Changing Neutral Currents and Their Implications for CP Asymmetries in B^0 Decays*, *Phys. Rev.* **D42** (1990) 1477–1484.

¹¹We thank Sebastien Descotes-Genon for providing us an update of a tree-level CKM fit from CKMfitter [89].

general [67]	
$M_W = 80.385(15)$ GeV	$M_Z = 91.1876(21)$ GeV
$G_F = 1.16638(1) \times 10^{-5}$ GeV ⁻²	$s_W^2 \equiv \sin^2\theta_W = 0.23126(13)$
$\alpha(M_Z) = 1/127.9$	$\alpha_s(M_Z) = 0.1185(6)$
quark masses	
$m_d(2 \text{ GeV}) = 4.68(16)$ MeV [124]	
$m_s(2 \text{ GeV}) = 93.8(24)$ MeV [124]	$m_c(m_c) = 1.275(25)$ GeV [67]
$m_b(m_b) = 4.18(3)$ GeV [67]	$m_t(m_t) = 163(1)$ GeV [125]
CKM	
$\lambda = 0.22541(^{+30}_{-21})$	$A = 0.8212(^{+66}_{-338})$
$\bar{\rho} = 0.132(21)$	$\bar{\eta} = 0.383(22)$
Kaon	
$m_K = 497.614(24)$ MeV [67]	$\kappa_\epsilon = 0.94(2)$ [126, 127]
$F_K/F_\pi = 1.194(5)$ [67]	$F_\pi = 130.41(20)$ MeV [67]
$\hat{B}_K = 0.750(15)$ [124, 128]	$\eta_{tt} = 0.5765(65)$ [129]
$\eta_{ct} = 0.496(47)$ [130]	$\eta_{cc} = 1.87(76)$ [131]
<i>B</i> -meson	
$m_{B^\pm} = 5279.29(15)$ MeV [67]	$\tau_{B^\pm} = 1.638(4)$ ps [70]
$m_{B_d} = 5279.61(16)$ MeV [67]	$\tau_{B_d} = 1.520(4)$ ps [70]
$m_{B_s} = 5366.79(23)$ MeV [67]	$\tau_{B_s} = 1.505(4)$ ps [70]
$F_{B_d} = 190.5(42)$ MeV	$F_{B_s} = 227.7(45)$ MeV [124]
$F_{B_d}(\hat{B}_{B_d})^{1/2} = 229.4(93)$ MeV	$F_{B_s}(\hat{B}_{B_s})^{1/2} = 276.0(85)$ MeV [57]
$\rho(F_{B_s}, F_{B_d}) = 61.7\%^*$	$\rho(F_{B_s}(\hat{B}_{B_s})^{1/2}, F_{B_d}(\hat{B}_{B_d})^{1/2}) = 95.1\%^{**}$
$\eta_B = 0.55(1)$ [129, 132]	$\Delta\Gamma_s/\Gamma_s = 0.124(9)$ [70]

Table 12: Values of the experimental and theoretical quantities used as input parameters as of March 2016. * : Calculated by demanding that the uncertainty of the ratio of the decay constants given above should equal the uncertainty given explicitly for the ratio, also given in Ref. [124]. ** : Calculated from information given in Ref. [57]. Note that their assumption for the SU(3) breaking from the charm sea contribution corresponds to the assumption of a 91.8% correlation for this uncertainty between B_d and B_s .

- [2] G. C. Branco, T. Morozumi, P. A. Parada, and M. N. Rebelo, *CP asymmetries in B^0 decays in the presence of flavor changing neutral currents*, *Phys. Rev.* **D48** (1993) 1167–1175.
- [3] F. del Aguila, M. Perez-Victoria, and J. Santiago, *Observable contributions of new exotic quarks to quark mixing*, *JHEP* **0009** (2000) 011, [hep-ph/0007316].
- [4] G. Barenboim, F. J. Botella, and O. Vives, *Constraining models with vector - like fermions from FCNC in K and B physics*, *Nucl. Phys.* **B613** (2001) 285–305,

- [hep-ph/0105306].
- [5] A. J. Buras, B. Duling, and S. Gori, *The Impact of Kaluza-Klein Fermions on Standard Model Fermion Couplings in a RS Model with Custodial Protection*, *JHEP* **0909** (2009) 076, [arXiv:0905.2318].
- [6] F. Botella, G. Branco, and M. Nebot, *The Hunt for New Physics in the Flavour Sector with up vector-like quarks*, *JHEP* **1212** (2012) 040, [arXiv:1207.4440].
- [7] S. Fajfer, A. Greljo, J. F. Kamenik, and I. Mustac, *Light Higgs and Vector-like Quarks without Prejudice*, *JHEP* **07** (2013) 155, [arXiv:1304.4219].
- [8] A. J. Buras, J. Girrbach, and R. Ziegler, *Particle-Antiparticle Mixing, CP Violation and Rare K and B Decays in a Minimal Theory of Fermion Masses*, *JHEP* **1304** (2013) 168, [arXiv:1301.5498].
- [9] W. Altmannshofer, S. Gori, M. Pospelov, and I. Yavin, *Quark flavor transitions in $L_\mu - L_\tau$ models*, *Phys. Rev.* **D89** (2014) 095033, [arXiv:1403.1269].
- [10] A. K. Alok, S. Banerjee, D. Kumar, S. U. Sankar, and D. London, *New-physics signals of a model with a vector-singlet up-type quark*, *Phys. Rev.* **D92** (2015) 013002, [arXiv:1504.00517].
- [11] K. Ishiwata, Z. Ligeti, and M. B. Wise, *New Vector-Like Fermions and Flavor Physics*, *JHEP* **10** (2015) 027, [arXiv:1506.03484].
- [12] P. Arnan, L. Hofer, F. Mescia, and A. Crivellin, *Loop effects of heavy new scalars and fermions in $b \rightarrow s\mu^+\mu^-$* , arXiv:1608.07832.
- [13] X. G. He, G. C. Joshi, H. Lew, and R. R. Volkas, *New Z-prime phenomenology*, *Phys. Rev.* **D43** (1991) 22–24.
- [14] X.-G. He, G. C. Joshi, H. Lew, and R. R. Volkas, *Simplest Z-prime model*, *Phys. Rev.* **D44** (1991) 2118–2132.
- [15] W. Altmannshofer and I. Yavin, *Predictions for lepton flavor universality violation in rare B decays in models with gauged $L_\mu - L_\tau$* , *Phys. Rev.* **D92** (2015), no. 7 075022, [arXiv:1508.07009].
- [16] A. J. Buras and J. Girrbach, *Left-handed Z' and Z FCNC quark couplings facing new $b \rightarrow s\mu^+\mu^-$ data*, *JHEP* **1312** (2013) 009, [arXiv:1309.2466].
- [17] **RBC, UKQCD** Collaboration, Z. Bai et al., *Standard Model Prediction for Direct CP Violation in $K \rightarrow \pi\pi$ Decay*, *Phys. Rev. Lett.* **115** (2015), no. 21 212001, [arXiv:1505.07863].
- [18] A. J. Buras, M. Gorbahn, S. Jäger, and M. Jamin, *Improved anatomy of ε'/ε in the Standard Model*, *JHEP* **11** (2015) 202, [arXiv:1507.06345].
- [19] A. J. Buras and J.-M. Gerard, *Upper Bounds on ε'/ε Parameters $B_6^{(1/2)}$ and $B_8^{(3/2)}$ from Large N QCD and other News*, *JHEP* **12** (2015) 008, [arXiv:1507.06326].

- [20] T. Kitahara, U. Nierste, and P. Tremper, *Singularity-free Next-to-leading Order $\Delta S = 1$ Renormalization Group Evolution and ϵ'_K/ϵ_K in the Standard Model and Beyond*, [arXiv:1607.06727](#).
- [21] A. Crivellin, G. D'Ambrosio, and J. Heeck, *Explaining $h \rightarrow \mu^\pm \tau^\mp$, $B \rightarrow K^* \mu^+ \mu^-$ and $B \rightarrow K \mu^+ \mu^- / B \rightarrow K e^+ e^-$ in a two-Higgs-doublet model with gauged $L_\mu - L_\tau$* , *Phys. Rev. Lett.* **114** (2015) 151801, [[arXiv:1501.00993](#)].
- [22] **SLD Electroweak Group, DELPHI, ALEPH, SLD, SLD Heavy Flavour Group, OPAL, LEP Electroweak Working Group, L3 Collaboration**, S. Schael et al., *Precision electroweak measurements on the Z resonance*, *Phys. Rept.* **427** (2006) 257–454, [[hep-ex/0509008](#)].
- [23] B. Grzadkowski, M. Iskrzynski, M. Misiak, and J. Rosiek, *Dimension-Six Terms in the Standard Model Lagrangian*, *JHEP* **1010** (2010) 085, [[arXiv:1008.4884](#)].
- [24] E. E. Jenkins, A. V. Manohar, and M. Trott, *Renormalization Group Evolution of the Standard Model Dimension Six Operators I: Formalism and lambda Dependence*, *JHEP* **10** (2013) 087, [[arXiv:1308.2627](#)].
- [25] E. E. Jenkins, A. V. Manohar, and M. Trott, *Renormalization Group Evolution of the Standard Model Dimension Six Operators II: Yukawa Dependence*, *JHEP* **01** (2014) 035, [[arXiv:1310.4838](#)].
- [26] R. Alonso, E. E. Jenkins, A. V. Manohar, and M. Trott, *Renormalization Group Evolution of the Standard Model Dimension Six Operators III: Gauge Coupling Dependence and Phenomenology*, *JHEP* **04** (2014) 159, [[arXiv:1312.2014](#)].
- [27] C. Arzt, M. B. Einhorn, and J. Wudka, *Patterns of deviation from the standard model*, *Nucl. Phys.* **B433** (1995) 41–66, [[hep-ph/9405214](#)].
- [28] W. Buchmuller and D. Wyler, *Effective Lagrangian Analysis of New Interactions and Flavor Conservation*, *Nucl.Phys.* **B268** (1986) 621–653.
- [29] J. Aebischer, A. Crivellin, M. Fael, and C. Greub, *Matching of gauge invariant dimension-six operators for $b \rightarrow s$ and $b \rightarrow c$ transitions*, *JHEP* **05** (2016) 037, [[arXiv:1512.02830](#)].
- [30] A. J. Buras, M. Misiak, and J. Urban, *Two loop QCD anomalous dimensions of flavor changing four quark operators within and beyond the standard model*, *Nucl.Phys.* **B586** (2000) 397–426, [[hep-ph/0005183](#)].
- [31] A. J. Buras, F. De Fazio, and J. Girrbach, *The Anatomy of Z' and Z with Flavour Changing Neutral Currents in the Flavour Precision Era*, *JHEP* **1302** (2013) 116, [[arXiv:1211.1896](#)].
- [32] A. J. Buras, *Minimal flavour violation and beyond: Towards a flavour code for short distance dynamics*, *Acta Phys.Polon.* **B41** (2010) 2487–2561, [[arXiv:1012.1447](#)].

- [33] A. J. Buras, F. De Fazio, J. Girrbach, and M. V. Carlucci, *The Anatomy of Quark Flavour Observables in 331 Models in the Flavour Precision Era*, *JHEP* **1302** (2013) 023, [[arXiv:1211.1237](#)].
- [34] A. J. Buras and J. Girrbach, *Complete NLO QCD Corrections for Tree Level Delta F = 2 FCNC Processes*, *JHEP* **1203** (2012) 052, [[arXiv:1201.1302](#)].
- [35] C. Bobeth, M. Gorbahn, and E. Stamou, *Electroweak Corrections to $B_{s,d} \rightarrow \ell^+ \ell^-$* , *Phys. Rev.* **D89** (2014) 034023, [[arXiv:1311.1348](#)].
- [36] A. J. Buras, *New physics patterns in ε'/ε and ε_K with implications for rare kaon decays and ΔM_K* , *JHEP* **04** (2016) 071, [[arXiv:1601.00005](#)].
- [37] T. Blum et al., *$K \rightarrow \pi\pi$ $\Delta I = 3/2$ decay amplitude in the continuum limit*, *Phys. Rev.* **D91** (2015), no. 7 074502, [[arXiv:1502.00263](#)].
- [38] **NA48** Collaboration, J. Batley et al., *A Precision measurement of direct CP violation in the decay of neutral kaons into two pions*, *Phys. Lett.* **B544** (2002) 97–112, [[hep-ex/0208009](#)].
- [39] **KTeV** Collaboration, A. Alavi-Harati et al., *Measurements of direct CP violation, CPT symmetry, and other parameters in the neutral kaon system*, *Phys. Rev.* **D67** (2003) 012005, [[hep-ex/0208007](#)].
- [40] **KTeV** Collaboration, E. Abouzaid et al., *Precise Measurements of Direct CP Violation, CPT Symmetry, and Other Parameters in the Neutral Kaon System*, *Phys. Rev.* **D83** (2011) 092001, [[arXiv:1011.0127](#)].
- [41] A. J. Buras and J.-M. Gerard, *Final State Interactions in $K \rightarrow \pi\pi$ Decays: $\Delta I = 1/2$ Rule vs. ε'/ε* , [arXiv:1603.05686](#).
- [42] V. Antonelli, S. Bertolini, M. Fabbrichesi, and E. I. Lashin, *The $\Delta I = 1/2$ selection rule*, *Nucl. Phys.* **B469** (1996) 181–201, [[hep-ph/9511341](#)].
- [43] S. Bertolini, J. O. Eeg, and M. Fabbrichesi, *A New estimate of ε'/ε* , *Nucl. Phys.* **B476** (1996) 225–254, [[hep-ph/9512356](#)].
- [44] J. M. Frere, J. Galand, A. Le Yaouanc, L. Oliver, O. Pene, and J. C. Raynal, *$K^0 - \bar{K}^0$ in the $SU(2)_L \otimes SU(2)_R \otimes U(1)$ model of CP violation*, *Phys. Rev.* **D46** (1992) 337–353. [[329\(1991\)](#)].
- [45] E. Pallante and A. Pich, *Strong enhancement of ε'/ε through final state interactions*, *Phys. Rev. Lett.* **84** (2000) 2568–2571, [[hep-ph/9911233](#)].
- [46] E. Pallante and A. Pich, *Final state interactions in kaon decays*, *Nucl. Phys.* **B592** (2001) 294–320, [[hep-ph/0007208](#)].
- [47] M. Buchler, G. Colangelo, J. Kambor, and F. Orellana, *A Note on the dispersive treatment of $K \rightarrow \pi\pi$ with the kaon off-shell*, *Phys. Lett.* **B521** (2001) 29–32, [[hep-ph/0102289](#)].

- [48] M. Buchler, G. Colangelo, J. Kambor, and F. Orellana, *Dispersion relations and soft pion theorems for $K \rightarrow \pi\pi$* , *Phys. Lett.* **B521** (2001) 22–28, [[hep-ph/0102287](#)].
- [49] E. Pallante, A. Pich, and I. Scimemi, *The Standard model prediction for ϵ'/ϵ* , *Nucl. Phys.* **B617** (2001) 441–474, [[hep-ph/0105011](#)].
- [50] A. J. Buras, D. Buttazzo, and R. Knegjens, *$K \rightarrow \pi\nu\bar{\nu}$ and ϵ'/ϵ in Simplified New Physics Models*, *JHEP* **11** (2015) 166, [[arXiv:1507.08672](#)].
- [51] M. Blanke, A. J. Buras, and S. Recksiegel, *Quark flavour observables in the Littlest Higgs model with T -parity after LHC Run 1*, *Eur. Phys. J.* **C76** (2016), no. 4 182, [[arXiv:1507.06316](#)].
- [52] A. J. Buras and F. De Fazio, *ϵ'/ϵ in 331 Models*, *JHEP* **03** (2016) 010, [[arXiv:1512.02869](#)].
- [53] A. J. Buras and F. De Fazio, *331 Models Facing the Tensions in $\Delta F = 2$ Processes with the Impact on ϵ'/ϵ , $B_s \rightarrow \mu^+\mu^-$ and $B \rightarrow K^*\mu^+\mu^-$* , *JHEP* **08** (2016) 115, [[arXiv:1604.02344](#)].
- [54] M. Tanimoto and K. Yamamoto, *Probing the SUSY with 10 TeV stop mass in rare decays and CP violation of Kaon*, [arXiv:1603.07960](#).
- [55] T. Kitahara, U. Nierste, and P. Tremper, *Supersymmetric explanation of CP violation in $K \rightarrow \pi\pi$ decays*, *Phys. Rev. Lett.* **117** (2016), no. 9 091802, [[arXiv:1604.07400](#)].
- [56] M. Endo, S. Mishima, D. Ueda, and K. Yamamoto, *Chargino contributions in light of recent ϵ'/ϵ* , [arXiv:1608.01444](#).
- [57] **Fermilab Lattice, MILC Collaboration**, A. Bazavov et al., *$B_{(s)}^0$ -mixing matrix elements from lattice QCD for the Standard Model and beyond*, *Phys. Rev.* **D93** (2016), no. 11 113016, [[arXiv:1602.03560](#)].
- [58] M. Blanke and A. J. Buras, *Universal Unitarity Triangle 2016 and the tension between $\Delta M_{s,d}$ and ϵ_K in CMFV models*, *Eur. Phys. J.* **C76** (2016), no. 4 197, [[arXiv:1602.04020](#)].
- [59] G. Branco, P. Ferreira, L. Lavoura, M. Rebelo, M. Sher, et al., *Theory and phenomenology of two-Higgs-doublet models*, *Phys.Rept.* **516** (2012) 1–102, [[arXiv:1106.0034](#)].
- [60] A. J. Buras, F. De Fazio, and J. Girrbach, *331 models facing new $b \rightarrow s\mu^+\mu^-$ data*, *JHEP* **1402** (2014) 112, [[arXiv:1311.6729](#)].
- [61] A. Efrati, A. Falkowski, and Y. Soreq, *Electroweak constraints on flavorful effective theories*, *JHEP* **07** (2015) 018, [[arXiv:1503.07872](#)].

- [62] Z. Bai, N. H. Christ, T. Izubuchi, C. T. Sachrajda, A. Soni, and J. Yu, *$K_L - K_S$ Mass Difference from Lattice QCD*, *Phys. Rev. Lett.* **113** (2014) 112003, [arXiv:1406.0916].
- [63] W. Altmannshofer and D. M. Straub, *New physics in $b \rightarrow s$ transitions after LHC run 1*, *Eur. Phys. J.* **C75** (2015), no. 8 382, [arXiv:1411.3161].
- [64] W. Altmannshofer and D. M. Straub, *Implications of $b \rightarrow s$ measurements*, in *Proceedings, 50th Rencontres de Moriond Electroweak Interactions and Unified Theories: La Thuile, Italy, March 14-21, 2015*, pp. 333–338, 2015. arXiv:1503.06199.
- [65] S. Descotes-Genon, L. Hofer, J. Matias, and J. Virto, *Global analysis of $b \rightarrow s\ell\ell$ anomalies*, *JHEP* **06** (2016) 092, [arXiv:1510.04239].
- [66] T. Hurth, F. Mahmoudi, and S. Neshatpour, *On the anomalies in the latest LHCb data*, *Nucl. Phys.* **B909** (2016) 737–777, [arXiv:1603.00865].
- [67] **Particle Data Group** Collaboration, K. Olive et al., *Review of Particle Physics*, *Chin.Phys.* **C38** (2014) 090001. Updates available on <http://pdg.lbl.gov>.
- [68] **E949** Collaboration, A. V. Artamonov et al., *New measurement of the $K^+ \rightarrow \pi^+\nu\bar{\nu}$ branching ratio*, *Phys. Rev. Lett.* **101** (2008) 191802, [arXiv:0808.2459].
- [69] G. Isidori and R. Unterdorfer, *On the short-distance constraints from $K_{L,S} \rightarrow \mu^+\mu^-$* , *JHEP* **01** (2004) 009, [hep-ph/0311084].
- [70] **Heavy Flavor Averaging Group (HFAG)** Collaboration, Y. Amhis et al., *Averages of b -hadron, c -hadron, and τ -lepton properties as of summer 2014*, arXiv:1412.7515. <http://www.slac.stanford.edu/xorg/hfag>.
- [71] **LHCb** Collaboration, R. Aaij et al., *First measurement of the differential branching fraction and CP asymmetry of the $B^\pm \rightarrow \pi^\pm\mu^+\mu^-$ decay*, *JHEP* **10** (2015) 034, [arXiv:1509.00414].
- [72] **LHCb, CMS** Collaboration, V. Khachatryan et al., *Observation of the rare $B_s^0 \rightarrow \mu^+\mu^-$ decay from the combined analysis of CMS and LHCb data*, *Nature* **522** (2015) 68–72, [arXiv:1411.4413].
- [73] **LHCb** Collaboration, R. Aaij et al., *Differential branching fractions and isospin asymmetries of $B \rightarrow K^{(*)}\mu^+\mu^-$ decays*, *JHEP* **06** (2014) 133, [arXiv:1403.8044].
- [74] M. Jung, *Determining weak phases from $B \rightarrow J/\psi P$ decays*, *Phys. Rev.* **D86** (2012) 053008, [arXiv:1206.2050].
- [75] K. De Bruyn and R. Fleischer, *A Roadmap to Control Penguin Effects in $B_d^0 \rightarrow J/\psi K_S^0$ and $B_s^0 \rightarrow J/\psi\phi$* , *JHEP* **03** (2015) 145, [arXiv:1412.6834].

- [76] P. Frings, U. Nierste, and M. Wiebusch, *Penguin contributions to CP phases in $B_{d,s}$ decays to charmonium*, *Phys. Rev. Lett.* **115** (2015), no. 6 061802, [[arXiv:1503.00859](#)].
- [77] G. A. Rinella, R. Aliberti, F. Ambrosino, B. Angelucci, A. Antonelli, et al., *Prospects for $K^+ \rightarrow \pi^+ \nu \bar{\nu}$ at CERN in NA62*, [arXiv:1411.0109](#).
- [78] A. Ceccucci, *Direct CP Violation and Rare K Decays Perspectives*, *Acta Phys. Polon.* **B47** (2016) 261–266.
- [79] **E391a** Collaboration, J. Ahn et al., *Experimental study of the decay $K_L^0 \rightarrow \pi^0 \nu \bar{\nu}$* , *Phys. Rev.* **D81** (2010) 072004, [[arXiv:0911.4789](#)].
- [80] **LHCb** Collaboration, R. Aaij et al., *Measurement of the $B_s^0 \rightarrow \mu^+ \mu^-$ branching fraction and search for $B^0 \rightarrow \mu^+ \mu^-$ decays at the LHCb experiment*, *Phys. Rev. Lett.* **111** (2013) 101805, [[arXiv:1307.5024](#)].
- [81] **LHCb** Collaboration, R. Aaij et al., *Angular analysis of the $B^0 \rightarrow K^{*0} \mu^+ \mu^-$ decay using 3 fb^{-1} of integrated luminosity*, *JHEP* **02** (2016) 104, [[arXiv:1512.04442](#)].
- [82] **BaBar** Collaboration, J. Lees et al., *Search for $B \rightarrow K^{(*)} \nu \bar{\nu}$ and invisible quarkonium decays*, *Phys. Rev.* **D87** (2013) 112005, [[arXiv:1303.7465](#)].
- [83] **Belle** Collaboration, O. Lutz et al., *Search for $B \rightarrow h^{(*)} \nu \bar{\nu}$ with the full Belle $Y(4S)$ data sample*, *Phys. Rev.* **D87** (2013) 111103, [[arXiv:1303.3719](#)].
- [84] C. Bobeth, G. Hiller, and G. Piranishvili, *CP Asymmetries in bar $B \rightarrow \bar{K}^*(\rightarrow \bar{K}\pi)\bar{\ell}\ell$ and Untagged $\bar{B}_s, B_s \rightarrow \phi(\rightarrow K^+K^-)\bar{\ell}\ell$ Decays at NLO*, *JHEP* **0807** (2008) 106, [[arXiv:0805.2525](#)].
- [85] C. Bobeth, G. Hiller, and D. van Dyk, *General Analysis of $\bar{B} \rightarrow \bar{K}^{(*)} \ell^+ \ell^-$ Decays at Low Recoil*, *Phys.Rev.* **D87** (2013) 034016, [[arXiv:1212.2321](#)].
- [86] W. Altmannshofer, A. J. Buras, D. M. Straub, and M. Wick, *New strategies for New Physics search in $B \rightarrow K^* \nu \bar{\nu}$, $B \rightarrow K \nu \bar{\nu}$ and $B \rightarrow X_s \nu \bar{\nu}$ decays*, *JHEP* **04** (2009) 022, [[arXiv:0902.0160](#)].
- [87] A. J. Buras, J. Girrbach-Noe, C. Niehoff, and D. M. Straub, *$B \rightarrow K^{(*)} \nu \bar{\nu}$ decays in the Standard Model and beyond*, *JHEP* **1502** (2015) 184, [[arXiv:1409.4557](#)].
- [88] T. Aushev, W. Bartel, A. Bondar, J. Brodzicka, T. Browder, et al., *Physics at Super B Factory*, [arXiv:1002.5012](#).
- [89] **CKMfitter Group** Collaboration, J. Charles et al., *CP violation and the CKM matrix: Assessing the impact of the asymmetric B factories*, *Eur.Phys.J.* **C41** (2005) 1–131, [[hep-ph/0406184](#)]. <http://www.ckmfitter.in2p3.fr>.
- [90] L. Basso, S. Moretti, and G. M. Pruna, *A Renormalisation Group Equation Study of the Scalar Sector of the Minimal B-L Extension of the Standard Model*, *Phys. Rev.* **D82** (2010) 055018, [[arXiv:1004.3039](#)].

- [91] K. S. Babu, C. F. Kolda, and J. March-Russell, *Implications of generalized $Z - Z'$ mixing*, *Phys. Rev.* **D57** (1998) 6788–6792, [[hep-ph/9710441](#)].
- [92] M. Ciuchini, E. Franco, V. Lubicz, G. Martinelli, I. Scimemi, et al., *Next-to-leading order QCD corrections to $\Delta F = 2$ effective Hamiltonians*, *Nucl.Phys.* **B523** (1998) 501–525, [[hep-ph/9711402](#)].
- [93] A. J. Buras, S. Jager, and J. Urban, *Master formulae for $\Delta F = 2$ NLO QCD factors in the standard model and beyond*, *Nucl.Phys.* **B605** (2001) 600–624, [[hep-ph/0102316](#)].
- [94] M. Gorbahn, S. Jager, U. Nierste, and S. Trine, *The supersymmetric Higgs sector and $B - \bar{B}$ mixing for large $\tan \beta$* , *Phys. Rev.* **D84** (2011) 034030, [[arXiv:0901.2065](#)].
- [95] G. Buchalla, A. J. Buras, and M. E. Lautenbacher, *Weak decays beyond leading logarithms*, *Rev.Mod.Phys.* **68** (1996) 1125–1144, [[hep-ph/9512380](#)].
- [96] A. J. Buras, *Weak Hamiltonian, CP violation and rare decays*, [hep-ph/9806471](#). In 'Probing the Standard Model of Particle Interactions', F.David and R. Gupta, eds., 1998, Elsevier Science B.V.
- [97] T. Inami and C. Lim, *Effects of Superheavy Quarks and Leptons in Low-Energy Weak Processes $K_L \rightarrow \mu^+ \mu^-$, $K^+ \rightarrow \pi^+ \nu \bar{\nu}$ and $K^0 - \bar{K}^0$* , *Prog.Theor.Phys.* **65** (1981) 297.
- [98] G. Buchalla, A. J. Buras, and M. K. Harlander, *Penguin box expansion: Flavor changing neutral current processes and a heavy top quark*, *Nucl. Phys.* **B349** (1991) 1–47.
- [99] G. Buchalla and A. J. Buras, *Qcd corrections to rare k and b decays for arbitrary top quark mass*, *Nucl. Phys.* **B400** (1993) 225–239.
- [100] M. Misiak and J. Urban, *QCD corrections to FCNC decays mediated by Z penguins and W boxes*, *Phys.Lett.* **B451** (1999) 161–169, [[hep-ph/9901278](#)].
- [101] G. Buchalla and A. J. Buras, *The rare decays $K \rightarrow \pi \nu \bar{\nu}$, $B \rightarrow X \nu \bar{\nu}$ and $B \rightarrow \ell^+ \ell^-$: An Update*, *Nucl.Phys.* **B548** (1999) 309–327, [[hep-ph/9901288](#)].
- [102] J. Brod, M. Gorbahn, and E. Stamou, *Two-Loop Electroweak Corrections for the $K \rightarrow \pi \nu \bar{\nu}$ Decays*, *Phys. Rev.* **D83** (2011) 034030, [[arXiv:1009.0947](#)].
- [103] A. J. Buras, D. Buttazzo, J. Girrbach-Noe, and R. Knegjens, *$K^+ \rightarrow \pi^+ \nu \bar{\nu}$ and $K_L \rightarrow \pi^0 \nu \bar{\nu}$ in the Standard Model: status and perspectives*, *JHEP* **11** (2015) 033, [[arXiv:1503.02693](#)].
- [104] A. J. Buras, M. Gorbahn, U. Haisch, and U. Nierste, *Charm quark contribution to $K^+ \rightarrow \pi^+ \nu \bar{\nu}$ at next-to-next-to-leading order*, *JHEP* **11** (2006) 002, [[hep-ph/0603079](#)].

- [105] F. Mescia and C. Smith, *Improved estimates of rare K decay matrix-elements from $K_{\ell 3}$ decays*, *Phys. Rev.* **D76** (2007) 034017, [[arXiv:0705.2025](#)].
- [106] C. Bobeth, G. Hiller, and G. Piranishvili, *Angular distributions of $\bar{B} \rightarrow \bar{K} \ell^+ \ell^-$ decays*, *JHEP* **12** (2007) 040, [[arXiv:0709.4174](#)].
- [107] T. Hermann, M. Misiak, and M. Steinhauser, *Three-loop QCD corrections to $B_s \rightarrow \mu^+ \mu^-$* , *JHEP* **1312** (2013) 097, [[arXiv:1311.1347](#)].
- [108] B. Grinstein and D. Pirjol, *Exclusive rare $B \rightarrow K^* \ell^+ \ell^-$ decays at low recoil: Controlling the long-distance effects*, *Phys. Rev.* **D70** (2004) 114005, [[hep-ph/0404250](#)].
- [109] M. Beylich, G. Buchalla, and T. Feldmann, *Theory of $B \rightarrow K^{(*)} l^+ l^-$ decays at high q^2 : OPE and quark-hadron duality*, *Eur.Phys.J.* **C71** (2011) 1635, [[arXiv:1101.5118](#)].
- [110] C. Bobeth, G. Hiller, D. van Dyk, and C. Wacker, *The Decay $B \rightarrow K \ell^+ \ell^-$ at Low Hadronic Recoil and Model-Independent $\Delta B = 1$ Constraints*, *JHEP* **01** (2012) 107, [[arXiv:1111.2558](#)].
- [111] D. Seidel, *Analytic two loop virtual corrections to $b \rightarrow d \ell^+ \ell^-$* , *Phys. Rev.* **D70** (2004) 094038, [[hep-ph/0403185](#)].
- [112] C. Greub, V. Pilipp, and C. Schupbach, *Analytic calculation of two-loop QCD corrections to $b \rightarrow s \ell^+ \ell^-$ in the high q^2 region*, *JHEP* **0812** (2008) 040, [[arXiv:0810.4077](#)].
- [113] **Fermilab Lattice, MILC Collaboration**, J. A. Bailey et al., *$|V_{ub}|$ from $B \rightarrow \pi \ell \nu$ decays and $(2+1)$ -flavor lattice QCD*, *Phys. Rev.* **D92** (2015), no. 1 014024, [[arXiv:1503.07839](#)].
- [114] **Fermilab Lattice, MILC Collaboration**, J. A. Bailey et al., *$B \rightarrow \pi \ell^+ \ell^-$ form factors for new-physics searches from lattice QCD*, *Phys. Rev. Lett.* **115** (2015), no. 15 152002, [[arXiv:1507.01618](#)].
- [115] J. A. Bailey et al., *$B \rightarrow K \ell^+ \ell^-$ decay form factors from three-flavor lattice QCD*, *Phys. Rev.* **D93** (2016), no. 2 025026, [[arXiv:1509.06235](#)].
- [116] D. Du, A. X. El-Khadra, S. Gottlieb, A. S. Kronfeld, J. Laiho, E. Lunghi, R. S. Van de Water, and R. Zhou, *Phenomenology of semileptonic B -meson decays with form factors from lattice QCD*, *Phys. Rev.* **D93** (2016), no. 3 034005, [[arXiv:1510.02349](#)].
- [117] C. Bobeth, G. Hiller, and D. van Dyk, *The Benefits of $\bar{B} \rightarrow \bar{K}^* l^+ l^-$ Decays at Low Recoil*, *JHEP* **1007** (2010) 098, [[arXiv:1006.5013](#)].
- [118] A. Bharucha, D. M. Straub, and R. Zwicky, *$B \rightarrow V \ell^+ \ell^-$ in the Standard Model from light-cone sum rules*, *JHEP* **08** (2016) 098, [[arXiv:1503.05534](#)].

- [119] R. R. Horgan, Z. Liu, S. Meinel, and M. Wingate, *Lattice QCD calculation of form factors describing the rare decays $B \rightarrow K^* \ell^+ \ell^-$ and $B_s \rightarrow \phi \ell^+ \ell^-$* , *Phys. Rev.* **D89** (2014) 094501, [arXiv:1310.3722].
- [120] R. R. Horgan, Z. Liu, S. Meinel, and M. Wingate, *Rare B decays using lattice QCD form factors*, *PoS LATTICE2014* (2015) 372, [arXiv:1501.00367].
- [121] G. D’Ambrosio, G. Isidori, and J. Portoles, *Can we extract short-distance information from $B(K_L \rightarrow \mu^+ \mu^-)$?*, *Phys. Lett.* **B423** (1998) 385–394, [hep-ph/9708326].
- [122] A. J. Buras, M. Jamin, and M. E. Lautenbacher, *The anatomy of ε'/ε beyond leading logarithms with improved hadronic matrix elements*, *Nucl. Phys.* **B408** (1993) 209–285, [hep-ph/9303284].
- [123] A. L. Kagan, *Right-handed currents, CP violation, and $B \rightarrow VV$* , hep-ph/0407076.
- [124] S. Aoki, Y. Aoki, C. Bernard, T. Blum, G. Colangelo, et al., *Review of lattice results concerning low-energy particle physics*, *Eur. Phys. J.* **C74** (2014), no. 9 2890, [arXiv:1310.8555].
- [125] **HPQCD** Collaboration, I. Allison et al., *High-Precision Charm-Quark Mass from Current-Current Correlators in Lattice and Continuum QCD*, *Phys.Rev.* **D78** (2008) 054513, [arXiv:0805.2999].
- [126] A. J. Buras and D. Guadagnoli, *Correlations among new CP violating effects in $\Delta F = 2$ observables*, *Phys. Rev.* **D78** (2008) 033005, [arXiv:0805.3887].
- [127] A. J. Buras, D. Guadagnoli, and G. Isidori, *On ε_K beyond lowest order in the Operator Product Expansion*, *Phys.Lett.* **B688** (2010) 309–313, [arXiv:1002.3612].
- [128] A. J. Buras, J.-M. Gérard, and W. A. Bardeen, *Large- N Approach to Kaon Decays and Mixing 28 Years Later: $\Delta I = 1/2$ Rule, \hat{B}_K and ΔM_K* , *Eur. Phys. J.* **C74** (2014), no. 5 2871, [arXiv:1401.1385].
- [129] A. J. Buras, M. Jamin, and P. H. Weisz, *Leading and next-to-leading QCD corrections to ε parameter and $B^0 - \bar{B}^0$ mixing in the presence of a heavy top quark*, *Nucl. Phys.* **B347** (1990) 491–536.
- [130] J. Brod and M. Gorbahn, *ε_K at Next-to-Next-to-Leading Order: The Charm-Top-Quark Contribution*, *Phys. Rev.* **D82** (2010) 094026, [arXiv:1007.0684].
- [131] J. Brod and M. Gorbahn, *Next-to-Next-to-Leading-Order Charm-Quark Contribution to the CP Violation Parameter ε_K and ΔM_K* , *Phys.Rev.Lett.* **108** (2012) 121801, [arXiv:1108.2036].

-
- [132] J. Urban, F. Krauss, U. Jentschura, and G. Soff, *Next-to-leading order QCD corrections for the $B^0 - \bar{B}^0$ mixing with an extended Higgs sector*, *Nucl. Phys.* **B523** (1998) 40–58, [[hep-ph/9710245](#)].